สเลอร์รีถ่านหินผสมน้ำโดยใช้ตัวกระจายที่สังเคราะห์จากของเหลวของเปลือกเมล็ดมะม่วงหิมพานต์

นางสาวปณิธา พูลเกิด

วิทยานิพนธ์นี้เป็นส่วนหนึ่งของการศึกษาตามหลักสูตรปริญญาวิทยาศาสตรดุษฎีบัณฑิต
สาขาวิชาปิโตรเคมี
คณะวิทยาศาสตร์ จุฬาลงกรณ์มหาวิทยาลัย
ปีการศึกษา 2554

COAL-WATER SLURRY USING DISPERSANTS SYNTHESIZED FROM CASHEW NUT SHELL LIQUID

Miss Panitha Phulkerd

A Dissertation Submitted in Partial Fulfillment of the Requirements
for the Degree of Doctor of Philosophy Program in Petrochemistry
Faculty of Science
Chulalongkorn University
Academic Year 2011

Thesis Title	COAL-WATER SLURRY USING DISPERSANTS SYNTHESIZED FROM CASHEW NUT SHELL LIQUID
By	Miss Panitha Phulkerd
Field of Study	Petrochemistry
Thesis Advisor	Associate Professor Amorn Petsom, Ph.D.
Thesis Co-advisor	Associate Professor Kunchana Bunyakiat
	Nuttha Thongchul, Ph.D

Accepted by the Graduate School, Chulalongkorn University in Partial Fulfillment of the Requirements for the Doctoral Degree

.....Dean of the Faculty of Science
(Professor Supot Hannongbua, Dr.rer.nat.)

THESIS COMMITTEE

.....Chairman
(Professor Pattarapan Prassassarakich, Ph.D.)

.....Thesis Advisor
(Associate Professor Amorn Petsom, Ph.D.)

.....Thesis Co-advisor
(Associate Professor Kunchana Bunyakiat)

.....Thesis Co-advisor
(Nuttha Thongchul, Ph.D.)

.....Examiner
(Associate Professor Nuanphun Chantarasiri, Ph.D.)

.....Examiner
(Associate Professor Voravee Hoven, Ph.D.)

.....External Examiner
(Damrong Sommit, Ph.D.)

ปณิธา พูลเกิด: สเลอร์รีถ่านหินผสมน้ำโดยใช้ตัวกระจายที่สังเคราะห์จากของเหลวของเปลือกเมล็ดมะม่วงหิมพานต์ (COAL-WATER SLURRY USING DISPERSANTS SYNTHESIZED FROM CASHEW NUT SHELL LIQUID) อ.ที่ปรึกษาวิทยานิพนธ์หลัก: รศ.ดร. อมร เพชรสม, อ.ที่ปรึกษาวิทยานิพนธ์ร่วม: รศ. กัญจนา บุณยเกียรติ, ดร. ณัฏฐา ทองจุล, 155 หน้า.

งานวิจัยนี้มีวัตถุประสงค์ในการสังเคราะห์ตัวกระจายประเภทแอนไอออนิกสามชนิดเพื่อใช้ในการเตรียมสเลอร์รีถ่านหินผสมน้ำจากของเหลวของเปลือกเมล็ดมะม่วงหิมพานต์ ได้แก่ ไดเอทาโนลามีน อะนาคาร์เดต, ไตรเอทาโนลามีน อะนาคาร์เดต, และคาดานอลฟอร์มัลดีไฮด์ซัลโฟเนต และเปรียบเทียบสมบัติตัวกระจายที่สังเคราะห์ได้กับตัวกระจายที่ใช้ในทางการค้า คือโซเดียมลิกโนซัลโฟเนต จากผลการทดลองพบว่าตัวกระจายที่เตรียมขึ้นจากกระบวนการซัลโฟเมทิเลชันของคาร์ดานอล, ฟอร์มัลดีไฮด์, และโซเดียมซัลไฟต์ เป็นตัวกระจายใหม่ที่มีประสิทธิภาพดีกว่าไดเอทาโนลามีน อะนาคาร์เดตและไตรเอทาโนลามีน อะนาคาร์เดตสำหรับสเลอร์รีถ่านหินผสมน้ำ โดยสัดส่วนที่เหมาะสมที่สุดสำหรับการเตรียมสเลอร์รีถ่านหินผสมน้ำ คือ ถ่านหิน 50 เปอร์เซ็นต์ และคาร์ดานอลฟอร์มัลดีไฮด์ซัลโฟเนต 1.0-1.8 เปอร์เซ็นต์ คาร์ดานอลฟอร์มัลดีไฮด์ซัลโฟเนตมีความสามารถในการลดแรงตึงผิวที่ดี โดยมีค่าเท่ากับ 51 มิลลินิวตันต่อเมตร นอกจากนี้ค่าซีต้าโพเทนเชียลของสเลอร์รีถ่านหินผสมน้ำ จะเพิ่มขึ้นเมื่อเพิ่มความเข้มข้นของตัวกระจาย ซึ่งสเลอร์รีมีเสถียรภาพนานประมาณ 1 เดือน โดยมีอัตราส่วนการตกตะกอนต่ำกว่า 50 เปอร์เซ็นต์ ในขณะที่สเลอร์รีที่ไม่เติมตัวกระจายจะมีอัตราส่วนการตกตะกอนต่ำกว่า 30 เปอร์เซ็นต์ จากการเปรียบเทียบกับตัวกระจายที่ใช้ในทางการค้าพบว่าคาดานอลฟอร์มัลดีไฮด์ซัลโฟเนตมีคุณสมบัติคล้ายกับโซเดียมลิกโนซัลโฟเนตและให้ค่าอยู่ในช่วงที่ได้รับการยอมรับ

สาขาวิชา ปิโตรเคมี ลายมือชื่อนิสิต.....

ปีการศึกษา 2554 ลายมือชื่ออ.ที่ปรึกษาวิทยานิพนธ์หลัก.....

ลายมือชื่ออ.ที่ปรึกษาวิทยานิพนธ์ร่วม.....

ลายมือชื่ออ.ที่ปรึกษาวิทยานิพนธ์ร่วม.....

5073839723: PETROCHEMISTRY
KEYWORDS: COAL-WATER SLURRY/ DISPERSANT/ RHEOLOGICAL BEHAVIOR/ NON-NEWTONIAN/ VISCOSITY/ STABILITY

PANITHA PHULKERD: COAL-WATER SLURRY USING DISPERSANTS SYNTHESIZED FROM CASHEW NUT SHELL LIQUID
ADVISOR: ASSOC. PROF. AMORN PETSOM, Ph.D.,
CO-ADVISOR: ASSOC. PROF. KUNCHANA BUNYAKIAT,
NUTTHA THONGCHUL, Ph.D., 155 pp.

The purpose of this study was to synthesize three anionic dispersants for the formulation of highly concentrated coal-water slurry from cashew nut shell liquid. The performance of the three synthesized dispersants, which are diethanolamine anacardate, triethanolamine anacardate and cardanol-formaldehyde sulfonate, were investigated and compared with a commercial dispersant, sodium lignosulfonate. It was found that cardanol-formaldehyde sulfonate as a *new dispersant*, synthesized from sulfomethylation reaction of cardanol, formaldehyde and sodium sulfite, was more efficient dispersant for coal-water slurry application than diethanolamine anacardate and triethanolamine anacardate. In the presence of 1.0-1.8 wt% of cardanol-formaldehyde sulfonate, coal-water slurry containing 50% weight fraction of coal could be achieved. Cardanol-formaldehyde sulfonate had a surface activity with the surface tension of 51 mNm^{-1}. In addition, the zeta potential was substantially increased with concomitant shift of the progressive dispersant concentration. The slurry stability for a period of as long as 1 month gave below 50% of penetration ratio in contrast to below 30% in the case of bare coal-water slurry. As compared with a commercial dispersant, it was found that cardanol-formaldehyde sulfonate gave similar properties to those of sodium lignosulfonate, within acceptable ranges.

Field of Study : Petrochemistry Student's Signature.....

Academic Year : 2011 Advisor's Signature.....

Co-advisor's Signature.....

Co-advisor's Signature.....

ACKNOWLEDGEMENTS

I would like to express my sincere appreciation and the greatest gratitude to my advisor, Associate Professor Dr. Amorn Petsom and co-advisors, Associate Professor Kunchana Bunyakiat and Dr. Nuttha Thongchul, for intellectual support, encouraging guidance, supervision and enthusiasm throughout the course of this research.

I am also grateful to Professor Dr. Pattarapan Prassassarakich, Associate Professor Dr. Nuanphan Chantarasiri, Associate Professor Dr. Voravee Hoven and Dr. Damrong Sommit for serving as the chairman and members of my thesis committee, respectively, for their valuable suggestions and comments.

Furthermore, I would like to express special thanks to Indonesia Coal Mine Company for their kindness in donating the Indonesian coal used in this research.

I would like to sincerely thank the Faculty of Science, Graduate School, Chulalongkorn University for financial support. Appreciation is also extended to the Program of Petrochemistry, Faculty of Science, Chulalongkorn University and Department of Chemical Technology, Faculty of Science, Chulalongkorn University for providing the experimental facilities.

Gratitude is expressed towards everyone who has contributed suggestions and support throughout this work. Finally, I am very grateful to my family and my good friends whose names are not mentioned here for their love, assistance and encouragement throughout the entire education. Without them, I would have never been able to achieve this goal.

CONTENTS

Page

CHAPTER **Page**

CHAPTER **Page**

CHAPTER **Page**

LIST OF TABLES

LIST OF FIGURES

Figure **Page**

Figure **Page**

LIST OF ABBREVIATION

ASTM	=	american standard test method
c	=	concentration
cm	=	centimetre
cSt	=	centistokes
^{o}C	=	degree Celsius
CFS	=	cardanol-formaldehyde sulfonate
CMC	=	carboxymethyl cellulose
CMW	=	coal-methanol-water fuel
CNSL	=	cashew nut shell liquid
COD	=	coal-oil dispersion
COM	=	coal-oil mixture fuel
COW		coal-oil-water fuel
CWF	=	coal-water fuel
CWO	=	coal-water-oil fuel
CWS	=	coal-water slurry
dl	=	deciliter
DI water	=	deionized water
DTA	=	differential thermal analysis
DVLO	=	Derjaguin–Landua–Verwey–Overbeek
EDL	=	electric double layer
FTIR	=	Fourier transform infrared Spectroscopy
g	=	gram
GPC	=	gas permeation chromatography
Hz	=	hertz
kgf	=	kilogram force
kPa	=	kilogram.Pascal
K	=	Kelvin
m	=	meter
mg	=	milligram
min	=	minute
ml	=	millilitre

mm	=	millimetre
mmHg	=	millimetre of Hg
mPa	=	milliPascal
mV	=	millivolt
m/z	=	mass to charge ratio
MHz	=	megahertz
MSL	=	modified wheat straw alkali lignin
MW	=	molecular weight
NaDDBS	=	sodium dodecyl benzenesulfonate
Na_2SO_3	=	sodium sulfite
NMR	=	nuclear magnetic resonance
N	=	Newton
ppm	=	part per million
psi	=	pound per square inch
PSD	=	particle size distribution
rpm	=	round per minute
SEM	=	scanning transmission electron microscope
SL	=	sodiumlignosulfonate
TEA	=	triethanolamine anacardate
TG	=	thermogravimetric
UV	=	ultraviolet
wt	=	weight
w/w	=	weight by weight
WAL	=	wheat straw alkali lignin
WCF	=	water-coal fuel
μm	=	micron
$[\eta]$	=	intrinsic viscosity
η_{inh}	=	inherent viscosity
η_{red}	=	reduced viscosity
η_{rel}	=	relative viscosity
η_{sp}	=	specific viscosity

CHAPTER 1

INTRODUCTION

1.1 World coal consumption [1]

Coal is a solid fossil fuel which accounts for 25 percent of global energy consumption, significantly less than crude oil (39 percent), but more than natural gas (22%). Coal is cheap, abundant compared to crude oil and natural gas and used mainly in electricity production and in the manufacturing of steel. As prices for crude oil, natural gas and even uranium have risen more than 100% in the last year, coal and coal stocks have not been part of this rally because of environmental problem. China and India account for 70 percent of the projected increase in world coal consumption and much of the increase in their demand for energy, particularly in the industrial and electricity sectors, is expected for coal [2]. As seen in Figure 1.1, the demand for coal continues to surge ahead of recent data put by the World Coal Institute; including clear evidence that the use of coal has risen dramatically, and has outpaced any other fuel. Even more compelling, the use of coal is expected to rise by over 50% over the next fifteen years. Developing countries will be responsible for over 90% of this increase.

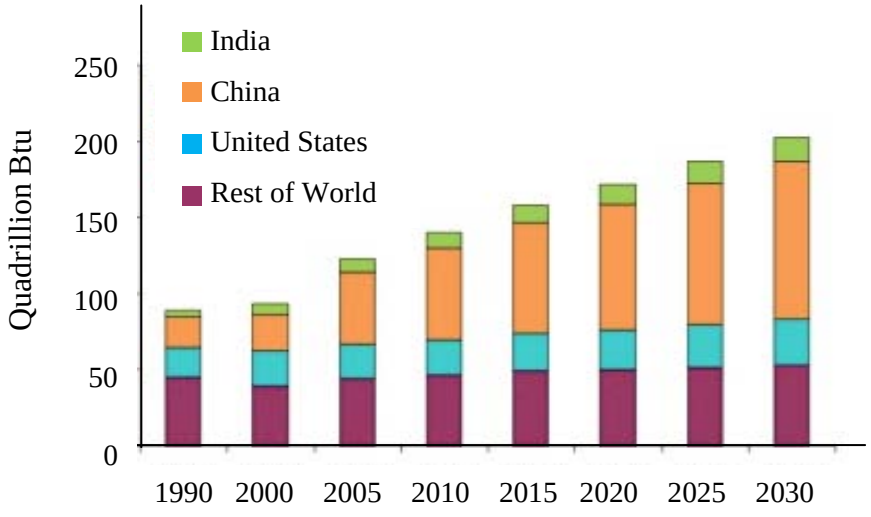

Figure 1.1 World coal consumption between 1990-2030 [2].

Burning coal produces enormous amounts of ash, flue gasses containing pollutants such as sulfur dioxide, nitrogen oxides, sulfuric acids and arsenic, and other greenhouse gas emissions that contribute to global warming. It also produces almost twice as much carbon dioxide. Therefore, clean coal technologies (CCT) is one of the best choices for turning coal into a more energy efficient and lower emission fuel, are being widely developed.

1.2 Clean coal technology [3]

Clean coal technology is one of the technologies being developed with the aim to reduce the environmental impact of coal energy generation. It is possible to make coal a fuel source that is free (or very low) for carbon dioxide emissions and other pollutant emissions. Some of the techniques can be used to accomplish growth-friendly environment, including chemically washing minerals and impurities from the coal, gasification, treating the flue gases with steam to remove sulfur dioxide, carbon capture and storage technologies to capture the carbon dioxide from the flue gas and dewatering lower rank coals (brown coals) to improve the calorific value, and thus the efficiency of the conversion into electricity. Clean coal technology usually addresses atmospheric problems resulting from burning coal. Historically, the primary focus was on sulfur dioxide and particulates, since it is the most important gas in the causation of acid rain. More recent focus has been on carbon dioxide as well as other pollutants due to its impact on global warming.

From the above problems including energy crisis and global warming, coal slurry has received considerable attention nowadays due to many benefits as followed:

- Presence of water in coal-water slurry reduces harmful emissions into the atmosphere and makes the coal explosion-proof. By converting coal into a liquid form, delivery and dispensing of the fuel can be simplified.

- Because of the relatively low cost of coal when compared to other energy sources, coal-water slurry is a very competitive alternative to heating oil and gas.

Depending on geographical area the price per unit energy of coal-water slurry may be 30% to 70% lower than the equivalent oil or gas.

- Low emissions and low BTU (Gcal or MWh) make coal-water slurry as very cost effective and environmental friendly fuel for heat and power generation.

- One side effect of the coal-water slurry making process is the separation of non carbon material mixed in with the coal before treatment. This results in a reduction of ash content to as low as 2% for the treated coal-water slurry, making it a viable alternative to diesel fuel for use in large stationary engines or diesel electric motives.

1.3 Coal-water slurry overview

The fact that coal is a solid causes some challenges; it requires more complex handling than a fluid does, environmental measures must be undertaken to prevent the dispersion of its dust, and a lot of space is required to store it. Utilizing it in a slurry form offers the potential to make the use of coal cleaner, comparable to heavy oil. One type of coal slurry, coal-oil mixture, is prepared by adding heavy oil to coal. This is different than another slurry, coal water slurry, a mixture of coal and water. While coal-oil mixture is convenient for burning and while it was tested before coal-water slurry, it failed to catch on because of the demand for heavy oil for other uses. Coal-water slurry, on the other hand, poses no problems relative to spontaneous combustion or dust dispersion and can be handled as an easy-to-treat liquid. Conventional coal slurry, without additives could be piped but, due to an approximate 50% water content, exhibited poor long-run stability, and required dehydration before firing. High-concentration coal-water slurry can now, as a result of studies on the particle size distribution of coal and the development of a dispersant and other additives, be kept fluid as well as stable even when less water is added, allowing it to be directly combusted without being de-watered. The inclusion of only a small amount of additives stabilizes the coal-water slurry in which coal particles of a certain size distribution are uniformly dispersed, constituting a weight concentration of approximately 50-70% [4,5].

Many nonionic, cationic, and anionic surfactants were tested for potential coal-water slurry. For example, saponin [6], sodium lignosulfonate [7], and various polymers [8], are attractive additives to be used as the dispersant. From the detailed study, coal-water slurry containing 64% wt of coal at 0.8% saponin was stable for a period of as long as 1 month in contrast to 4-5 h in the case of bare coal-water slurry [6]. Sodium lignosulfonates was obtained from a by-product of pulp and paper processes, acted as an effective dispersant for dispersed improvement of coal-water slurry. The higher adsorption amount and compact adsorption film of sodium lignosulfonate with molecular weight ranging from 10,000 to 30,000 and the zeta potential, which is influenced by the sulfonic and carboxyl group contents of the lignosulfonate molecule on coal surface, affect significantly on reducing the viscosity of the coal-water slurry [7]. On the other hand, the anionic polymers (carboxymethyl cellulose, polystyrene sulfonate, and humic acids) and nonionic polymer (hydroxyethyl cellulose, hydroxypropyl cellulose, dextrin) were also used as good dispersants which showed also strong flotation performance. Although the anionic polymers adsorbed less densely on the coal surfaces but they were much stronger coal dispersants since their action was a combination of steric and electrostatic repulsive forces. In contrast, the nonionic cellulose ethers could act only through steric effects [8]. As discussed above, all additives were proved to be used as the dispersant compound providing a beneficial effect on significant reduction of viscosity and perform good rheological behavior.

1.4 Manufacturing process for high-concentration coal-water slurry [4]

High-concentration coal-water slurry can be produced by pulverizing coal into a particle size distribution suitable for coal-water slurry, selecting the correct additives such as a dispersant and a stabilizer, and appropriately blending the coal, water, and additives to manufacture a highly concentrated, low-viscosity, highly stable, and good-quality of coal- water slurry. A diagram of the coal-water slurry process is shown in Figure 1.2.

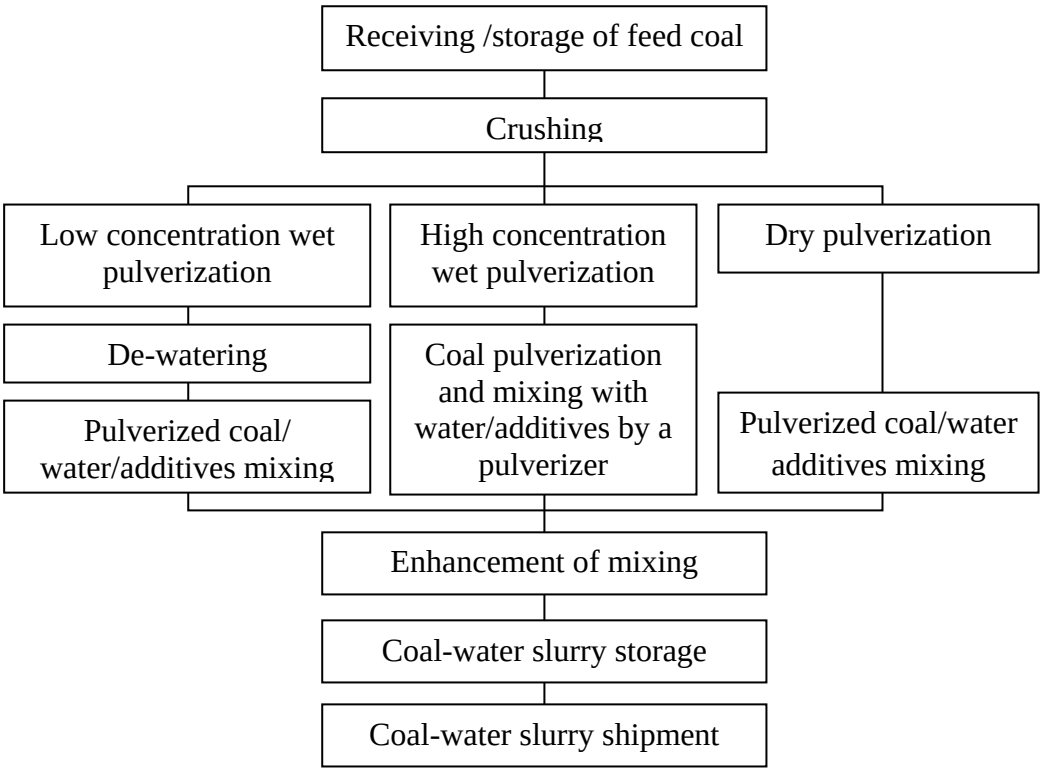

Figure 1.2 Coal-water slurry manufacturing process [4].

The goal of the present study was to develop new anionic dispersants from modified cashew nut shell liquid for the formulation of highly concentrated coal-water slurry. This may result in the decreased use of polymer dispersant obtained from petroleum fuel. Not only coal-water slurry can be developed one of clean coal technology, but the use of green dispersant is also responsive to environmentally friendly world.

In this work, three dispersants were synthesized from cashew nut shell liquid; two carboxylate derivatives as diethanolamine anacardate and triethanolamine anacardate, were obtained from anacadic acid, whereas cardanol-formaldehyde sulfonate was obtained from cardanol. The highly concentrated coal-water slurry was prepared and their properties were investigated in the presence and absence of the synthesized dispersant comparing with a commercial dispersant. Practical aspects regarding the type and amount of dispersant were also evaluated.

1.5 Objectives

The principal objectives of this research were to synthesize anionic dispersants from anacardic acid and cardanol and to investigate the performance of synthesized dispersants blended with the coal-water slurry, which were viscosity, rheological behavior and stability.

1.6 Scope of the research work

1.6.1 To study the preparation of dispersants from carboxylate derivatives of cardanol and anacardic acids, which are the main phenolic components of cashew nut shell oil.

- Two anacardate salts were prepared by the neutralization reaction of anacardic acid with diethanolamine and triethanolamine.
- The cardanol-formaldehyde sulfonate was prepared by sulfomethylation reaction.

1.6.2 To study the parameters on the synthesis of cardanol-formaldehyde sulfonate as followed;

- The ratio of raw materials such as sulfonating agent and formaldehyde
- The reaction time
- The reaction temperature

1.6.3 To characterize the physical properties of dispersants such as IR, NMR, and surface tension, etc.

1.6.4 To study the fundamental properties of coal such as proximate analysis (ASTM D 3172-3175) and ultimate analysis (ASTM D 3177-89).

1.6.5 To study the preparation of highly concentrated coal water slurry.

1.6.6 To study the effect of the factors that influences on the viscosity and the rheological property of coal-water slurry as followed;

- Effect of coal concentration: 30-60 wt%
- Effect of particle size of powdered coal: -45 to 200 microns.
- Effect of dispersant concentration: 0.2-2.0 wt%

- Effect of temperature range of 25-60^{o}C

1.6.7 To study the zeta potential of coal particles in aqueous solution at the variation of pHs and dispersant concentrations.

1.6.8 To study the stability of coal-water slurry by glass rod penetration method.

1.6.9 To study the suspension phenomena of synthesized dispersant and flocculated behavior of coal in presence and absence of dispersant using SEM observation.

1.6.10 To study the combustion phenomena by Thermal analysis (Thermogravimetry analysis).

CHAPTER 2

THEORY AND LITERATURE REVIEW

This chapter presents the chemical structure and physic properties of natural raw materials that are modified by a chemical process to give dispersants employed for clean coal technology, coal-water slurry. The basic properties of surfactant are also described. In addition, the theory of fundamental rheological properties of viscoelastic materials including the applicable flow models for fluids, are presented. The important purpose of the development of a novel dispersant for coal-water slurry is to respond to the energy crisis and the failing environment, is also discussed in detail.

2.1 Cashew Tree [9]

The cashew is a tree in the family *Anacardiaceae*. It is now widely grown in tropical climates for its cashew nuts and cashew apples. The main commercial product of the cashew tree is the nut. In the main producing areas of East Africa and India, 95% or more of the apple crop is not eaten, as the taste is not popular.

Figure 2.1 Cashew fruit [9].

The true fruit of the cashew tree is a kidney or boxing-glove shaped drupe that grows at the end of the cashew apple. The drupe develops first on the tree, and then the pedicel expands into the cashew apple. Within the true fruit is a single seed, the cashew nut. The seed is surrounded by a double shell containing an allergenic

phenolic resin, anacardic acid, a potent skin irritant chemically related to the more well known allergenic oil which is also a toxin found in the related poison ivy.

2.1.1 Cashew nut processing

In the cashew composition, the shell of the nut is leathery, not brittle. It contains the thick vesicant oil, cashew nut shell liquid, within a sponge-like interior. The primary products of cashew nuts are the kernels which have value as confectionery nuts. Cashew nut shell liquid (CNSL) is an important industrial raw material for resin manufacture and the shells can be burned to provide heat for the decorticating operation.

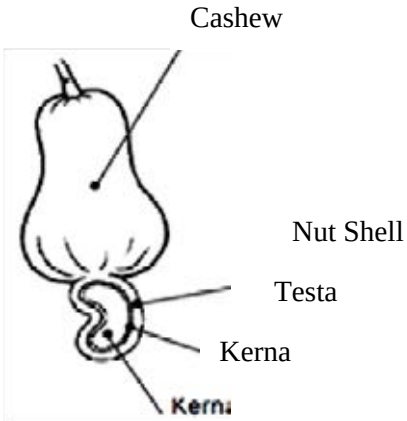

Figure 2.2 Cross-section of cashew fruit [9].

2.1.2 Processing overview [10]

Traditionally, extraction of the kernel from the shell of the cashew nut has been a manual operation. The nut is roasted which makes the shell brittle and loosens the kernel from the inside of the shell. By soaking the nuts in water, the moisture content of the kernel is raised, reducing the risk of it being scorched during roasting and making it more flexible so it is less likely to crack. The cashew nut shell liquid is released when the nuts are roasted. Its value makes collection in sufficient quantities economically advantageous. However, for very small-scale processors, this stage is unlikely to take place due to the high cost of the special roasting equipment required for the cashew nut shell liquid collection. The shell can be cracked either manually, using a hammer, or mechanically. Manually operated blade openers are relatively

inexpensive, however the more successful mechanical methods depend on the nuts having passed through the ‘hot oil’ cashew nut shell liquid extraction operation. Care must be taken not to break or split the kernel at this or subsequent stages as whole kernels are more valuable than broken ones. Once the kernel is removed from the shell, it is dried, the testa is peeled off and the kernel is graded. Figure 2.3 gives an overview of cashew nut processing and the various choices in methods.

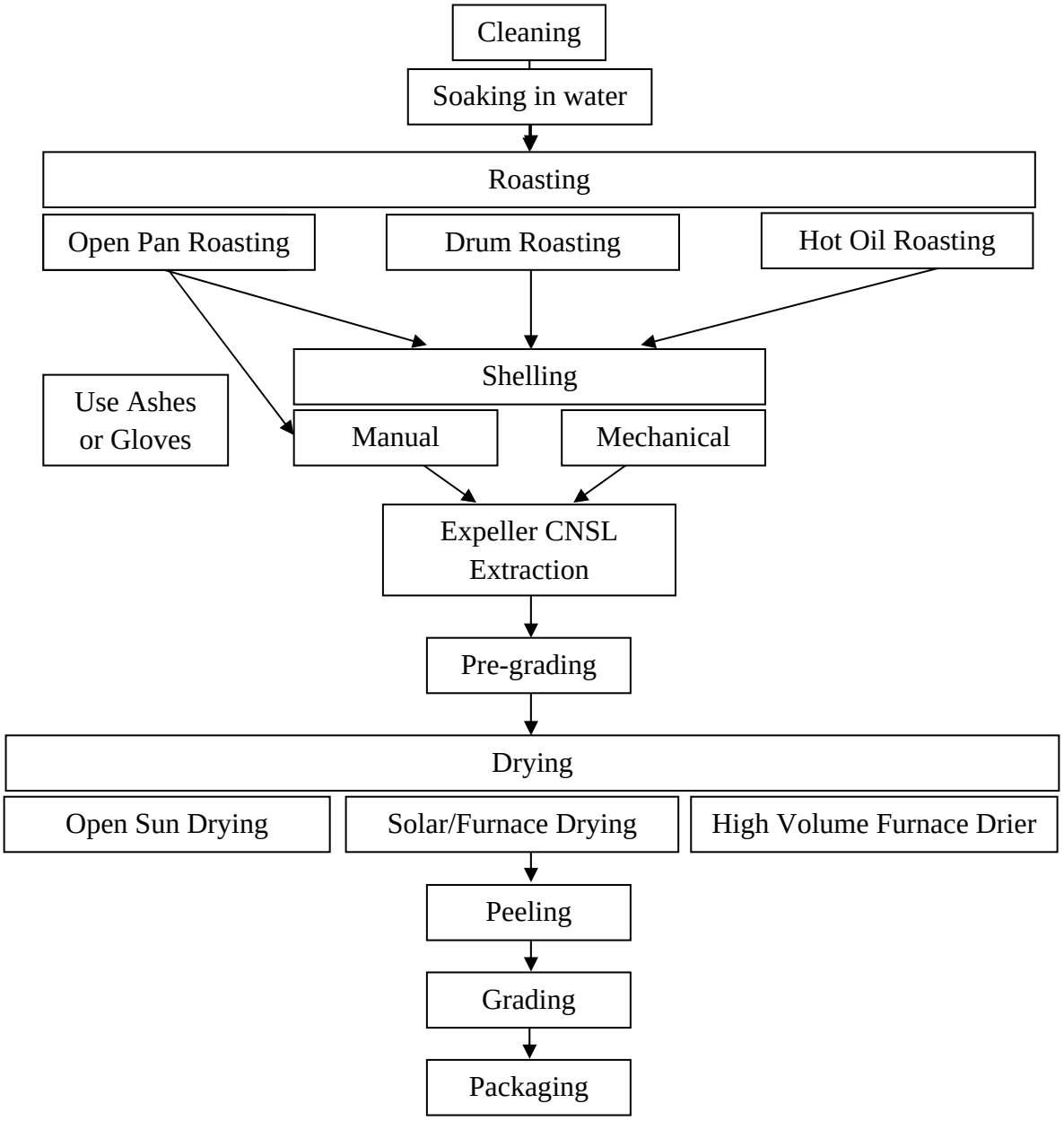

Figure 2.3 Overview of cashew nut processing [11].

2.2 Cashew nut shell liquid

Cashew nut shell liquid is a mixture of four substituted phenols as anacardic acid, cardanol, cardol and 2-methyl cardol.

2.2.1 Cashew nut shell liquid structure

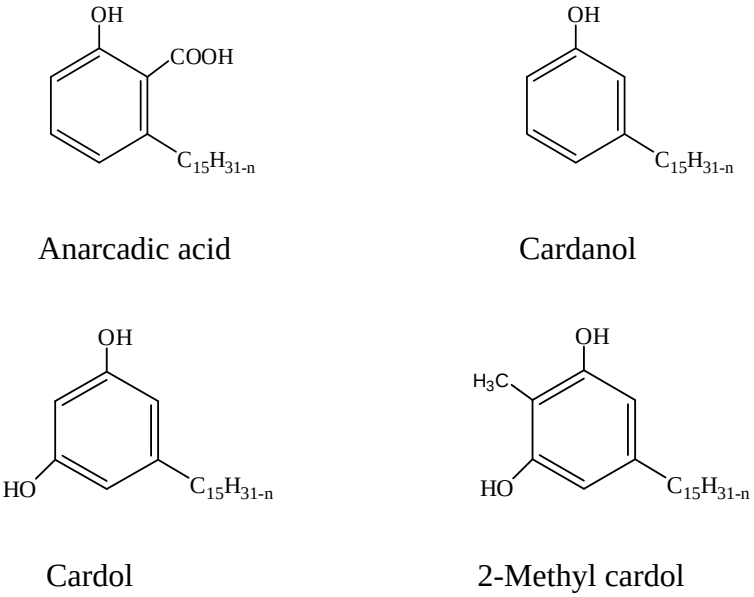

Figure 2.4 Structures of cashew nut shell liquid constituents [12].

The first two are monohydric phenols whereas the other two are dihydric phenols. In the nut, cashew nut shell liquid occurs mainly as anacardic acid (~90%) and cardol around slightly lower than 10%. During the hot-oil bath process for extraction of cashew nut shell liquid, anacardic acid is decarboxylated to cardanol. Therefore, in the technical grade cashew nut shell liquid, the main components will be cardanol and cardol and some polymerized cashew nut shell liquid.

Cashew nut shell liquid can be extracted by the expeller method but the oil has to be heated after extraction to convert anacardic acid to cardanol. The expelled and heated cashew nut shell liquid will have less amount of polymerized cashew nut shell liquid. However, if there is a requirement for pure monomers, the best source will be solvent extracted cashew nut shell liquid. Each component again is a mixture of four structurally related monomers, the difference being only in the degree of unsaturation.

Thus, cardanol is a mixture of a four components; saturated (~5%), monoene (~49%), diene (l6.8%) and triene (29.3%). Thus, cashew nut shell liquid contains a total of 16 components, which makes it a complicated system [12-14].

2.2.2 Cashew nut shell liquid application

Cashew nut shell liquid undergoes all the conventional reactions of phenols, cashew nut shell liquid-aldehyde condensation products and cashew nut shell liquid based phenolic resins [13] are used in applications such as surface coatings, adhesives. Various polyamines synthesized from cashew nut shell liquid are used as curing agents for epoxy resins. Cashew nut shell liquid and its derivatives have been used as antioxidants, plasticizers, demulsifying agents for water in oil type petroleum, processing aids for rubber compounds, modifiers for plastic materials, and used to provide oxidative resistance sulfur-cured natural rubber products. It is also added to rubber gum stock or nitrile rubber to improve the processability, mechanical properties and resistance to crack and cut properties of the vulcanization. Further, soluble metal derivatives of cashew nut shell liquid are used to improve the resistance to oxidation and sludge formation of lubricating oils [15-17].

2.3 Cardanol

Cardanol is a naturally occuring phenol manufactured from cashew nut shell liquid. It is a monohydroxyl phenol having a long hydrocarbon chain ($C_{15}H_{27}$) in the meta position. The products obtained from cardanol have many advantages over these manufactured from other substituted phenols. It is therefore widely used in the manufacture of surface coatings, insulating varnishes, oil and alcohol soluble resins, laminating resins, rubber compounding, azo dyes, etc.

2.3.1 Cardanol structure

The components of commercial cardanol differ in the degree of unsaturation of the side chain but for the practical purposes it can be represented by the following formula.

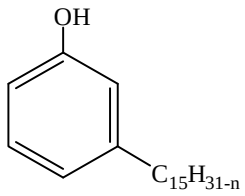

Figure 2.5 The chemical structure of cardanol [18].

The average unsaturation of about two double bonds in the side chain of the cardanol molecules make cross linking easy and give a satisfactory gradual drying and baking properties to paints prepared from it. Because of its peculiar structure, cardanol varnishes have high electric insulation, greater resistance to water chemicals and good flexibility. The long hydrocarbon side chain imparts to cardanol aldehyde condensate greater solubility in drying oils such as linseed DCO, or tung oil and aliphatic hydrocarbons. Cardanol can be substituted by 30% in phenolic resins used for phenol bonded resins for plywood and lamination industries.

2.3.2 Specification for cardanol

Cardanol is obtained from the distillation of commercial cashew nut shell liquid under reduced pressure (1mm of Hg) approximately 225 ^{o}C, gives a pale yellow

to brown liquid with refractive index 1.5 at 30 ^{o}C. Since cardanol is a phenol which has a C-15 unsaturated alkyl chain with 1-3 double bonds at m-position so cardanol has a tendency to oxidise and acquire colour on exposure to light and air depending upon the time of storage.

Table 2.1 Cardanol specification [19]

Particulars	Normal grade
Structural formula	$OHC_6H_4C_{15}H_{27}$
Density	0.9272-0.9350
Viscosity at 30°C	55.65 cp
Melting point (Less than)	50°C
Volatiles maximum	1%
Ash contents	negligible
Iodine value (Catalytic method)	min 250
Acid value	max 5
Hydroxyl value	180-190
Color gardener (Freshly distilled)	light brown
Moisture	1% V/V

2.3.3 Extraction of isolation cardanol from cashew nut shell liquid

Paramshivappa et al. [20] reported an efficient method for the separation of mono- and diphenolic components from technical cashew nut shell liquid. Cashew nut shell liquid was dissolved in a mixture of methanol and ammonium hydroxide (8:5) and extracted with hexane to obtain cardanol. The resultant methanolic ammonia layer was extracted with a mixture of ethyl acetate and hexane to yield cardol. cardol. This is the first industrially feasible process based on solvent extractions for the isolation of cardanol from technical cashew nut shell liquid.

Devi et al. [21] described the separation of cashew (*Anacardium occidentale* L.) nut shell liquid components (anacardic acid, cardol, and cardanol) for industrial application. Anacardic acid was selectively isolated as calcium anacardate. The acid-free cashew nut shell liquid was treated with liquor ammonia and extracted with

hexane/ethyl acetate (98:2) to separate the mono phenolic component, cardanol. Subsequently, ammonia solution was extracted with ethyl acetate/hexane (80:20) to obtain cardol.

2.3.4 Applications of cardanol

The average unsaturation of about two double bonds in the side chain of the cardanol molecules make cross linking easy and give a satisfactory gradual drying and baking properties to paints prepared from it. Because of its peculiar structure cardanol varnishes have high electric insulation, greater resistance to water chemicals and good flexibility. The long hydrocarbon side chain imparts to cardanol aldehyde condensate greater solubility in drying oils such as linseed, or tung oil and aliphatic hydrocarbons. Cardanol can be substituted by 30% in phenolic resins used for phenol bonded resins for plywood and lamination industries. On the other hand, water soluble phenol-cardanol-formaldehyde resin is developed by substituting 30% cardanol in phenolic resins [22]. The resins will give additional property of antifungus and antithermic when used in plywood industries. In lamination industries it gives additional advantage in non-edge cracking and also cost saving.

2.4 Surfactant

A surfactant is an amphiphilic (amphipathic) molecule that has a hydrophilic head group (polar region), which has a high affinity for water, and a lipophilic tail group (non-polar region), which has a high affinity for oil. A surfactant work reduces surface tension of a liquid and increase the contact between the liquid and another substance. Surface acting agent refer to the fact that a surfactant interacts with the surface of a liquid to change its properties through the adsorption process. They accrete on the surface of a liquid creating a film which reduces its surface tension.

2.4.1 Functional properties

The dual character of a surfactant is responsible for the phenomenon of surface activity and spontaneous aggregation in solution. As a class, association colloids indicate their tendency to aggregate spontaneously in solution to form a variety of thermodynamically stable structures (e.g. micelles, bi-layers, vesicles, and reverse micelles). These structures are adopted because they minimize the unfavorable contact area between the non-polar tails of the surfactant molecules and water. For example, surfactant monomers are amphiphilic and have a high level of surface activity, whereas micelles have little surface activity. Consequently, the interfacial tension decreases when surfactants are monomers, whereas it remains fairly constant in the presence of micelles [23,24].

A surfactant forms micelles or reverse micelles in a solution when its concentration exceeds some critical level, known as the critical micelle concentration (CMC). Below the CMC, the surfactant molecules are dispersed, predominantly as monomers, but once the CMC is exceeded, any additional surfactant molecules form micelles, and the monomer concentration remains fairly constant. When surfactant is added to a solution above the CMC, the number of micelles, rather than the size or shape of the individual micelles, tends to increase [25].

2.4.2 Surfactant classification [26]

Surfactants can be classified according to their physical properties or functionalities. The following is the common classification and is based on the nature of the hydrophilic group.

2.4.2.1 Anionic

Anionics are used mainly in detergent formulations and alkyl and alkylarye chains in the C12–C18 range obtain the best detergency. The counterions most frequently used are sodium, potassium, ammonium, calcium and various protonated alkyl amines. Sodium and potassium impart water solubility, whereas calcium and magnesium promote oil solubility. Amine/alkanol amine gives both oil and water solubility. Soap is still the largest single type of surfactant. Sodium dodecyl sulfate (SDS) with the formula $CH_3(CH_2)_{11}OSO_3Na$, is by far the most important surfactant within this type [27].

2.4.2.2 Cationic

The majority of cationic surfactants are based on the nitrogen atom carrying the cationic charge. Both amine and quaternary ammonium-based products are common [28]. The amines only function as a surfactant in the protonated state, therefore, they cannot be used as high pH. Quaternary ammonium compounds are not pH sensitive. Non-quaternary cations are also much more sensitive to polyvalent anions.

2.4.2.3 Nonionic

Nonionic surfactants do not have any surface charge and have either a polyether or a polyhydroxyl unit as the non-polar group. In the vast of non-ionics, the polar group is a polyether consisting of oxyethylene unites, prepared by the polymerization of ethylene oxide [28]. The classic number of oxyethylene unites in the polar chain is five to ten, although some surfactants, e,g. dispersants, often have much longer oxyethylene chains.

2.4.2.4 Zwitterionic

Zwitterionic surfactants have two charged groups of different size such as 2-(trimethylamino)ethane-1-sulfonate ($(CH_3)_3N^+CH_2CH_2SO_3^-$), 2(trimethylamino) ethylmethylphosphate ($(CH_3)_3N^+CH_2CH_2OP(O)_2^-OCH_3$) [29]. While the positive charge is almost in availably ammonium, the source of negative charge may vary, although carboxylate is by far the most common. An amorphic surfactant is one that changes from net cationic via zwitterionics to net anionic on going from low to high pH. All these properties strongly depend on the solution pH.

2.4.3 Emulsion process [26]

An emulsion is a mixture of two immiscible liquids, one of which is dispersed in the continuous phase of the other, typically created by rupturing droplets down to colloidal sizes through mixing. To inhibit recombination or coalescence, a surfactant, which is concentrated at the interfaces must be added to create short-ranged interfacial repulsion between the droplets. For an appropriate surfactant, a quantity much less than the mass of the liquids is often sufficient to make this interfacial repulsion strong enough to render the emulsion kinetically stable against coalescence and de-mixing. The process of converting two separate immiscible liquids into an emulsion, or reducing the size of the droplets in a pre-existing emulsion, that are kinetically stable (metastable), could be provided by the addition of emulsifiers and/or thickening agents prior homoginization.

The structure of an emulsion explosive is directly relevant to its rheology, stability and detonation properties. To serve as a complete description of emulsions, a theory must be able to explain all aspects of emulsion formation, stability, the influence of environmental factors such as temperature and pressure, the role of emulsifiers, stabilizers, the chemical structures of the immiscible phases, and the effects of additives. An emulsion or metastable system tends to revert back to the thermodynamically most stable state of the system, which consist of a layer of oil on top of a layer of water.

2.5 Coal clean energy

The massive use of coal has significantly promoted the progress of human civilization and industrial development in early days, however, the pollutants generated by coal burning and the emission of green house gases have also affected air pollution and climate change. People are striving to find other relatively clean energy to replace or at the least partially substitute coal that currently plays the primary role in energy.

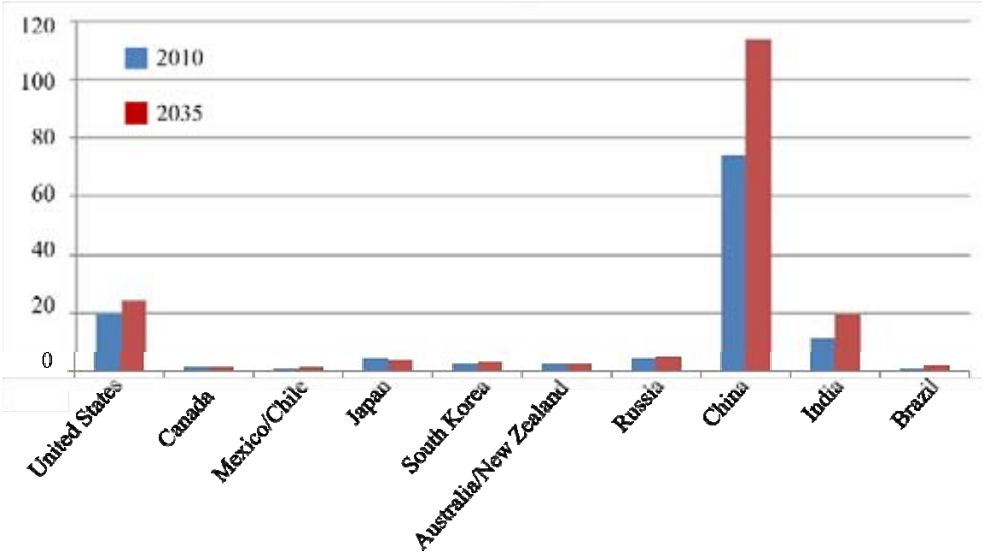

Figure 2.6 World coal consumption by country 2010 and 2035 [30].

Currently in China, 60% of the energy comes from coal, and over 70% of the power supply is generated by coal burning [30]. However, for the United States that uses less coal, proven coal reserves are sufficient to last 250 years without the use of other energy. Its energy consumption has been fueled by the burgeoning economic growth over the past two decades. Therefore, how to utilize coal resources in a cleaner manner are the common topic different countries have when facing the current and future problems in relation to resource situation. The fact that coal is a solid causes some challenges; it requires more complex handling than a fluid does, environmental measures must be undertaken to prevent the dispersion of its dust, and a lot of space is required to store it. Utilizing it in a slurry form offers the potential to make the use of coal cleaner, comparable to heavy oil.

2.5.1 Coal slurry [31]

Coal slurry fuel consists of finely ground coal dispersed into one or more liquids such as water, oil, or methanol. Slurry fuels have the advantages of being convenient to handle (similar to heavy fuel oil) as liquid fuel and processing high energy density, as illustrated in Table 2.2. It have been investigated as potentially efficient replacement for oil in boilers and furnaces, fuel in internal combustion engines, and recently energy feedstock for cofiring of coal fines in utility boilers. Nowadays, coal slurry is used around the world in countries such as the U.S., Russia, Japan, China, and Italy. Indeed, coal slurry fuels have been investigated since the 19th century, but economic constraints have kept it from becoming a major energy source. Typically, interest in coal slurry develops whenever regional or short-term oil availability is in doubt, such as periods during both world wars and again in the energy crises of 1973 and 1979. Much of the work during these time periods was focused on coal-oil fuels, which could quickly and readily replace oil or liquid fuel in furnaces and boilers. However, recent research, since 1980, has concentrated more on coal water slurry (CWS) for the complete replacement of oil in industrial steam boilers, utility boilers, blast furnaces, process kilns, and diesel engines.

Table 2.2 Fuel energy densities [32]

Fuel	Density (lb/gal)	Btu/lb	Btu/gal
Coal in bulk	6.2-9.4	12,500	76,000-116,500
Residue oil	8.2	18,263	150,000
Mixture of coal (60%) and water (40%)	9.8	8,000	78,700
Mixture of coal (70%) and water (30%)	10.2	9,373	95,600

2.5.2 Types of coal slurry fuel

Coal-slurry mixtures can be made from a combination of various liquids and coal, the most common liquid ingredients being oil, water, and methanol

2.5.2.1 Coal-oil mixture fuel (COM)

Coal-oil means any mixture of finely divided solid hydrocarbon, such as coal, lignite, oil shale, and torbanite, suspended in any hydrocarbons that are liquid or semi-liquid at ordinary atmospheric temperatures, such as petroleum fractions and heavy residues, tars, or oils from the carbonization of the solid hydrocarbons as well as their heavy residues, and the heavier fractions of the mixed oils and tars resulting from the particular process. COM, a suspension of coal on fuel oil, may contain up to 10% by weight of water that sometimes COM are referred to as coal-oil dispersion (COD) [33].

2.5.2.2 Coal-oil-water fuel (COW) and coal-water-oil fuel (CWO)

COW and CWO are the suspension of coal in fuel oil and in water of 10% or more. Depend on the type of fuel and application, therefore oil is the main ingredient in COW and water in COW.

2.5.2.3 Coal-water fuel (CWF) or water-coal fuel (WCF)

CWF consists of fine-dispersive mixture of powdered coal, water and (sometimes) plasticizer. In general, the ratio of coal and water is in the range of 58%-70% and 29%-40%, respectively, in the presence of less 1% additives [34].

2.5.2.4 Coal-Methanol-water fuel (CMW)

CMW is a suspension of coal in methanol and water [35].

The CMF and CMW slurries possess favorable properties; however, the cost of methanol has all but eliminated them from further development. COM, once actively investigated, has now been shelved for economic reasons. CWF has been

investigated for complete oil replacement in boilers and furnaces and internal combustion engines, but low oil prices in the past decades have reduced the economic advantage and somewhat cooled the interest. However, CWF developed from waste streams and tailings were being investigated for co-firing in boilers and furnaces. The comparative economics of coal-water slurry against the conventional fuel in the 21st century is undoubtedly far more favorable. Furthermore, CWF provides a valuable mode of coal transportation through a long pipeline. Important slurry characteristics are stability, pumping, atomization, and combustion characteristics. These properties control the hydrodynamics and rheology of the coal slurry system. Coal slurry must have low viscosity at pumping shear rates (10-200 s^{-1}) and at atomization shear rates (5,000-30,000 s^{-1}) [36]. This allows for low pumping power requirements and increased boiler and furnace efficiencies through smaller droplets sizes. There are several types of pumps that are developed for coal slurry pumping. In order to understand coal slurry hydrodynamics and rheology, an understanding of dispersed systems is required. Solid-liquid dispersed systems are classified into two, based on their particle sizes, namely, colloidal and coarse-particle systems. Colloidal dispersed systems consist of particles smaller than 1 μm and coarse particle dispersion systems (suspension) consist of particles larger than 1 μm. In colloidal dispersion systems, sedimentation is prevented by Brownian motion (thermal activity). However, suspensions are thermodynamically unstable and will tend to precipitate owing to the overwhelming gravitational force on large-size particles [37].

2.5.3 Particle size distribution

Typical coal slurry fuels have a particle size distribution (PSD) with 10–80% of the particles smaller than 74 μm (-200 mesh). The sizing of coal is a multistep process consisting of coal crushing, pulverization, and finishing steps. The finishing processes can be carried out by wet or dry grinding. They reduce the particle size to <1 mm for coarse, <250 μm for fine, and <44 μm for ultrafine grinding. In slurry preparation, wet grinding is often used to minimize oxidation of the coal, which is normally detrimental to many beneficiation or treatment processes. Coal slurries are most economical when they have the maximum amount of coal (i.e., highest solid

loading) at the lowest possible viscosity. To obtain the highest possible loading, a bimodal or multimodal PSD is utilized, as shown in Figure 2.7. Finer coal particles fit into the interstices of the larger coal particles, forming a higher concentrated network of particles. These particles may also act as a lubricant, leading to a lower viscosity [32].

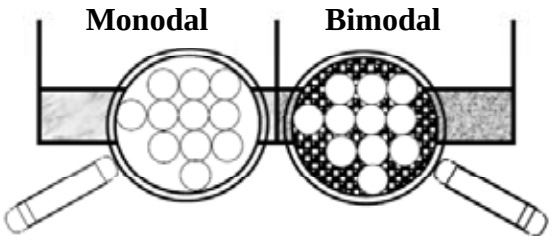

Figure 2.7 Particle size distribution for unimodal and bimodal distributions [32].

An unimodal slurry has a peak solid loading of ~65% at which time the viscosity becomes infinite. Multimodal systems are commonly used, because they can easily be generated by a common grinding and the obtained minimum viscosity with a typical multimodal distribution formulation. The settling of coal particles is a complex phenomenon from a theoretical point of view, involving hydrodynamic and physiochemical forces. The falling movement of fine coal in slurries has a Reynolds number (Re) <<1, which leads to the use of *Stokes' equation* for hindered settling rate as shown in equation 2.1 and 2.2 [36].

$$v = \frac{d^2 g(\rho_1 - \rho_2)}{18\mu} f(\emptyset) \qquad 2.1$$

$$f(\emptyset) = \frac{v}{v_t} \leq 1 \qquad 2.2$$

Where v is hindered settling rate, v_t is single-particle settling velocity and μ is viscosity of dispersing medium. For ρ_1 and ρ_2 are densities of dispersed and dispersing mediums, respectively. Otherwise, d is diameter of dispersed particles, g is gravitational acceleration, $f(\emptyset)$ is a function of volume fraction of suspended solids.

Stokes' law suggests that to reduce the sedimentation velocity, the particle diameter should be reduced, the viscosity of the dispersing medium should be

increased, and the difference in density between the solid and the liquid phase should be decreased. However, optimal slurry processing demands high loading at low viscosity for transportation and atomization requirements. Therefore, low viscosity slurry inherently promotes the sedimentation of the fines. To alleviate this obvious difference in the property requirements of the resultant slurry, various additives and surfactants have been developed.

2.5.4 Rheology

Rheology is the study of a system's response to a mechanical perturbation in terms of elastic deformations and viscous flow. In most rheological systems, elastic response is associated with solids, whereas viscous response is associated with liquids. Therefore, a suspension system such as coal slurry exhibits behaviors of both elastic and viscous responses. These responses in coal slurry are a function of the type of coal, coal concentration, PSD, properties of dispersing phase, and additive package.

2.5.5 Viscosity

Viscosity is the measure of the internal friction of a fluid. This friction becomes apparent when a layer of fluid is made to move relatively to another layer. The greater the friction the greater the amount of force required to cause this movement which is called shear. Shearing occurs whenever the fluid is physically moved by pouring, spreading, spraying, mixing, etc. High viscous liquids require more force to move than less viscous liquids. If we have two parallel planes of fluid of equal area A and they are separated by a distance dx and are moving in the same direction at different velocities v_1 and v_2. The force required to maintain this difference in velocities is proportional to the difference in speed through the liquid, or the velocity gradient:

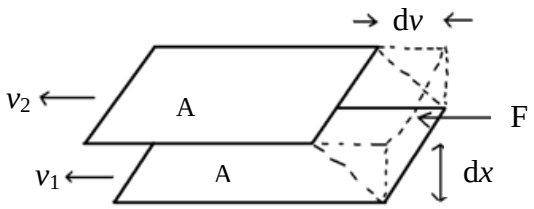

Figure 2.8 Fluid flow model [37].

The velocity gradient, d*v*/d*x*, is a measure of the speed at which the intermediate layers move with respect to each other. It describes the shearing the liquid experiences and is called shear rate and its unit of measure is called reciprocal second (sec^{-1}).

The term F/A indicates the force per unit is required to produce the shearing action and it is called shear stress, *S* and its unit is Nm^{-2}. Therefore, viscosity can be defined as:

$$viscosity = \frac{shear\ stress,S}{shear\ rate,R} \qquad 2.3$$

The fundamental unit of viscosity is the poise. A material requiring a shear stress of one dyne per square centimeter to produce a shear rate of s^{-1} has a viscosity of a poise or 100 centipoise (cP). One pascal-second, Pa.s equals 10 poises [37].

2.5.6 Flow Behavior [38]

2.5.6.1 Newtonian fluids

All gases and fluids such as air, water, ethanol, and benzene are Newtonian. This means that a plot of shear stress versus shear rate at a given temperature is a straight line with a constant slope that is independent of the shear rate. Also, low molecular weight liquids, and solutions of low molecular weight substances in liquids are usually Newtonian.

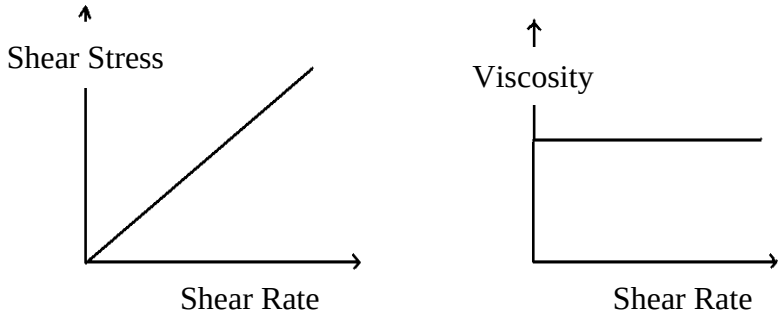

Figure 2.9 Flow diagrams of Newtonian fluid [36].

The behavior of Newtonian liquids in experiments conducted at constant temperature and pressure has the following features:

1. The only stress generated in simple shear flow is the shear stress, the two normal stress differences are zero.
2. The shear viscosity doesn't vary with shear rate.
3. The viscosity is constant with respect to the time of shearing and the stress in liquid falls to zero immediately the shearing is stopped.
4. The viscosities measured in different types of deformation are always in simple proportion to one another.

Any fluid that does not obey the Newtonian relationship between the shear stress and shear rate is called non-Newtonian. High molecular weight liquids, which include polymer melts and solutions of polymers, as well as liquids in which fine particles are suspended (slurries and pastes), are usually non-Newtonian.

2.5.6.2 Non-newtonian fluids [39]

Regarding its flow behavior, a non-Newtonian fluid is one whose flow curve shows an apparent viscosity, shear stress divided by shear rate, which is shear rate and, sometimes, shear time dependent. Accordingly, such materials may be conveniently grouped as follows:

2.5.6.2.1 Non-Newtonian fluids (Time independent)

Fluids for which the rate of shear at any point is determined only by the value of the shear stress at that point at any instant; these fluids are known as time independent, equilibrium behavior", "purely viscous" or "inelastic" fluids.

Coal slurries, in general, exhibit non-Newtonian behavior which the slope of the shear stress versus shear rate curve will not be constant with changing the shear rate. Further, the viscosity of non-Newtonian fluids also changes as the shear rate is varied. Thus, the parameters of viscometer model, spindle and rotational speed al have an effect on the measured viscosity. This measured viscosity is called apparent viscosity and is accurate when explicit experimental parameters are adhered to. There are several types of non-Newtonian flow behavior, characterized by the way a fluid's viscosity changes in response to variations in shear rate [40,41].

2.5.6.2.2 Pseudoplastic

Pseudoplastic fluid encompasses most non-Newtonian fluids. In these fluids the shear stress is increasing proportionally and the viscosity decreasing by growth of the shear rate (gradient of speed). This group practically includes all dispersion systems (e.g. suspensions of particles in water). Some examples include paints and emulsions. This type of behavior is called shear-thinning.

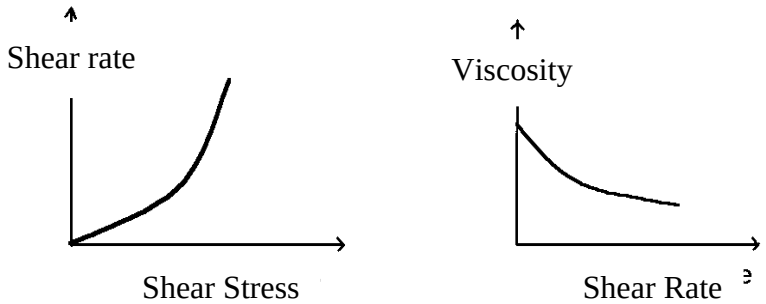

Figure 2.10 Flow diagrams of pseudoplastic fluid (shear-thinning) [40].

The relationship between the shear stress τ and shear rate $\dot{\theta}$ as follows.

$$\tau = \eta\dot{\theta} \qquad 2.3$$

Here, η is called the “apparent viscosity” of the fluid, and is a function of the shear rate. In the above example, a plot of η as a function of the shear rate also is shown in Fig. 2.10.

Many shear-thinning fluids will exhibit newtonian behavior at extreme shear rates, both low and high. For such fluids, when ln (apparent viscosity) is plotted against ln (shear rate) as shown in Fig. 2.11.

The regions where the apparent viscosity is approximately constant are known as Newtonian regions. The behavior between these regions can usually be approximated by a straight line on these axes.

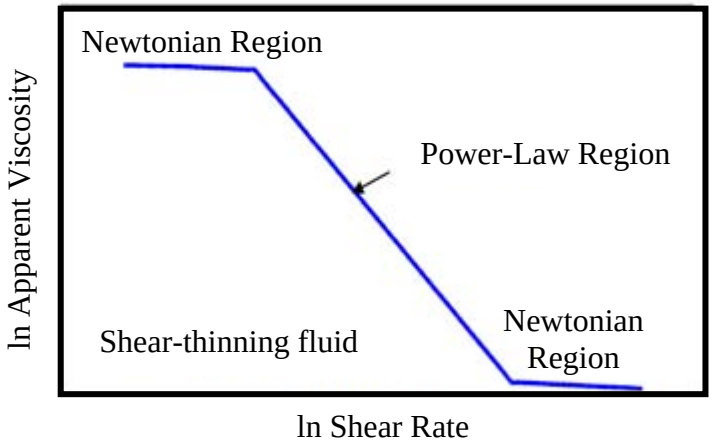

Figure 2.11 Rheogram of shear-thinning fluid [40].

It is known as the power-law region. In this region, we can evaluate the behavior by

$$ln\ \eta = a + b\ ln\ \dot{\theta} \qquad 2.4$$

which can be rewritten as

$$\eta = K\dot{\theta}^{b} \quad 2.5$$

where K = exp(a). Instead of b we commonly use (n-1) for the exponent and write a result for the apparent viscosity as follows

$$\eta = K\dot{\theta}^{n-1} \quad 2.6$$

Upon using the connection among the shear stress, apparent viscosity, and the shear rate we get the power-law model.

$$\tau = K\dot{\theta}^{n} \quad 2.7$$

where n is called the power-law index. Note that n = 1 corresponds to Newtonian behavior. Typically, for shear thinning fluids, n lies between $^1/_3$ and $^1/_2$, even though other values are possible.

2.4.8.2.1.2 Dilatant

Dilatant fluids is characterized by the increasing shear stress and viscosity superproportionally with the growth of shear rates. Some examples of shear-thickening fluids are corn starch in water, clay slurries, sand/water mixtures and solutions of certain surfactants. Dilatancy is also referred to as shear- thickening liquids. Most shear-thickening fluids tend to show shear-thinning at very low shear rates.

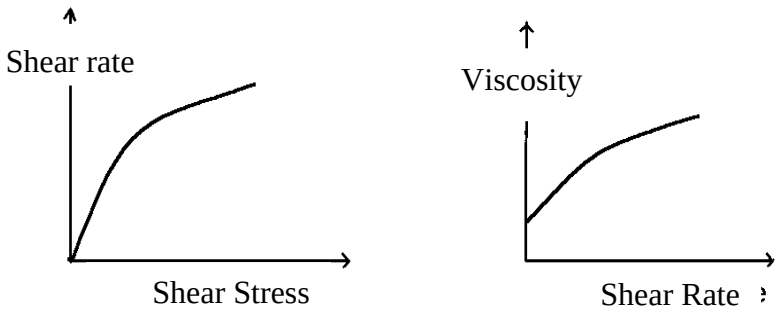

Figure 2.12 Flow diagrams of dilatant fluid (shear-thickening) [40].

2.4.8.2.1.3 Bingham

The fluid behaves like solid under static conditions. A certain amount of force must be applied to the fluid before any flow is induced. The shear stress must exceed a critical value known as the yield stress, τ_0, for the fluid to flow. Plastic fluids start to yield only at a certain characteristic minimum yield stress. The viscoplastic fluid behaves like solids when the applied shear stress is less than the yield stress. Once it exceeds the yield stress, the viscoplastic fluid will flow just like an ordinary fluid. If the shear stress, $\tau > \tau_0$ linearly increases in dependence on the shear rate called the Bingham fluid [39].

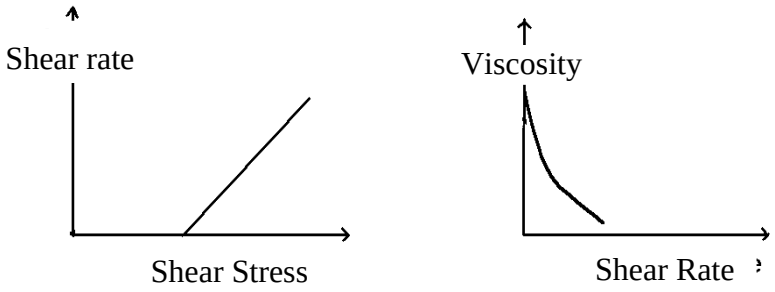

Figure 2.13 Flow diagrams of Bingham fluid.

While the dilute and more concentrated suspensions of mineral particles in water behave like pseudoplastic (shear thinning) non-newtonian fluids, the highly concentrated suspensions (paste) exhibit nearly such properties as the Bingham fluids. Once the yield value is exceeded and flow begins, plastic fluids may display newtonian, pseudoplastic or dilatant flow characteristics.

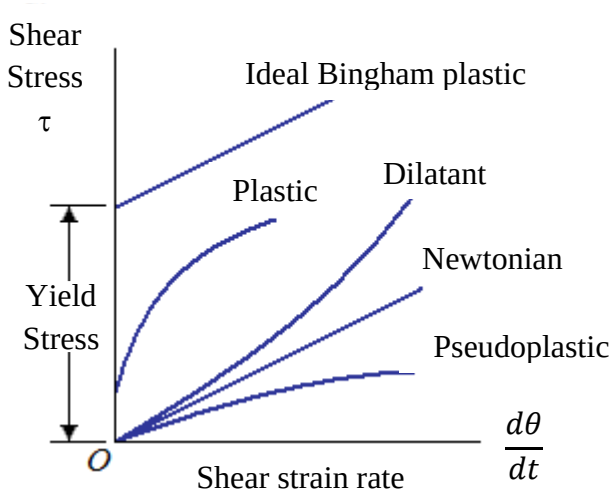

Figure 2.14 Diagram summary of non-Newtonian fluids [40].

2.4.8.2.2 Non-Newtonian fluids (Time dependent)

Some fluids exhibit a change in viscosity with time under conditions of constant shear rate.

2.4.8.2.2.1 Thixotropic

The fluid undergoes a decrease in viscosity with time, while it is subjected to constant shearing (greases). Further, a fluid that thins out with time and requires decreasing stress is termed thixotropic.

2.4.8.3.2 Rheopectic

Fluid's viscosity increases with time as it is sheared at a constant rate. Some fluids require a gradually increasing shear stress to maintain a constant strain rate and are called rheopectic. A further complication of non-newtonian behavior is the transient effect shown in the following figure:

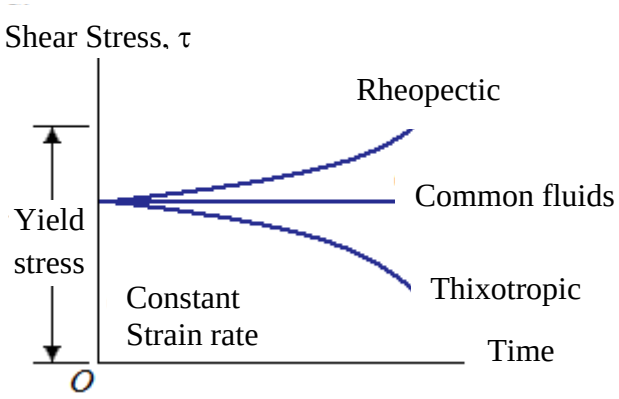

Figure 2.15 Rheogram of non-Newtonian fluids with the dependence of time [39].

Viscosity has proved to be very difficult to model because it exhibits both elastic and viscous responses. The Einstein equation for viscosity in dilute suspensions is given by equation 2.8 [39].

$$\mu_r = \frac{\mu}{\mu_0} = 1 + 2.5\phi \qquad 2.8$$

Note: μ_0 is viscosity of dispersing phase, and μ are relative and absolute viscosities, respectively, and ϕ is volume fraction of solids.

This equation works well for dilute systems. To describe higher concentrations, a number of investigators have developed relations in the form of $\mu_r = f(\phi)$ that asymptotically reduce to Einstein's equation at low concentrations. Modeling of these systems, however, utilizes only one parameter, the volume fraction of solids.

2.5.7 Stability [32]

Slurry stability is classified into three broad categories, namely, sedimentative (static), mechanical (dynamic), and aggregative. The stability of slurry is a crucial factor in its processability and applicability, which ultimately determine the value of the slurry. The factors that affect slurry stability are density, particle size, solid concentration, surface properties (relative hydrophilic nature), surface charge (zeta potential), morphology of coal, and type of slurry liquid. The stability of slurry

against gravity is called sedimentative stability. A statically unstable slurry will settle, but as the system becomes more stable, the degree of settling decreases. Static stability in a fluid requires a yield stress in the fluid sufficient to support the largest particle. The stability in a dynamic system is called dynamic stability. Dynamic stability involves the superposition of mechanical stresses; some examples are pumping and mixing. The third stability type, aggregative stability, is a function of inter-particle forces [36,37].

2.5.7.1 Suspension types

A suspension can be classified into three broad categories, namely, aggregative stable, flocculated, and coagulated, as shown in Figure 2.16. In an aggregative stable of suspension, repulsion forces do not allow particles to adhere to each other. They tend to settle owing to gravity, leading to highly classified and compact sediment with coarse particles at the bottom and finest particles on the top. In the second suspension type, flocculated, the particles weakly interact to form porous clusters called flocs.

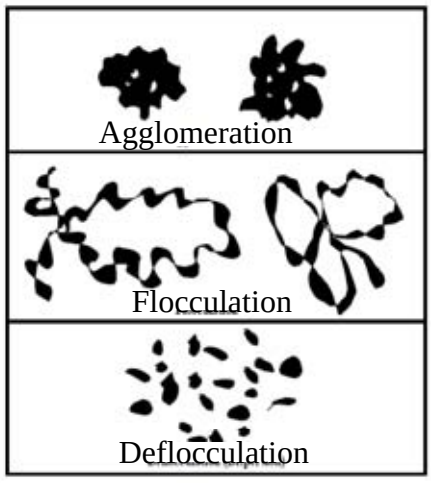

Figure 2.16 Illustrations of suspension types [42].

The formed sediments are very loose and occupy a large fraction of the original slurry volume. The slurry is easily brought back to original uniform concentrations with mild agitation. In the last suspension type, coagulated, the

particles interact strongly. The strong attractive inter-particle forces promote the formation of compact and tightly bound clusters, which are difficult to break loose without significant agitation. These unstable slurries have fast settling rates and often display non-Newtonian behavior like thixotropic (time-dependent behavior), pseudo-plastic (shear thinning), or plastic behavior.

2.5.7.2 Interparticle interactions

Recent studies [32,36,37,43] have shown that stability in slurries is achieved by promoting networks through weak interparticle interactions. The properties of coal slurries are governed by the nature of the forces between particles. Six important particle-particle interactions may exist in aqueous dispersions.

The attractive force, van der Waals force, encourages aggregation between particles when the distance between particles is very small. These forces are due to spontaneous electric and magnetic polarizations giving a fluctuating electromagnetic field within the dispersed solids and aqueous medium separating the particles.

Now, it is possible to predict the interactions of the electric double layer (EDL) and van der Waals forces by [43]:

$$V_T = V_A + V_R \qquad 2.9$$

in which V_T, V_A, and V_R refer to the total potential, van der Waals forces, and electrical double layer interactions, respectively.

This forms the basis of the DVLO (Derjaguin–Landua–Verwey–Overbeek) theory of colloid stability. The energy interactions for EDL and van der Waals forces are shown in Figure 2.17. The subsequent total energy curve allows for prediction of aggregation at close distances (primary minimum) and the possibility of a weak and reversible aggregation in the secondary minimum. The form of the curve depends on the size of the particles and surface charge. For example, coarse particles are more likely to be vulnerable to aggregation at the secondary minimum.

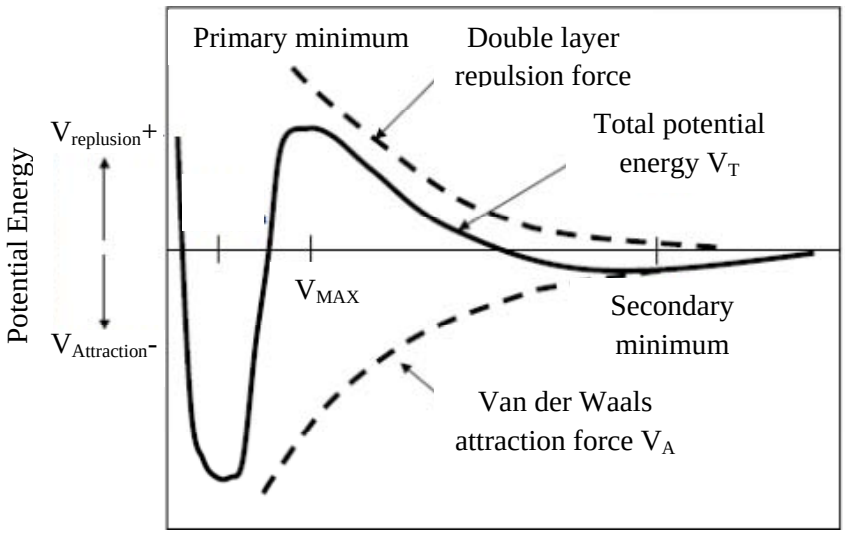

Figure 2.17 Particle-particle interaction potential energy [43].

The other types of interparticle interactions (steric interactions, polymer flocculation, hydration- and solvent-induced interactions, and hydrophobic interactions) represent special cases. The most significant of these are steric interactions and polymer flocculations. Steric interactions develop when molecules (usually polymers or macromolecues) are adsorbed onto the particle surface at high coverages. The polymer molecules protrude from the surface of the particle into solution. When particles approach one another, the polymer chains overlap and often dehydrate, increasing the stability of the slurry. Polymer flocculation occurs when the particle surface has low coverage of a high-molecular-weight polymer. The polymers bridge the particles and form flocs.

Hydration- and solvation-induced interactions become important when interparticle distance is on the order of a solvent molecule. For aqueous systems, these solvation effects are clearly visible in structuring of the water near the interfacial surface (with their bound water), which interacts with hydrated ions from solution. The net effect is an increased stability or net repulsion between particles as it becomes necessary for the ions to lose their bound water to allow the approach to continue. Hydrophobic interactions are analogous to hydration and solvation effects, because stability can be enhanced by the attraction between two hydrophobic particles. Therefore, hydrophobic particles tend to associate with each other. The hydrophobic forces are greater than the van der Waals force and have a longer range [43].

2.6 Coal-water slurry (CWS) [44]

Coal-water slurry is an environment friendly coal based liquid fuel that can be used to replace petroleum because of the relative ease of handling (similar to fuel oil and not explosive, unlike coal dust), storage in tanks, and injection into furnaces and boilers. It is prepared through particular technical process from 65%-70% coal, 29%-34% water, and minor (1%) quantities of chemical additives which leads to high energy densities per unit mass. Hence, CWS is slurry of powdered coal and water, which maintains a stable state over a long period when a small amount of additive is provided properly. Possible applications include gas turbines, diesel engines, fluid bed combustors, blast furnaces, and gasification systems. CWM with a lower coal loading of 50 wt% may be used for the internal combustion engine, especially when nonexplosive fuel is needed, for example, in military vehicles and helicopters.

2.6.1 Standard specifications of coal-water slurry

The physical properties of coal slurry are extremely important in the processing of the fuel. The slurry must be stable and exhibit low viscosity in the shear rates of pumping and atomization. The flow characteristics of coal-water slurry depend on: (1) physicochemical properties of the coal, (2) the volume fraction, φ, of the suspended solids, (3) the particle size range and distribution, (4) interparticle interactions (affected by the nature of surface groups, pH, electrolytes, and chemical additives), and (5) temperature [45].

Table 2.3 Standard specifications of coal-water slurry [45]

Physical Properties	Value
Density	65~70%
Viscosity	~1000CP
Size	d<50μm
Ash	<7%
Sulfur	<0.5%

Rheological and hydrodynamic behavior of coal water slurries varies from coal to coal. Each coal has a unique package of particle size distribution, concentration, and additives to reach the desired processability. Slurry capability is determined from the equilibrium moisture content of coal which ascribes to the hydrophilic nature of the coal. Therefore, proximate analysis and ultimate analysis of dry coal are required. The more hydrophilic the coal is, the more water it will hold and the less likely it is to produce a highly concentrated slurry. The coal-water slurry viscosity increases with the hydrophilicity of the coal. Therefore, a hydrophobic coal can more easily form a slurry of low viscosity at high solid loadings. Conventional high-rank coals (black coal), except anthracite, have a hydrophobic nature from the lack of acid groups and will form a slurry of ~80 wt% (dry coal weight basis). Anthracite coals have low reactivity and are not very volatile, leading to poor ignition stability. However, low-rank coals (brown coal) are hydrophilic from an abundance of oxygen functional groups and will form slurries of only 20–25 wt% (dry coal weight basis). These slurries have low concentrations but form slurries that are non-agglomerating and have high reactivities. Difference in coal slurry stability between types of coals is a function of the relative balance between acid and base groups on the coal surface. Coal-water slurry is loaded to the highest possible concentration at acceptable viscosities. However, viscosity increases with coal concentration (loading), though reducing the viscosity compromises the stability of the slurry**.** The viscosity of the slurry increases gradually with increasing solid loading until a critical point is reached at which inter-particle friction becomes important. Beyond this point, the viscosity increases very sharply until the slurry ceases to flow. To properly stabilize coal-water slurries, i.e., to enhance the stability of the coal dispersion, additives such as surfactants and electrolytes are added [46].

Surfactants are used as dispersants to wet and separate coal particles by reducing the interfacial tension of the coal-water system. Surfactants are short-chain molecules containing both a hydrophobic group and a hydrophilic oxide (nonionic) or a charged ionic group (ionic). These molecules attach themselves to the coal particles through adsorption or ionic interaction. Ionic surfactants adsorb onto the alkyl groups at hydrophobic sites on the coal particle. This gives the coal particles a negative charge, which affects the EDL, enhancing the repulsive forces and thus preventing

agglomeration [6,7]. Anionic surfactants decrease the viscosity of the slurry up to a critical loading. At this point the coal adsorption sites are saturated and the remaining surfactant forms micelles in the slurry, leading to an enhanced structure and increased viscosity. Nonionic surfactants function by two different methods depending on the nature of the coal. On a hydrophilic coal surface the hydrophobic end of the surfactant is toward the aqueous phase. The water then acts as a lubricating material between coal particles. The second method is via attachment of surfactant on a hydrophilic coal. The hydrophilic end of the surfactant attaches to the coal molecule, leaving the hydrophobic end into the aqueous medium. This increases the amount of water near the surface of the coal particle, producing a hydration layer or solvation shell. This prevents agglomeration by cushioning coal particles and lowers the viscosity. The ionic strength of water in the CWS is an important parameter in the rheological and hydrodynamic characteristics of a slurry. Because coal is a mixture of macromolecular carbonaceous materials and mineral matters rather than a uniformly homogeneous substance, the ionic strength of the water will affect the interaction with coal. In a hydrophobic colloidal system dispersed by electrically repulsive forces, the electrolyte concentration (and its ionic strength) has a considerable effect on the stability against flocculation of particles. The cation concentration causes an increase in the viscosity of the slurry with decreasing pH. Electrolytes strongly affect the degree of particle dispersion and, thus, rheology in coal-water mixture that uses anionic dispersant. The addition of electrolyte to a slurry using nonionic dispersants has no appreciable effect on the viscosity [44,46].

In highly concentrated slurries, minimal settling is expected, but viscosity reducing additives increase the settling rate. To stabilize the dispersion, flocculating agents are added, which produce a gel. Some examples of this are nonionic amphoteric polymers of polyoxyethylene, starches, natural gums, salts, clays, and water soluble polymeric resins that have been used for drag reduction, i.e., viscosity reduction. Both ionic and nonionic polymer solutions show reduction in viscosity, although the reduction is more pronounced for anionic polymers.

2.6.2 The coal-water slurry technology development and its application benefits [47]

Coal-water slurry technology has been developed and in place a few decades ago, but has gained more interest recently due to several reasons.

1. Using coal to replace oil reduces fuel cost of users.

2. Coal-water slurry is a clean coal technology, use energy source economically and rationally and improve environmental protection.

3. Energy saving effect is remarkable because coal-water slurry combustion is easy to control, its low waste, and low high combustion efficiency (above 95%-98%).

4. Providing new manner in coal transportation: coal-water slurry can be transported through pipelines and stored in storage tanks.

5. Burning coal-water slurry replaces loose coal and improves regional environment. CWS can be manufactured in the mine mouth to supply several power plants by using ships and pipelines. It’s s just like distribution system from oil refinery to power plants.

2.6.3 Coal-water slurry production process

In a typical production process, crushed coal is sent to storage tank and then ball mill, together with the right amount of water and additive, then to slurry tank and filter tank for separation by filtration. After filtering, the slurry is sent to a stirring tank with stabilizer addition then stored at storage tank before off take.

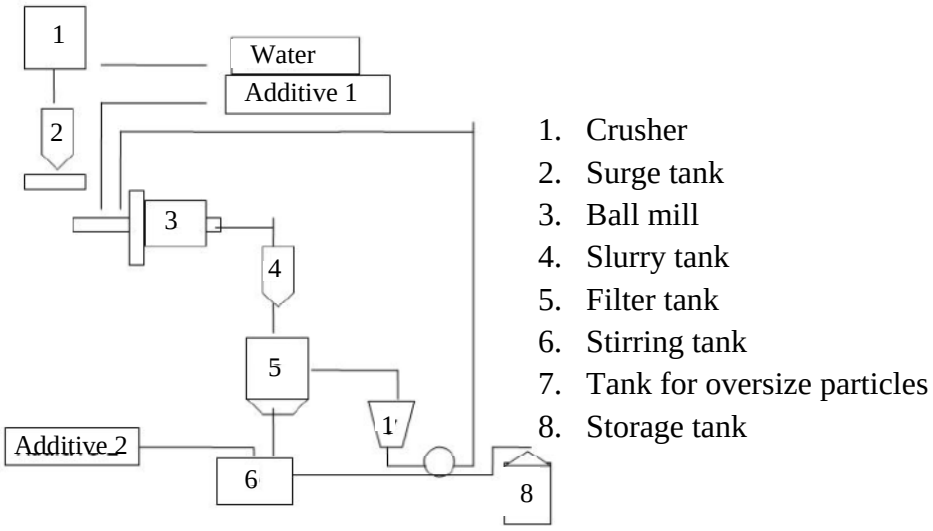

Figure 2.18 Coal-water slurry production process [47].

2.6.4 Current end users of the product and its market potential [24]

At present, there are more than 20 processing plants, producing coal-water slurry with the total production capacity of more than 4 million tons in China; there are more than 5,000 oil burning boilers, available to be converted to coal-water slurry fuel, with the annual oil burning amount of over 39 million tons and the demand of coal water slurry about 78 million tons, if the ratio of calorific value of oil to coal-water slurry is 2 to 1. Meanwhile, with the increase of petroleum price and strengthening of environmental protection, more and more coal burning boilers and petroleum burning boilers will be converted to coal-water slurry burning boilers. So, this product is in large demand and its marketplace is wide as well. Coal-water slurry are most likely to be used in boilers that were designed for coal but have changed over to oil, or in oil boilers that can burn coal-liquid mixtures without serious loss of output (de-rating). Other suggested uses have been in diesel engines, for blast-furnace injection, in process heating, and in rotary kilns.

2.7 Literature reviews

Das et al. [6] reported the surface activity of saponin, extracted from the fruits of plant *Sapindous laurifolia*, and the rhelogical characteristics of the highly concentrated coal-water slurry containing saponin. The results confirm the use of saponin of 0.8% as a suitable additive for coal-water slurry of 64% weight similar to the commercially available additive such as sodium dodecyl sulfate, which is stable for period as long as 1 month in contrast to 4-5 h in the case of bare coal-water slurry.

Yang et al. [7] revealed that the adsorption behavior of sodium lignosulfonates on the coal water interface has much greater effect on the viscosity of coal-water slurry. The higher adsorption amount and compact adsorption film of SL on the coal surface help reduce the viscosity of coal-water slurry, and the zeta potential is also an important factor, which is influenced by the sulfonic and carboxyl group contents of the lignosulfonate molecule. Furthermore, the sodium lignosulfonate with its molecular weight ranging from 10,000 to 30,000 has both a higher adsorbed amount and zeta potential on the coal surface and the best effect on reducing the viscosity of coal-water slurry.

Pawlik et al. [8] investigated the effect of several low molecular weight polymers (MW<100,000) on the surface properties of a medium-volatile bituminous coal in concentrated aqueous suspensions. The experimental results exhibit that the anionic polymers are much stronger coal dispersants since their action is a combination of steric and electrostatic repulsive forces. On the contrary, the nonionic cellulose ethers can act only through steric effects. The poor dispersing performance of hydroxypropyl cellulose correlates well with the inability of the polymer to depress the natural floatability of the bituminous coal. Therefore, rendering the coal particles hydrophilic is the common mode of the dispersing action of both anionic and nonionic polymers.

Zhou et al. [48] synthesized a new type of high-performance lignin series dispersant of coal water slurry from wheat straw alkali lignin (WAL), and determine the affecting factors for coal-water slurry preparation. It is found that the inherent

viscosity and the sulfonic group content of the modified wheat straw alkali lignin (MSL) are the key factors affecting its dispersing effect for coal-water slurry. Moreover, the MSL with intermediate inherent viscosity (6.0 mLg^{-1}) and higher sulfonic group content (1.80 $mmolg^{-1}$) was found to have excellent dispersing effect for coal-water slurry. The studies of the properties of coal-water slurry showed that MSL has similar dispersing effect with naphtalenesulfonate-formaldehyde condensate, and far better dispersing effect than lignosulfonate.

Mishra et al. [49] study the adsorption behavior of sodium dodecyl benzenesulfonate (NaDDBS) on a raw coal sample. It was observed that the isotherm exhibits two adsorption plateaus below and above the critical micelle concentration of NaDDBS. Low heats of adsorption suggest weak hydrophobic bonding between adsorbent and adsorbate. Otherwise, the results reveal that addition of a very small amount of NaDDBS approximately 0.3 wt% of coal with 60% (w/w) coal-water slurry results in a marked reduction of the apparent viscosity of the coal-water slurry at a shear rate of 100 s^{-1}.

Boylu et al. [50] studied the effect of carboxymethyl cellulose (CMC) used as stabilizer in the preparation of coal-water slurries on the stability. The results of the experiments showed that polymeric anionic CMC agent has much greater effect on the stability of coal-water slurry prepared from bituminous coal. Also, we found that inorganic mineral matters were able to be used as a stabilizer for preventing the sedimentation and separation of coal-water slurry.

Shin et al. [51] examined the rheological and thermal properties of coal-organic solvent slurries. It is shown that solvents with molecules containing unpaired electrons (high basicity) exhibit high extraction power and cause swelling of coal leading to higher viscosities compared to coal-water slurry. In addition, coal slurries prepared by alcohols and cyclohexanone demonstrated lower settling rates but a high specific sedimentation volume presumably because these solvents swelled coal particles well and led to the formation of weak gel structures in the bulk. In addition, ethanol and cyclohexanone are capable of breaking a considerable amount of hydrogen bonds in coal and subsequently opening up the structures.

CHAPTER 3

EXPERIMENTAL

This experimental research could be classified into two parts; the first one shows synthesis, characterization and property of dispersant, and the latter performs the preparation and properties of coal-water slurry containing synthesized dispersant.

3.1 Synthesis, characterization and properties of dispersants

3.1.1 Raw materials

3.1.1.1 Cashew nuts shell liquid (CNSL) was obtained from Chonburi Province as a dark colored viscous liquid. Diethanolamine and triethanolamine were obtained from Aldrich Chemicals.

3.1.1.2 Cardanol was obtained from S.N.B United Chemical, Co., Ltd., Thailand. Formaldehyde (40% solution), Carlo erba, Italy was used for formylation. Sodium sulfite, Merck from Germany was used for sulfonation reaction. Methanol (Mallinckrodt Chemical, USA) was used as solvent.

3.1.1.3 The commercial sodium lignosulfonate (SL) was part of a by-product of sulfite pulping from Guangzhou Paper Making Co. Ltd., China. This commercially available sodium lignosulfonate is a water soluble, red brown powder, changing to yellow brown when dissolved in water. The final pH of the product is above 9.Since the structure of lignosulfonate is complex and changes according to biomass source and isolation technique, thus it is difficult to explain a detailed composition and chemical structure.

3.1.2 Synthesis process

3.1.2.1 Diethanolamine anacardate (DEA) [52]

A 5.1 g sample of anacardic acid was dissolved in 100 ml of methanol. A 1 wt% solution of diethanolamine in methanol was added drop by drop until the pH reached approximately 8, then the solution was continuously stirred for 30 min. Methanol in the product was removed until dryness giving the dark colored viscous product.

3.1.2.2 Triethanolamine anacardate (TEA) [52]

A 5.1 g sample of anacardic acid was dissolved in 100 ml of methanol. Then a 1 wt% solution of triethanolamine in methanol was added drop by drop until the pH reached approximately 8. After methanol was removed, the dark colored viscous product was obtained.

3.1.2.3 Cardanol-formaldehyde sulfonate (CFS)

The 12 g anhydrous sodium sulfite was dissolved in 30 g water in a round-bottom flask equipped with a reflux condenser, a temperature controlled electric heating device, a motor stirrer, a thermometer, and a dropping funnel. Then, 10 g formaldehyde aqueous solution of 37% concentration was added into the reactor by means of a dropping funnel, and the reaction was carried out at 70°C for 30 minutes. After a certain reaction time, a mixture of 10 g cardanol and 30 g methanol was fed into the reaction containing sodium sulfite and aldehyde under stirring. Then 10 g formaldehyde aqueous solution was dropped into the mixtures for sulfomethylation. After adding the formaldehyde solution, the temperature was raised to 80^{o}C and the reaction continued for 8 hours till the end of the reaction. After sulfomethylation of cardanol was completed, 200 ml methanol was added into the mixture to precipitate the product and remove an intermediate solution and residual cardanol for several times. After that, the final product, cardanol-formaldehyde sulfonate, was dried to yield a solid content of approximately 35% with pH of 9. The proposed structure of cardanol-formaldehyde sulfonate is shown in Figure 3.1.

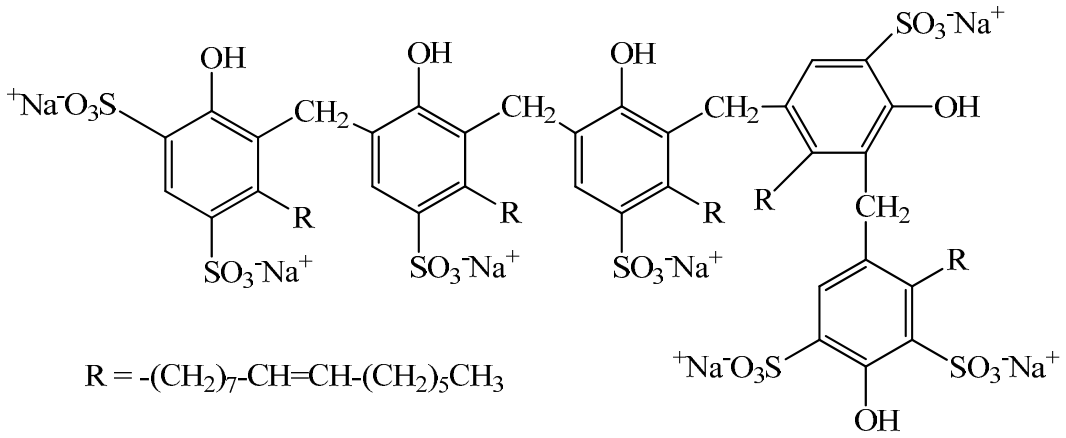

Figure 3.1 Chemical structure of cardanol-formaldehyde sulfonate.

Furthermore, the influence of the sulfonating agent concentration on dispersing effect of cardanol-formaldehyde sulfonate was studied. Finally, the effect of reaction time and temperature on molecular weight and sulfur content attributed to the sulfonic group content was also investigated and are shown in Table 3.1.

Table 3.1 The variation of reaction parameters

The ratio of sulfomethylating agent : total reactant mass		Reaction time (h)	Reaction temperature (^{o}C)
Sodium sulfite (%)	Formaldehyde (%)		
5.7	13.8	2	60
10.7	24.2	4	70
15.3	32.4	6	80
19.4	39.0	8	100
		10	120
		12	140

3.1.3 Characterization

3.1.3.1 Infrared spectroscopy (IR)

The Fourier transform infrared (FT-IR) spectra was carried out using Perkin Elmer Spectrum One spectrophotometer. A certain amount of sample was mixed with potassium bromide in a mortar box. After each grinding, the mortar box was thoroughly cleaned with acetone. The grinding powder of the sample and potassium bromide was pressed using the tablet machine for subsequent infrared spectrum analyses. The spectra were collected within a scanning range of 400–4000 cm^{-1}. The FT-IR was first calibrated for background signal scanning with a control sample, and then, the experimental sample scanning was conducted.

3.1.3.2 Nuclear magnetic resonance spectroscopy (NMR)

The structural study was carried out with varian, INOVA NMR spectrometer. ^{1}H and ^{13}C NMR spectra of the synthesized materials were operated at 500 MHz and 125 MHz, respectively. Spectra of surfactants as carboxylic salt species and cardanol-formaldehyde sulfonate, were recorded in CD_3Cl and D_2O at 25^{o}C, respectively.

3.1.4 Properties testing of synthesized dispersants

3.1.4.1 Sulfur content measurements

The wavelength dispersive X-ray fluorescence (Philips WD-XRF PW 2400) with energy dispersive (Oxford ED-2000) spectrometer coupled with microprocessor controlled chemical reactions has been applied to analyze the sulfur content of the dispersants collected in the simple screening study.

3.1.4.2 Gel-Permeation Chromatography (GPC) measurement

A Water GPC system (USA), equipped with a Water E600 columns connected to a refractive index (RI) detector, were used to measure the molecular weight and the

molecular weight distribution of the synthesized cardanol-formaldehyde sulfonate. The analyses were performed at 25.0±0.1^{o}C using THF as an eluent at a flow rate of 1 ml/min. Narrow PS standards were used for generating a calibration curve.

3.1.4.3 Surface tension measurements

The surface tension of the dispersant solution was measured on a tensionmeter (K8 model Kruss) by the platinum loop. Extreme care was taken with the platinum loop and experimental vessel. Before and after a measurement, the platinum loop was cleaned by acetone and then cleaned using the distilled water which was used for preparing the solutions. Every case was performed at about 30°C.

3.1.4.4 Inherent viscosity measurements

The inherent viscosity of the cardanol-formaldehyde sulfonate samples was measured using Ubbelohde viscometer. The dilution and extrapolation method was used for theoretical calculation.

3.2 The preparation and property of coal-water slurry containing synthesized dispersant

3.2.1 Materials

3.2.1.1 Beneficiated clean Bituminous coal from Indonesian Coal Mine was selected for study.

3.2.1.2 Synthesized dispersants obtained from section 3.1 including diethanolamine anacardate, triethanolamine anacardate, and cardanol-formaldehyde sulfonate, were compared with a commercial dispersant, sodium lignosulfonate.

3.2.2 Apparatus

3.2.2.1 Carborundum mill was used to reduce the size of coal from approximately 600 mm less than 10 mm.

3.2.2.2 Ball mill was used for wet grinding the coarse coal particles into fine coal powders.

3.2.2.3 ASTM sieves were used to separate coal powder size into particle size. Table 3.2 shows comparison between ASTM mesh sizes with SI size in micron.

Table 3.2 Sieve micron size comparison

ASTM Mesh No.	Size (micron)
325	45
200	75
140	106
120	125
70	212

3.2.2.4 A homogenizer (Nessei Ace Homogenizer**,** Japan) was used to prepare coal-water slurry, in which comprises of coal, water, and dispersant, to ensure the formation of a homogeneous mixture to be used in the further experiment.

Figure 3.2 Homogenizer for coal-water slurry preparation.

3.2.2.5 HAAKE rotational viscometer (HaakeRotoVisco1) was employed to study the viscosity and rheological behavior of coal-water slurry. The viscometer consists of a measuring drive unit, temperature vessel with circulator, sensor system, and a data logger (Thermo electron Corp.). The basic instrument was operated with a measuring cup (No.3 cylinder cup) and a rotor (E3 immersion geometry) according to ISO 3219as shown in Figure 3.2.

Figure 3.3 HAAKE rotational viscometer (HaakeRotoVisco 1).

3.2.3 Method for coal preparation

Bituminous coal from Indonesia Coal Mine was selected for this study. The ultimate and proximate analyses are the most often used analysis for characterizing coals in connection with their utilization which was carried out with Perkin Elmer (PE2400 Series II). It is well known that the optimum particle size of coal plays important roles in identifying rheological properties of slurry fuel. Therefore, a study of laboratory grinding tests was carried out by using a ball mill under wet processing to obtain the adequate slurry condition.

First, coal which was obtained as large lumps and agglomerates, was broken into small pieces by a hammer. Then, pulverized coal was prepared by crushing a lump of coal with carborundum to obtain coarse particles below 10 mm product and

was dried at 100^{o}C for 24 h. The crushed dry coal was comminuted in the ball mill (wet grinding) to obtain the products of different particle size distributions by controlling the grinding time. The fine particles coal was dried at 100^{o}C for 48 h for coal-water slurry preparation. The coal powder was screened through a sieve screener to obtain products with a required average particle size. The particle size distribution of coal sample is measured by Malvern particle size analyzer (Mastersizer S).

3.2.4 Grinding test procedure

The first set of grinding tests was carried out in a batch ceramic ball mill. The grinding ball, and pot mill are high alumina porcelain (46% alumina) with 7-8 hardness in Moh's scale. Pot mill size was 150 mm in diameter by 300 mm length. The mill was loaded to a bulk volume of 2000 cm^3 (75% loading) with 30 mm diameter grinding balls. All tests were run at 80 rpm with a constant slurry volume loading of approximately 1500 cm^3.The effects of the water-to-solids ratio on grinding were analyzed. Moreover, grinding tests in dense suspensions were also studied as a function of time. On the basis of the laboratory results, simulations were conducted to analyze grinding circuits for producing the recommended size distribution for coal-water slurry.

3.2.4.1 Variation of the percent coal

The coal powders were varied in range of 40-53 % by weight which was achieved by changing the water-to-coal ratio with total slurry volume of 1500 cm^3.

3.2.4.2 Variation of the grinding time

The gradient time variation was carried out using a new sample for each test which was study at 5, 10, 24, and 48 h.

3.2.5 Methodology for coal-water slurry preparation

Four dispersants were used for coal-water slurry preparation. Two dispersants, diethanolamine anacardate and triethanolamine anacardate, were synthesized from cashew nut shell liquid. The third dispersant, cardanol-formaldehyde sulfonate, was synthesized from cardanol. The forth one, sodium lignosulfonate, a commercial dispersant was used for comparison purpose.

About 120 g of slurry was prepared at known quantity of pulverized coal, dispersant and distilled water. The coal powder was mixed slowly in a pot containing known quantity of dispersant and deionized water. The content was stirred by means of a mixer until it became a slurry, and then the stirring of the slurry was continued for a further 15 min at 3000 rpm. After that the homogenization of the coal-water slurry can be achieved. All experiments were conducted at temperature of 25°C. The variation in temperature was $\pm$0.1°C, which is controlled through a constant temperature circulating bath connected to a viscometer. Before measurement the slurries were allowed to stand for 5 min. The measured viscosity value was the apparent viscosity. The rheological measurement was controlled by a software rotation version 3.0. The various parameters such as shear stress, shear rate, apparent viscosity, and temperature along with the curve were displayed on a computer screen.

Characteristic of coal-water slurry is more complex than its parent coal because of the consideration of both the physicochemical characteristic of its original coal and the behavior of coal mixture with water, which has to be understood through the science of rheology. Therefore, the effects of particle size distribution of coal, coal concentration, dispersant concentration, temperature were investigated on the viscosity of the slurry as follows;

3.2.5.1 Variation of coal particles size

The coal samples were then classified into; -45, 45-80,80-100, 100-125, 125-200, and +200 μm size fractions using standard U.S sieve screens.

3.2.5.2 Variation of coal concentration

Each slurry was made using dry coal concentration varying between 40-60 wt%.

3.2.5.3 Variation of dispersant concentration

The dispersant concentrations for coal-water slurry were varied from 0.2-2.0 wt% in steps of 0.2 wt% for constant weight concentrations of coal-water slurry.

3.2.5.4 Variation of temperature

The effect of varying temperatures was studied in range of 25-80^{o}C.

3.2.6 Properties testing of coal-water slurry

3.2.6.1 Viscosity and rheological measurements

Generally, the viscosity and flow behavior of slurry test materials were precisely measured by a rotational viscometer. All results like viscosity, shear stress, shear rate, yield point and operating temperature were reported. A rotational speed was preset and the flow resistance of the sample was measured, in other words, the torque required to maintain the set speed was proportional. Finally, the automatic characterization of the flow behavior of non-Newtonian fluids or the determination of the yield point using controlled deformation could be done.

3.2.6.2 Zeta potential measurement

The zeta potential of coal particles in the coal-water slurry was measured by a zeta potential of colloid system by zeta meter (brand 3.0).As this system was intended for a dilute state, that was prepared by different dispersant concentrations with dispersing coal powder of 10 wt% into 50 ml total solution. Before measurement, the solution was dispersed again for 10 min by a stirrer.

3.2.7 Coal-water slurry stability evaluation

The stability of coal-water slurry was evaluated by “glass rod penetration” method in a similar manner, in which the detail was described by Boylu et al. [50]. This test is designed to find the layer of the compact sediment deposited at the bottom of the cylinder. After each coal-water slurry was obtained, it was stored in a glass cylinder (3 cm in diameter; 15 cm in height) at room temperature ranging from 24 h to 360 h. The glass rod (5 mm in diameter, 9 g in weight) was spontaneously dropped down directly from the coal-water slurry surface to the cylinder bottom, and it stopped when the tip gets in contact with the hard sediment. The penetration ratio was calculated as follows;

$$\text{Penetration ratio (\%)} = d/dt \times 100$$

Where d distance of rod travel (cm)

dt maximum distance of rod travel (cm)

3.2.8 Scanning electron microscope (SEM) measurements

The synthesized dispersants used to prepare 10 gL^{-1} aqueous solutions were examined using the SEM (JEOL, JSM-5410LV). The pH values of the prepared aqueous solutions are 9 for purified cardanol-formaldehyde sulfonate and 8 for diethanolamine anacardate solution. Besides, the suspension of coal 0.1 % in each dispersant solution was also studied. During the SEM measurement, a drop of the prepared sample solution is deposited on the SEM stub. Then it is dried and kept in a desiccator overnight, and the dry substrate is examined. No additional sample treatment was performed, to avoid possible specimen coating artifacts.

3.2.9 Combustion test

Thermogravimetric analysis (TGA) was used to evaluate the thermal stability and to determine the decomposition temperature of materials. The thermal behavior of

coal-water slurries was monitored by differential thermal analysis (DTA) and thermogravimetric (TG) analysis (Netzsch STA 409C) with the conditions as follows:

Temperature: room temperature to 700 ^{o}C

Heating rate: 15 ^{o}C min

Air flow rate: 90 ml min^{-1}

CHAPTER 4

RESULTS AND DISCUSSION

In this investigation, coal-water slurry was prepared by mixing coal with water in the presence of efficient dispersant to obtain highly concentrated coal-water slurry. Anacardic acid and cardanol are the major components in cashew (*Anacardium occidentale sp.)* nut shell liquid of interest. The synthesized method and the basic properties of two dispersants; carboxylic salt species derivatized from anacardic acid, and cardanol-formaldehyde sulfonate, are reported in the present research. The dispersing performance and surface activity ability of these dispersants in coal-water slurry were studied. Compatibility of dispersant and coal was determined. Finally, the rheological properties and thermal properties were also investigated.

4.1 Preparation of diethanolamine anacardate and triethanolamine anacardate from anacardic acid in cashew nut shell liquid

4.1.1 Isolation of cashew nut shell liquid

The cashew nutshell liquid contained monohydric phenols as anacardic acids and cardanol, and dihydric phenols as cardol and 2-methyl cardol, as shown in Figure 4.1.

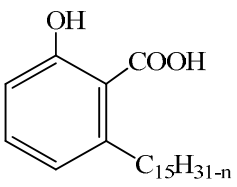

Anacardic acid

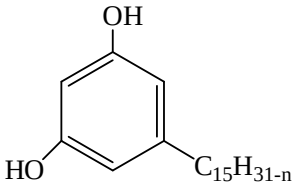

Cardol

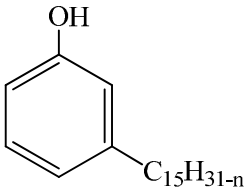

Cardanol

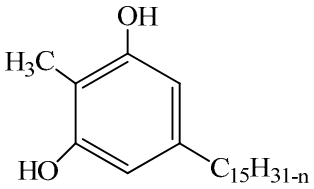

2-Methyl cardol

Figure 4.1 Chemical structures of cashew nut shell liquid components [12].

The major component of cashew nut shell liquid is anacardic acid whose structure was characterized by FTIR spectrometer, ^{1}H-NMR, and ^{13}C-NMR. The structure is shown in Figure 4.2 following assigned structure in Appendix A.1-A.3.

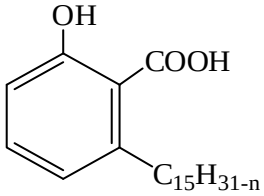

where n = 0,2,4,6

Figure 4.2 Chemical structure of anacardic acid.

The ^{1}H-NMR spectrum of cashew nut shell liquid, shows signals of aromatic proton at δ_H 6.9 - 7.4 ppm. In case of the proton signal influenced from carboxylic acid is detected at δ_H 9.4 ppm. For the signal of double bonds in side chain is detected at δ_H 4.9-5.4 ppm. In addition, the signal of methylene protons adjacent to the aromatic is detected at $\delta_{H\ H}$ 2.4-2.8 ppm, whereas that of methyl protons is also detected at δ_H 0.83-0.93 ppm.

The ^{13}C-NMR spectrum of cashew nut shell liquid shows signals at δ_C 116-156 ppm which belong to carbon in aromatic ring. The spectrum also demonstrates a signal of COOH at δ_C 172 ppm. In case of double bond in the aromatic ring and side chain is detected at δ_C 126-136 ppm whereas carbon signals of methylene and methyl groups appear at δ_C 13-35 ppm.

The infrared spectrum of cashew nut shell liquid shows absorption peaks at of 3390 cm^{-1} and 3006 cm^{-1} belonging to O-H stretching of phenol and =C-H stretching of aromatic, respectively. Furthermore, the adsorption peak of C-H stretching of aliphatic appears at 2940 cm^{-1} and 2846 cm^{-1}. The peaks at 1649 cm^{-1} and 1602 cm^{-1} demonstrating C=O stretching of carboxylic acid and C=C ring stretching of aromatic are also detected. Finally, the spectrum of C-O stretching is detected at 1221 cm^{-1} and 1160 cm^{-1}.

4.1.2 Characterization of diethanolamine anacardate

The neutralization reaction of anacardic acid with diethanolamine, forming diethanolamine anacardate, was essentially completed with a 98% yield product at the pH around 8. The final structure is illustrated in Figure 4.3 and the data proven by ^{1}H-NMR, ^{13}C-NMR, and FTIR, is shown in Appendix A.4-A.6.

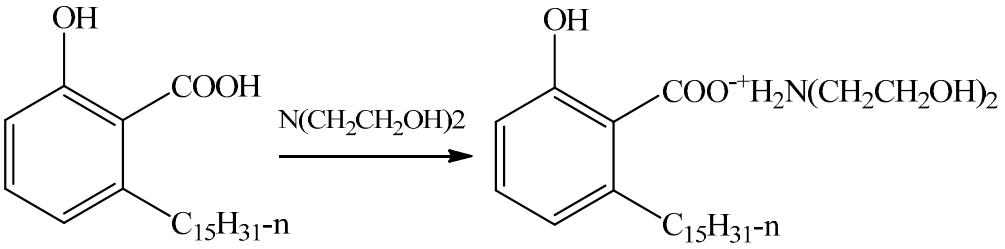

Figure 4.3 Chemical structure of diethanolamine anacardate.

The ^{1}H-NMR spectrum of diethanolamine anacardate shows signals of the methylene protons contained in the diethanol ammonium cation at δ_H 2.8-3.0 ppm. These are clear signals for methyl protons in side chain is also detected at δ_H 0.84-

0.94 ppm, the olefin methylene groups in the alkyl chain at δ_H 5.3 ppm and aromatic proton δ_H 6.6 - 7.1 ppm. Finally, the disappearance of the proton signal influenced from carboxylic acid at δ_H 9.4 ppm indicates the change of the structure from anacardic acid to diethanolamine anacardate.

The ^{13}C-NMR spectrum of diethanolamine anacardate is detected at δ_C 114-162 ppm for the carbon signals in aromatic ring. In addition, other spectrums demonstrate carbon signals of methylene and methyl groups at δ_C 13-36 ppm, the olefin methylene groups in the alkyl chain at δ_C 112 ppm, and carbon double bond in the aromatic ring and side chain at δ_C 126-136 ppm.

The FTIR spectrum of diethanolamine anacardate show a band of OH stretching phenol at 3300 cm^{-1} coupled with small peak of =C-H stretching aromatic (Ph-H) at 3079 cm^{-1}. The absorption peak belonging to C-H stretching of aliphatic (-CH_2-, -CH_3) and –C=O of carboxylate, were detected at 2927 cm^{-1} and 1585 cm^{-1}, respectively. Further, the appearance of the vibration band of the C–N bonds observed at 1069 cm^{-1} and 1156 cm^{-1}, can confirm the structural change of anacardic acid to diethanolamine anacardate.

4.1.3 Characterization of triethanolamine anacardate

Triethanolamine anacardate is obtained from the neutralization reaction of anacardic acid with triethanolamine at the pH around 8, in which the yield product is given approximately 98%. The structure shown in Figure 4.4 was analyzed by FTIR, ^{1}H-NMR and ^{13}C-NMR and shown in Appendix A.7-A.9.

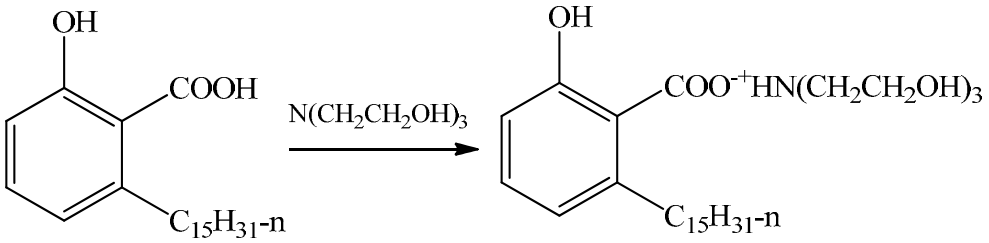

Figure 4.4 Chemical structure of triethanolamine anacardate.

The ^{1}H-NMR spectrum of triethanolamine anacardate structure elucidated by δ_H 2.9 and 3.2 ppm signals belongs to the methylene protons contained in the triethanol ammonium cation. The spectrum also demonstrated signals of methyl protons at δ_H 0.9 ppm, methylene protons adjacent to the aromatic at δ_H 2.4-2.8 ppm, the olefin methylene groups in the alkyl chain at δ_H 4.9-5.4 ppm, and aromatic proton δ_H 6.6 - 7.1 ppm. Further, there is no peak at δ_H 9.4 ppm ascribing to the proton signal influenced from carboxylic acid demonstrating a forward reaction produced from anacardic acid to triethanolamine anacardate.

The ^{13}C-NMR spectrum of triethanolamine anacardate is detected at δ_C 38 and 56 ppm for the methylene protons contained in the triethanol ammonium cation coupled with secondary carbon signals, respectively. The carbon signals in aromatic ring are also shown in range of δ_C 114-162 ppm. Other spectrums demonstrate carbon signals of methylene and methyl groups at δ_C 13-35 ppm, the olefin methylene groups in the alkyl chain at δ_C 111 ppm, and carbon double bond in the aromatic ring and side chain at δ_C 126-136 ppm. Finally, the spectrum demonstrates quaternary carbon atom in the triethanol ammonium at δ_C 176 ppm.

The FTIR spectrum of triethanolamine anacardate shows absorption peak at 3310 cm^{-1} and 3052 cm^{-1} which belong to OH stretching of phenol and aromatic C-H stretching (Ph-H), respectively. Furthermore, the peaks which belong to C-H stretching of aliphatic (-CH_2-, -CH_3) and the vibration of the carboxylate –C=O, were detected at 2928 cm^{-1} and 1585 cm^{-1}. For the adsorption peak of C–N bonds was also detected at 1077 cm^{-1} and 1035 cm^{-1}. As compared with IR spectrum of cashew nut shell liquid, the increase of FTIR band at 3310 cm^{-1} produced by the polyhydroxyl nature of the counterion, as well as the 1078 and 1034 cm^{-1} bands which are characteristic of the tension vibration of the C–N bonds, strongly suggests the structure of triethanolamine anacardate.

From the result, the same data structure of triethanolamine anacardate proved by NMR and IR spectroscopy was seen in the reference [52].

4.2 Preparation of cardanol-formaldehyde sulfonate from cardanol

4.2.1 Isolation of cardanol

The cardanol is a phenolic component obtained by heating at a high temperature in the presence of acid catalyst from anacardic acid, which is the main component of the cashew nut shell liquid, a byproduct of cashew nut processing. Mono-unsaturated cardanol, the major component (48.5%) is shown in Figure 4.5. The remaining cardanol is 29.3% tri-unsaturated, 16.8% bi-unsaturated, and 5.4% saturated.

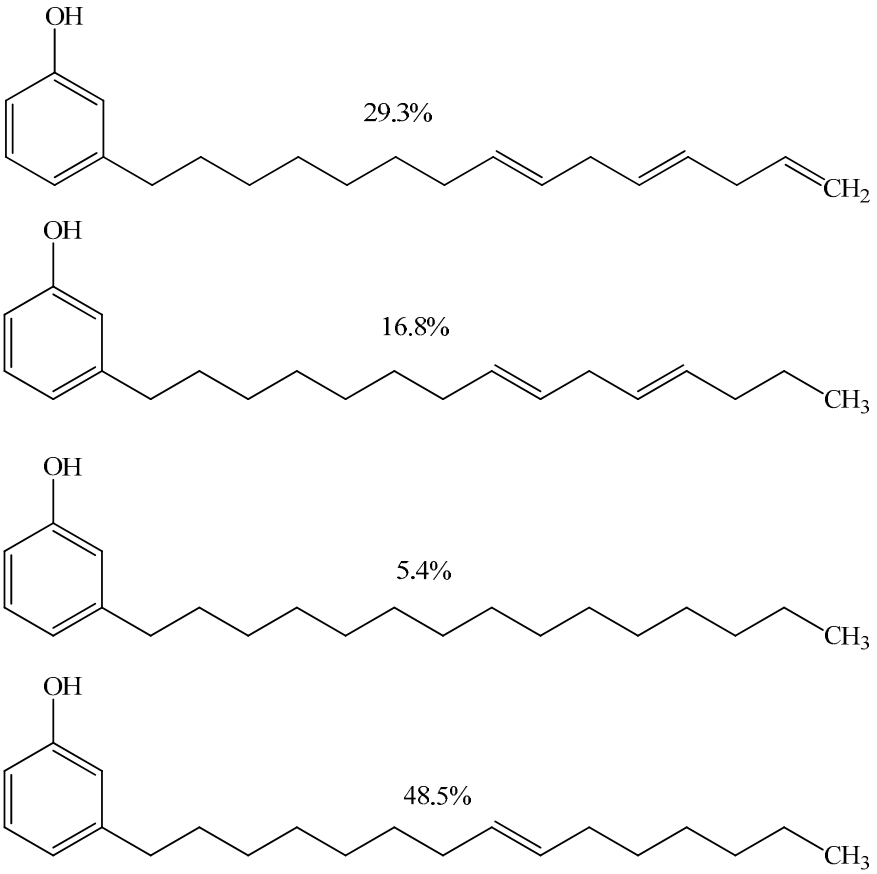

Figure 4.5 Chemical structure of cardanol [18].

The structure was characterized by ^{1}H-NMR, ^{13}C-NMR and FT-IR spectrometer. The results are given in Figure A.10-A12 in Appendix A.

The ^{1}H-NMR spectrum of purified cardanol showed signals at δ_H 6.7-7.1 ppm belonged to aromatic proton. In addition, the spectrum also demonstrated signals of methylene protons adjacent to the aromatic at δ_H 2.5-2.7 ppm, olefinic proton in side chain at δ_H 4.9-5.8 ppm and methyl protons at δ_H 0.8-0.9 ppm.

The ^{13}C-NMR spectrum of purified cardanol shows signal at δ_C 116-157 ppm which belongs to carbon in aromatic ring. In addition, the spectrum also demonstrated signals of double bonds in the aromatic ring and side chain at δ_C 127-137 ppm. Finally, the carbon signals of methylene and methyl groups are also detected at δ_C 13-36 ppm.

The infrared spectrum of purified cardanol showed absorption peaks at 3390 cm^{-1} (O-H stretching of phenol), 3006 cm^{-1} (=C-H stretching of aromatic), 2940 cm^{-1} and 2846 cm^{-1} (C-H stretching of aliphatic), 1592 cm^{-1} (C=C ring stretching of aromatic), and 1160 cm^{-1} (C-O stretching).

4.2.2 Synthesis and characterization of cardanol-formaldehyde sulfonate

The cardanol-formaldehyde sulfonate was obtained from sulfomethylation reaction by mixing cardanol, formaldehyde, and sodium sulfite. The chemical equation of sulfomethylation is represented in Figure 4.6.

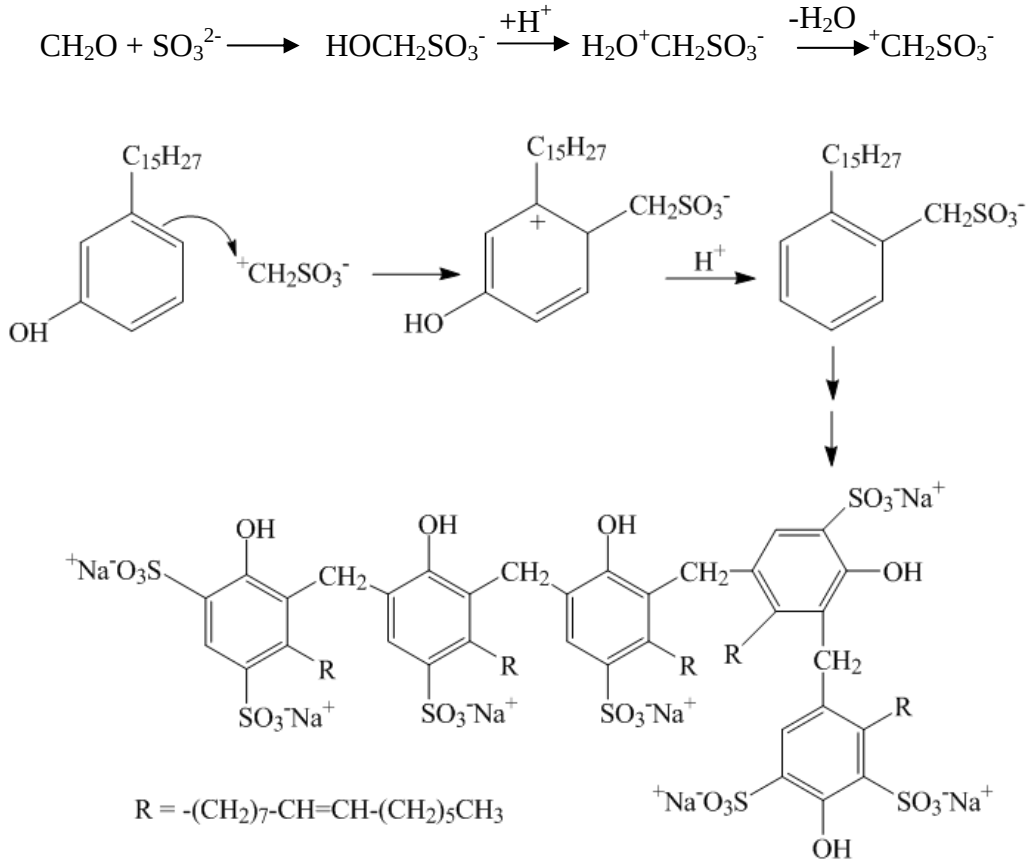

Figure 4.6 Mechanism and chemical structure of cardanol-formaldehyde sulfonate.

After completing sulfomethylation of cardanol with sulfomethylating agent, the product was removed from the residual materials, and then kept in an oven for 24 hours. Finally, cardanol-formaldehyde sulfonate with red-violet color was obtained.

4.2.3 Characterization of cardanol-formaldehyde sulfonate

The ^{1}H-NMR spectrum of cardanol-formaldehyde sulfonate was determined in D_2O. Aryl protons of aromatic ring appear as multiplet at δ_H 6.6-6.8 ppm and the peak around δ_H 7.1-7.3 ppm appears due to the phenolic hydroxyl. The peaks around the region of δ_H 4.6 -5.4 might be attributed to the methylene protons whereas the peaks between δ_H 0.8-2.8 ppm appear due to the presence of long alkyl aliphatic side-chain, originally observed in cardanol. The terminal methyl group of akyl side chain may also be seen as a small peak at δ_H 0.8 ppm. The peak at δ_H 3.6 indicates the presence of methylene protons of C_6H_5-CH_2-C_6H_5 for the bridge between the phenyl rings.

The ^{13}C-NMR spectrum of cardanol-formaldehyde sulfonate shows signals of carbon atom in the aromatic ring around δ_C 116-146 ppm. Other spectrums also demonstrate signals of methylene and methyl groups at δ_C 22-36 ppm and double bonds in the aromatic ring and side chain at δ_C 127-137 ppm. Besides, the appearance of the peak at δ_C 56 ppm indicates the presence of methylene protons of C_6H_5-CH_2-C_6H_5 for the bridge between the phenyl rings.

The infrared spectrum was employed to analyze the chemical structure and the changing chemical composition of cardanol-formaldehyde sulfonate from cardanol. The spectrum of cardanol-formaldehyde sulfonate shows the broad band of at 3436 cm^{-1} indicating the presence of hydroxyl group and the peak at 3010 cm^{-1} indicating -CH- stretching of aromatic ring. The absorbance peaks at 2925 and 2854 cm^{-1} belonging to -CH- stretching of alkyl side chain are also detected. For the peaks at 1638 and 1620 belong to C=C in aromatic ring. There is the appearance of bands at 1464 cm^{-1} and 1436 cm^{-1} (CH) corresponding with ring stretching C-H in plane deformation in the spectrum. Furthermore, the adsorption peaks at 1188, and 1051 cm^{-1} belong to sulfonic group in cardanol-formaldehyde sulfonate molecule. From comparison between cardanol-formaldehyde sulfonate and cardanol, it is found that the absorbance peaks at -CH- stretching of aromatic ring and aromatic skeleton vibration decrease evidently which indicates the breaking of aromatic structure in cardanol molecule from the reaction.

All these spectral data indicates that the condensation of methyolated cardanol has been completed under experimental conditions and was fully consisted of the proposed structure shown in Figure 4.6.

4.2.4 The factors influencing sulfomethylation reaction

In order to obtain the efficient cardanol-formaldehyde sulfonate for dispersing ability in coal-water slurry, the sulfomethylation reaction conditions were optimized by varying the amount of sodium sulfite and formaldehyde in the system, reaction time and temperature. The apparent viscosity was measured in all conditions, in which coal-water slurry was prepared employing the coal content of 50 wt% in the presence of dispersant concentration of 1.0 wt%.

4.2.4.1 Effect of the ratio of sulfomethylating agent

In the synthesis reaction, sulfonic group content of cardanol-formaldehyde sulfonate are greatly influenced by the sulfonating agent dosage and formaldehyde dosage used in the modification reaction. Therefore, the mass ratios of the total reaction materials except the sulfonating agent; sodium sulfite; were kept constant, and the sodium sulfite dosage is adjusted to obtain cardanol-formaldehyde sulfonate products with different sulfonic group contents. The effect of the mole ratios of sodium sulfite mass to total reactant mass concentration on the apparent viscosity and dispersing property of cardanol-formaldehyde sulfonate (1 wt%) were studied and illustrated in Figure 4.7.

In Figure 4.7, it is found that the sulfur contents ascribing the existence of sulfonic group contents in cardanol-formaldehyde sulfonate, increase abruptly with increasing the weight ratio of sodium sulfite and reactant mass concentration, and then level off. On the contrary, the apparent viscosity of the coal-water slurry containing cardanol-formaldehyde sulfonate of 1.0 wt% decreases rapidly and then increases after that. This result demonstrates the suitable ratio of sodium sulfite mass

to total reactant mass is 15.3%. At this mass ratio, the cardanol-formaldehyde sulfonate has the best dispersing performance in the coal-water slurry.

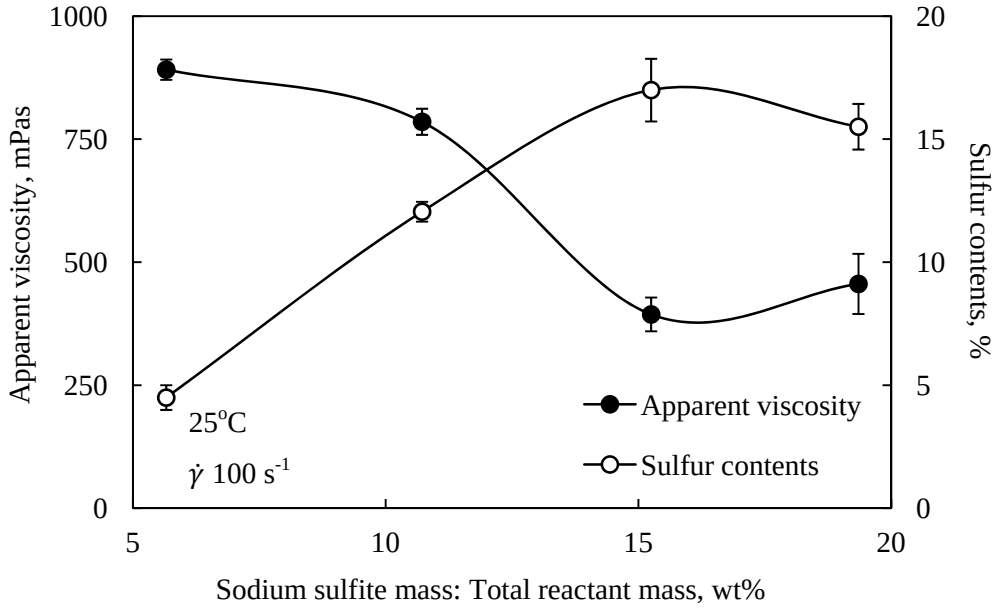

Figure 4.7 Effect of sodium sulfite mass concentration in sulfomethylation reaction on sulfur contents of cardanol-formaldehyde sulfonate and apparent viscosity of coal-water slurry containing cardanol-formaldehyde sulfonate of 1 wt% by carrying out at 80^{o}C for 8 h.

In the synthesis process, the reaction between sodium sulfite and formaldehyde generates the reactive intermediate ($NaSO_3.CH_2OH$) at first, then the $NaSO_3.CH_2OH$ is engrafted in the ortho/para-position of phenolic hydroxyl groups in cardanol molecules by sulfomethylation. The increasing Na_2SO_3 dosage in the total reaction materials generates more reactive $NaSO_3.CH_2OH$ intermediate, and the reactive $NaSO_3.CH_2OH$ occupies more active site in the cardanol molecules, which increase the sulfonic group contents of the cardanol molecules in cardanol-formaldehyde sulfonate. As to the reason, less addition of sodium sulfite causes the poor water solubility of obtained cardanol-formaldehyde sulfonate, so its sulfonic groups has only slight influence on the improvement of dispersing performance in coal-water slurry in comparison with the mixture of coal with deionized water. The

similar behavior appears with cardanol-formaldehyde sulfonate obtained by using excess sodium sulfite. Therefore, the sulfonating agent dosage should not be excessive or insufficient, and a suitable intermediate value can yield the cardanol-formaldehyde sulfonate with higher sulfonic group content.

4.2.4.2 Effect of formaldehyde dosage

Since the synthesis reaction is complex, not only the amount of sodium sulfite but also formaldehyde should be considered. The formaldehyde dosage in the reaction is also an important factor affecting the efficiency of cardanol-formaldehyde sulfonate. In the study, the raw materials ratio in the reaction solution was kept constant and the formaldehyde dosage was changed to obtain cardanol-formaldehyde sulfonate products with different sulfonic group contents and molecular weights, and the result is shown in Figure 4.8.

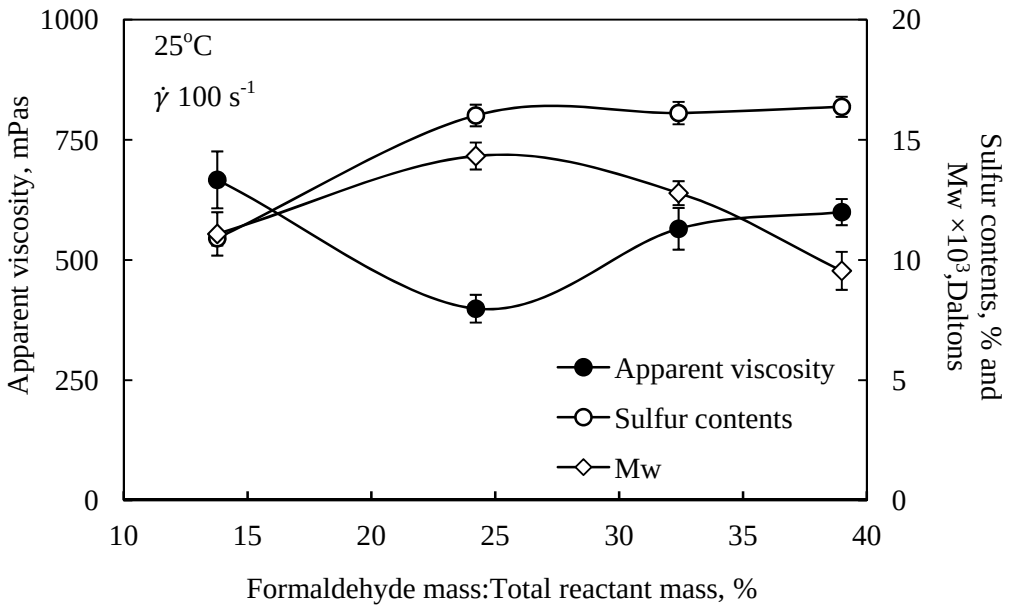

Figure 4.8 Effect of formaldehyde mass concentration in sulfomethylation reaction on sulfur contents and molecular weight of cardanol-formaldehyde sulfonate and apparent viscosity of coal-water slurry by carrying out at 80°C for 8 h.

When the ratio of formaldehyde and total reactant mass increases from 13.8 to 24.2%, the sulfonic group content and the molecular weight of cardanol-formaldehyde sulfonate increase, while the apparent viscosity of coal-water slurry decreases. The increase of formaldehyde dosage generates more $NaSO_3.CH_2OH$ intermediate, which can easily react with the active hydroxyl groups and reduce the active sites for condensation reaction. Therefore, negligible increase of the sulfonic group contents and the reduction of the molecular weight of the cardanol-formaldehyde sulfonate are obtained at formaldehyde dosage above 24.2 %. However, the extremely low contents of either sulfonic group content or molecular weight of cardanol-formaldehyde sulfonate results in the worse dispersing ability in coal-water slurry, because only the cardanol-formaldehyde sulfonate with high sulfonic group content and molecular weight can have excellent dispersing ability in coal-water slurry. Therefore, the optimized formaldehyde dosage as 24.2% gives cardanol-formaldehyde sulfonate having the sulfur contents of 16.1% and molecular weight of 14,333 daltons with the minimum apparent viscosity of 399 mPa s.

4.2.4.3 Effect of reaction time in sulfomethylation reaction

The molecular weight and sulfur content are important factors affecting the performance of the dispersant in the disperse system. Therefore, in the synthesized process of condensation polymerization, the variation of reaction times and temperatures were studied together with the control of sulfomethylating agent dosages and formaldehyde dosage. Besides, the performance of coal-water slurry containing cardanol-formaldehyde sulfonate obtained in each condition also was evaluated by apparent viscosity at shear rate of 100 s^{-1}. The results based on dispersing ability of dispersant will be explained by the effect of molecular weight and sulfur contents as shown in Figure 4.9.

The result given in Figure 4.9 shows that the molecular weight of cardanol-formaldehyde sulfonate tends to increase upon an increase of the reaction times. In case of sulfur contents in cardanol-formaldehyde sulfonate, it is found that sulfur contents vary with the reaction times, and then become constant at beyond 8 hours.

Increasing molecular weight and sulfur contents, the apparent viscosity of coal-water slurry tends to markedly decreases at first, and then increases significantly. However, at above reaction time of 8 hours, the molecular weight still sharply increases without any further sulfur content increase, demonstrating the additional crosslink of cardanol-formaldehyde sulfonate. This is reasonable for the enhancement of apparent viscosity beyond reaction time of 8 hours. Therefore, the optimized reaction time for the synthesis in sulfomethylation process is 8 hours, for which obtained cardanol-formaldehyde sulfonate has the molecular weight about 14,631 Daltons with sulfur contents of 17.2% resulting in the lowest apparent viscosity of coal-water slurry of approximately 375 mPa s.

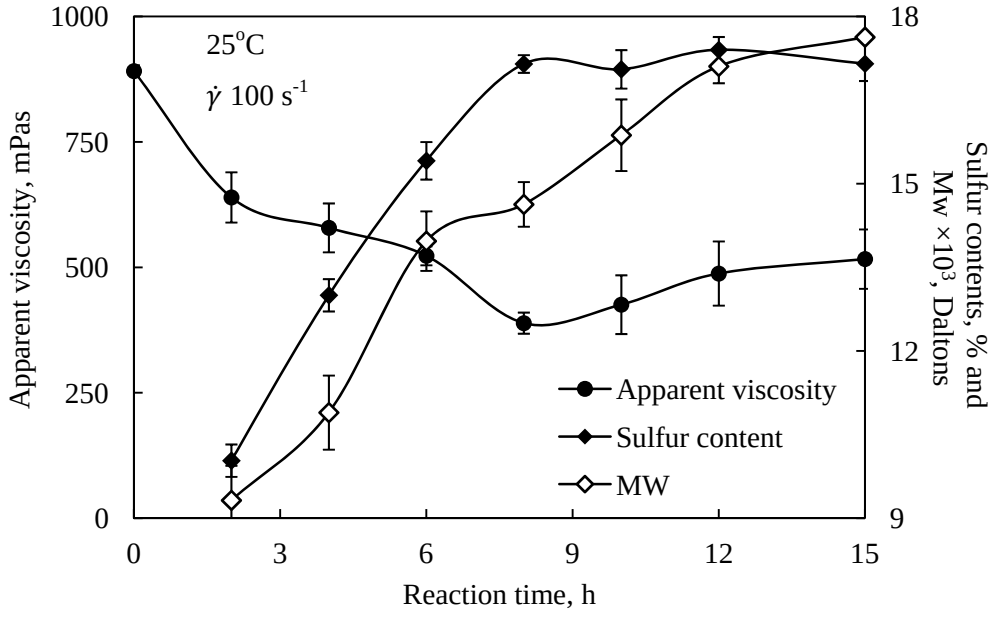

Figure 4.9 Effect of reaction time in sulfomethylation reaction of cardanol-formaldehyde sulfonate on a relation between apparent viscosity of coal-water slurry and, sulfur content and molecular weight, of cardanol-formaldehyde sulfonate.

4.2.4.4 Effect of the reaction temperature in sulfomethylation reaction

As seen in Figure 4.10, the apparent viscosity and sulfur content were plotted against the reaction temperature under the optimal reaction time of 8 hours. It is found that sulfur content increases considerably at first, and then decreases slightly corresponding with the decreased apparent viscosity of the coal-water slurry and also increase again. At the reaction temperature of 80^{o}C, the obtained product has the sulfur contents of 17.5% which affects the lowest viscosity in coal-water slurry as 359 mPas. It should be noted that the exceed temperature above 100^{o}C influences to the high evaporation rate of methanol that is used to dissolve a raw material as cardanol affecting the poor compatibility of reactants. On the contrary, at the low reaction temperature, although the existence of methanol could dissolve easily cardanol but the reaction takes place slowly and incompletely resulting in much remained cardanol in the reaction.

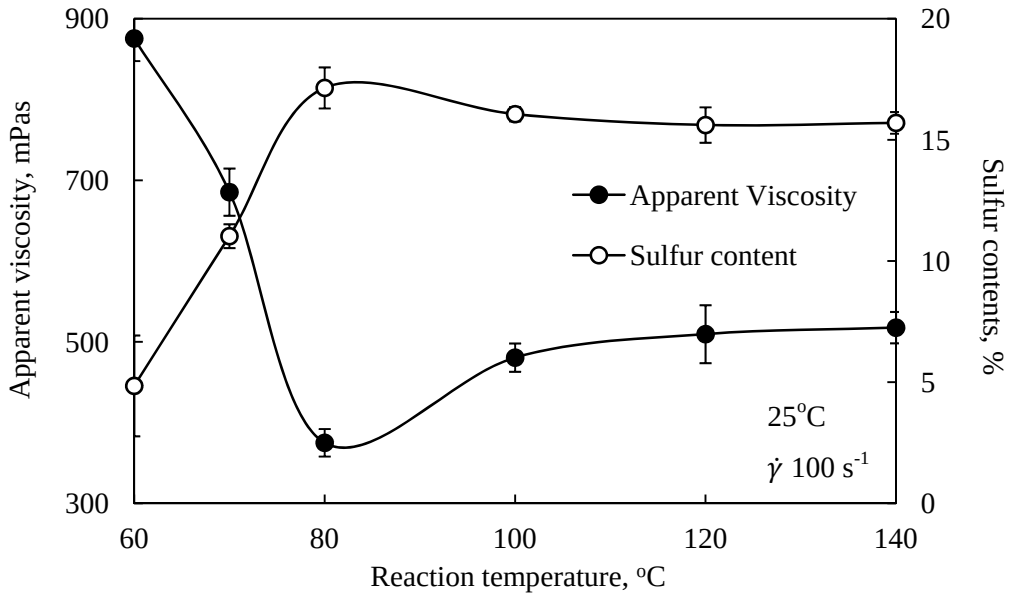

Figure 4.10 Effect of reaction temperature in sulfomethylation reaction of cardanol-formaldehyde sulfonate and apparent viscosity of coal-water slurry.

From the above results, the optimized condition of sulfomethylation reaction that was carried out at 80^{o}C for 8 hours with the suitable amount of sodium sulfite of

15% and formaldehyde of 24%, gives 35 percent yield of cardanol-formaldehyde sulfonate product with the good dispersing performance for coal-water slurry. The final product characterized by, ^{1}H-NMR, and ^{13}C-NMR, and FTIR spectrometer, respectively, is shown in Appendix A.13-A.15.

4.2.5 Physico-chemical properties of cardanol-formaldehyde sulfonate

Physico-chemical properties are explained below. The cardanol formaldehyde sulfonate possesses high molecular weight due to high degree of condensation between cardanol and formaldehyde.

4.2.5.1 Surface tension analysis

The surface tension of dispersant solution, *i.e.*, diethanolamine anacardate, triethanolamine anacardate, cardanol-formaldehyde sulfonate, and sodium lignosulfonate, was prepared with various concentrations in deionized water and measured at 30 ^{o}C. The relation between the surface tension and dispersant concentration is shown in Figure 4.11.

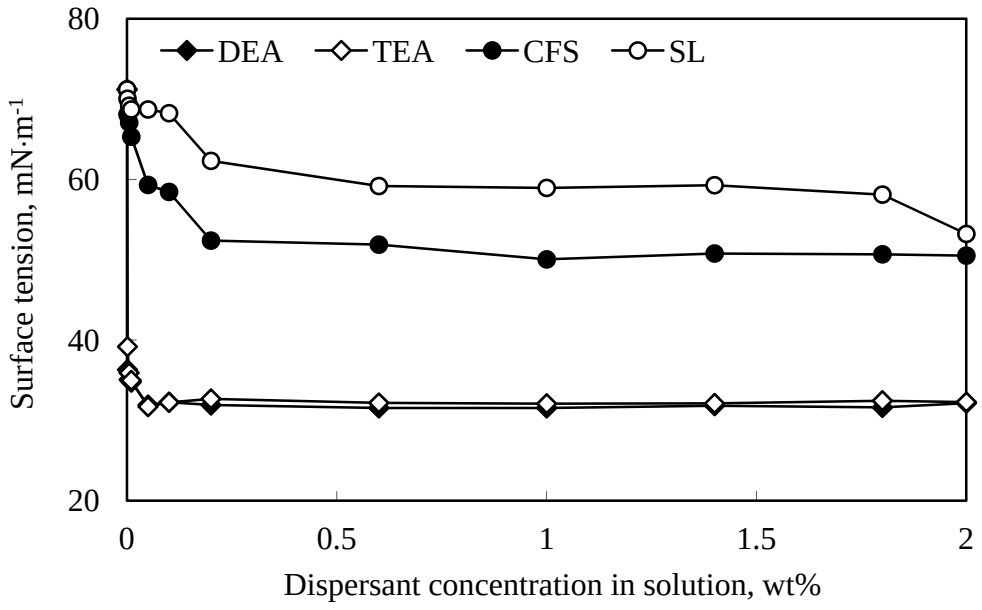

Figure 4.11 Surface tension of the dispersant aqueous solution.

Generally, the surface tension of distilled water is about 71.2 $mN \cdot m^{-1}$ at $30^{o}C$. Figure 4.11 shows that the surface tension of dispersant solution is influenced strongly by various dispersant concentrations especially at low concentration. As the addition of each anacardate salt, diethanolamine anacardate and triethanolamine anacardate, the surface tension of solution tends to decrease sharply and keeps constant beyond 0.05 wt%, in both which gives the same lowest values of surface tension as around 32 $mN \cdot m^{-1}$. Similar behavior is also shown in the surface tension of cardanol-formaldehyde sulfonate solution and sodium lignosulfonate solution that decreases slightly at the increased concentration at first, then the decreased values vary markedly with increasing dispersant concentration in the range of 0.01-0.30 wt% and become constant. Remarkably, decreasing the surface tension of aqueous solution as diethanolamine anacardate, triethanolamine anacardate, and cardanol-formaldehyde sulfonate solutions is greater than that of sodium lignosulfonate, indicating the existence of many hydrophilic structures in dispersant molecules. This result is reasonable for the performance of three synthesized dispersants with high surface activity in water.

4.2.5.2 Inherent viscosity

In general, all polymers increase the viscosity of the solvent when they are dissolved. Increasing viscosity of a polymer solution depends on concentration, size, and molecular weight of the dissolved polymer. Several important viscosity functions are used in this viscosity studies [20-21,38-39].

Since cardanol-formaldehyde sulfonate is a new dispersant expected for coal-water slurry application, it is necessary to study the relationship between the structure of polymers and its viscosity in order to understand the particular rheologic behavior of the polymer solution. For the measurement of the intrinsic and inherent viscosity of cardanol-formaldehyde sulfonate, the viscometer should be selected with the flow time is greater than 100 seconds. When $t > 100$ seconds, it is permissible to ignore the kinetic energy terms. It is then a simple matter to calculate relative viscosity and

specific viscosity by comparing the flow time of the solution, t, to the flow time of the pure solvent, t_0 [53].

$$\eta_r = \frac{t}{t_0} \quad and \quad \eta_{sp} = \frac{t-t_0}{t_0} \tag{4.1}$$

As consideration for viscosity experiments, the relative viscosity is restricted to less than 5 for a linear extrapolation. The intrinsic viscosity requires extrapolation of η_{sp}/c to zero concentration. The simplest approach is to do a simple linear extrapolation 4.2 [53]:

$$\frac{\eta_{sp}}{c} = [\eta] + kc \tag{4.2}$$

In the experimental result, it is revealed that the slope of the η_{sp}/c vs. c curve, k, depends on molecular weight of the polymer. In this case, k is not known, so the typical viscosity experiment is to measure reduced viscosity and inherent viscosity at several concentrations.

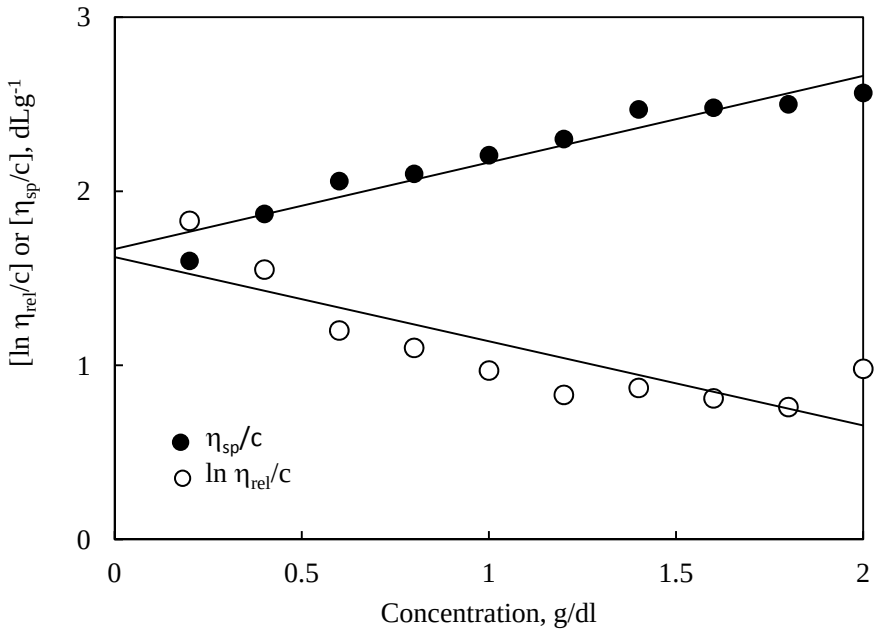

Figure 4.12 Plots of η_{sp}/c and ln η_{rel}/c as a function of concentration of cardanol-formaldehyde sulfonate aqueous solution.

As seen in Figure 4.12, a specific viscosity expresses the incremental viscosity due to the presence of the polymer in the solution. Normalizing specific viscosity to concentration gives η_{sp}/c which expresses the capacity of a polymer to cause the solution viscosity to increase. As with other polymer solution properties, the solutions used for viscosity measurements will be nonideal and therefore η_{sp}/c will depend on c. As with osmotic pressure, it will probably be useful to extrapolate to zero concentration. The extrapolated value of η_{sp}/c at zero concentration is known as the intrinsic viscosity $[\eta]$, will be shown to be a unique function of molecular weight (for a given polymer-solvent pair) and measurements of $[\eta]$ can be used to measure molecular weight. While the inherent viscosity-like specific viscosity, ln η_{rel} is zero for pure solvent and increases with increasing concentration, thus ln η_{red} also expresses the incremental viscosity due to the presence of the polymer in the solution. Normalizing ln η_{rel} to concentration or ln η_{rel}/c gives the inherent viscosity. In the limit of zero concentration, η_{inh} extrapolates the same as η_{sp}/c and becomes equal to the intrinsic viscosity. This can be proved by 4.3 [53]:

$$[\eta] = \lim_{n\to\infty} \frac{\eta_{sp}}{c} = \lim_{n\to\infty} \frac{\ln \eta_{rel}}{c} \qquad 4.3$$

Therefore, the extrapolating either η_{sp}/c or η_{inh} to zero concentration can be determined. When c is not equal to zero the specific viscosity and inherent viscosities will be different, even for an ideal solution.

Indeed, extrapolation to zero polymer concentration is intended to eliminate polymer intermolecular interactions. When the polymer concentration is expressed in g/dl, the units of $[\eta]$ will be dl/g. The plots used to find the intrinsic viscosity are called the Huggins plot (η_{red} vs. c) and the Kraemer plot ($\ln(\eta/\eta_o)$ vs. c). As shown in Figure 1, the curves of both plots should be linear and have a common intercept that is the intrinsic viscosity. For the average viscosity at zero concentration of cardanol-formaldehyde sulfonate is estimated as 1.7 dl/g.

In the industry, as a norm, the polymer molecular weight is reported by inherent viscosity, denoted by [η]. It is related to the molecular weight, M, through the Mark–Houwink equation 4.4 [53]:

$$[\eta] = KM^{\propto} \qquad 4.4$$

where K and α are constants specific to the solvent and temperature used in the measurements.

The inherent viscosity determines the polymer molecular weight and, further, influences the dispersing property of the cardanol-formaldehyde sulfonate. Therefore, the relation between inherent viscosity and apparent viscosity at the variation of concentrations was studied and reported in Figure 4.13.

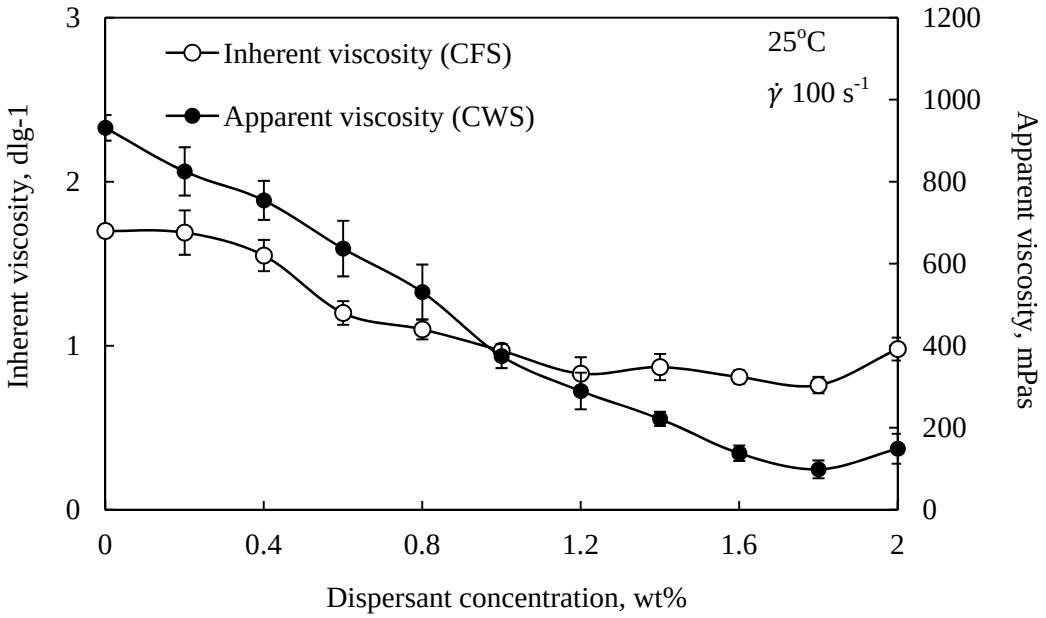

Figure 4.13 The relation of inherent viscosity and dispersing ability of cardanol-formaldehyde sulfonate.

With the increase of dispersant concentration, the inherent viscosity decrease markedly at first and varies slightly at the dispersant concentration above 1.0 wt%. While the viscosity of coal-water slurry also decreases abruptly and then increases a

little. From this relation, it is noted that the dispersing ability of cardanol-formaldehyde sulfonate is influenced by its inherent viscosity, which is affected by the variation of synthesis reaction; sulfomethylation polymerization; such as the mixture ratio of the crude materials and reaction conditions. Therefore, the inherent viscosity of cardanol-formaldehyde sulfonate is close to 1.0 dl/g, performs a good dispersing ability due to low apparent viscosity of coal-water slurry. Finally, it should be noted that the cardanol-formaldehyde sulfonate having the molecular weight of 14,333 Daltons obtained at the ratios of sulfomethylating agent mass to total reactant mass, and formaldehyde mass to total reactant mass as 15% and 24.21 %, respectively, can act as a good dispersant and give lowest apparent viscosity at 1.8 wt% concentration.

4.3 Analysis of coal properties

4.3.1 Proximate and ultimate analysis

Coal analysis is the fundamental understanding before the preparation and handling of highly concentrated coal-water slurry with low viscosity.

Table 4.1 Proximate and ultimate analyses of the bituminous coal sample on dry bases

Component	Items	Value
Proximate analyses	Moisture content (%)	2.73
	Volatile matter (%)	36.04
	Ash (%)	29.71
	Fixed carbon (%)	31.52
	Gross heat of combustion (cal/g)	4,815
Ultimate analyses, dry basis	Carbon (%)	58.97
	Hydrogen (%)	4.65
	Oxygen (%)	35.42
	Nitrogen (%)	0.92
	Sulfur (%)	0.04
	C/O ratio	1.66
Degree of oxidation[a]		0.087
C/O		1.66
O/C		0.60
C/H		12.68

[a]Degree of oxidation: (%O+%N+%S+%H)/(8×%C).

Generally, coal is characterized by proximate analysis which represents the moisture content, volatile content consisting of gases and vapors driven off during pyrolysis (when heated to 950 ^{o}C), the fixed carbon and the ash as the inorganic residue remaining after combustion in the sample, and the heating value based on the completed combustion of the sample to carbon dioxide and liquid water. Further, the

ultimate analysis is also studied to demonstrate the composition of the coal in weight percent of carbon, hydrogen and oxygen (the major components) as well as sulfur and nitrogen (if any). The characteristic of coals is seen in Table 4.1.

From detailed chemical and mineralogical analyses of the Indonesian bituminous coal sample, as well as the calorific values of coal from certain deposits, can be described the degree of oxidation. Oxidation reduces the coal quality by altering the chemical and physical properties of coal. In particular, the calorific value is lowered, and caking is eliminated. There is also floatability during washing of the coal. The weathering of coal results in its physical break-down to fine particles, which enhances hydration and hydrolysis. If the coal is structurally fractured, the extent of oxidation will be greater. The degree of oxidation is determined by the maceral and mineral matter content. All ranks of coal are affected by oxidation, and the degree to which this may occur is influenced by the coal rank, pyrite content, climate, hydrology and by the surface area within the coal accessible to oxidation. One direct side-effect of oxidation is that of spontaneous combustion. This occurs when the rate of heat generation by oxidation exceeds the rate of heat dissipation. As the functional-group oxygen increases with the oxygen content of a coal, it is expected that the number of the hydrophilic sites increases as well. Therefore, the carbon/oxygen ratio (C/O) on the surface of the coal is of great importance.

4.3.2 Particle size distribution analysis

Not only coal type but also the particle size distribution is also an important factor for determining the coal loading and subsequent viscosity. It is generally considered that either a broad size distribution is required to produce highly concentrated coal-water slurry with minimum viscosity. Ball mills have been widely used for the preparation of coal-water slurry because of their availability and capacity. However, the grinding of high-density slurries is not completely understood due to the complexity arising from the dependence of breakage properties on the slurry

characteristics such as the solids concentration, the fineness of the size distribution, and the chemical environment.

Coal obtained from bituminous coal mine should be broken as smaller sizes in order to obtain coarse particles that this research used crushing a lump of coal with carborundum mill twice. After that, the crushed coals were comminuted in conventional ball mill to obtain products of different particle size distributions by controlling the grinding tests that were conducted under various conditions to optimize the properties of coal-water slurry. This research studied the effect of grinding time and grinding ratio by the mixture of coal and water without the use of a dispersant. Finally, particle size distributions varying sizes from 1 to 600 μm were achieved.

4.3.3 Grinding Test

4.3.3.1 Grinding Time

In laboratory scale, the cone and roll crushers were used to reduce the particle size of crush coals less than 1 mm. Then, a typical set of size distribution data for various grinding times is processed by using the ball mill, of which the feed curve shows broad particle size distribution as illustrated in Figure 4.14.

As the grinding procedure, the curves of coal grinding time at 5 and 10 hours show similar patterns due to the closed grinding time whereas percent cumulative coal at grinding time of 24 hours is dramatically increased around cumulative under size of 86 % with finer particle sizes approximately 100 μm. While the curve of grinding time at 48 hours exhibits a lower level and parallel manner with that of grinding time of 24 h. However, it is expected that ball mill process with long grinding time could conduct high-efficiency grinding for small particles. But the experimental result indicates that grinding time process carried out for a long period of time leads to the poorer grinding ability. This result may be explained by some heatup effect during

grinding and insertion of smaller particles in larger particles sizes causing coal-coal aggregation.

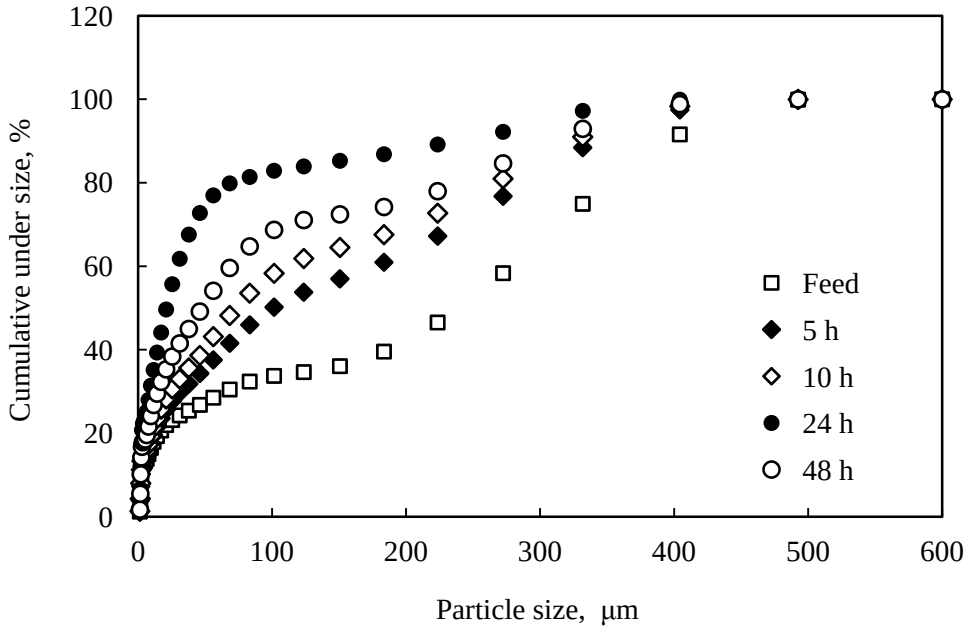

Figure 4.14 Particle size distribution of coal powder at various grinding times.

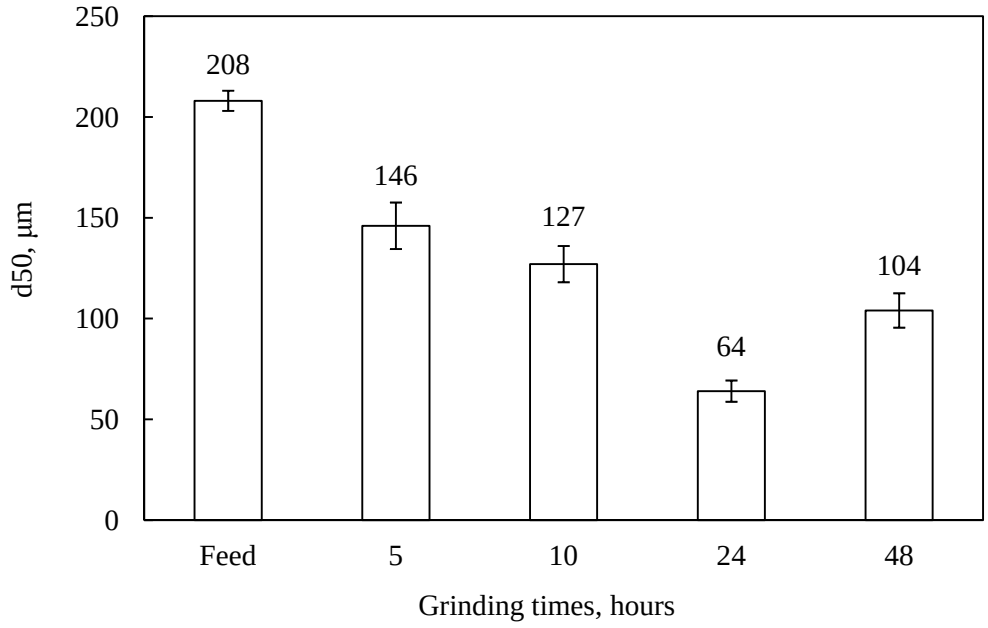

Figure 4.15 d_{50} of coal samples at various grinding times.

In Figure 4.15 shows the averaged particle size, d_{50}, is defined as the diameter where 50 mass percent of the coal particles has a larger equivalent diameter, and the other 50 mass percent has a smaller equivalent diameter. This value was estimated by Malvern particle size analyzer. The above results correspond with the d_{50} value that the best averaged coal particles size as 64 μm is obtained at the grinding time of 24 h.

4.3.3.2 Grinding ratio

Figure 4.16 shows various grinding ratios of coal and water carried out at a fixed grinding time of 24 hours. It can be found that at grinding ratio of low concentrated coals, numerous finer product sizes less than 100 m is obtained at more 80% cumulative size whereas fine coal sizes after grinding at high concentrated coals tend to decrease indicating slow grinding rates. By the coal concentration of 48 percent by weight exhibits the highest grinding rate, attaining more 80% cumulative size with 100 μm particle size which has mean particle size of 64 μm. It should be noted that changing the slurry density also changed the shape of the size distribution.

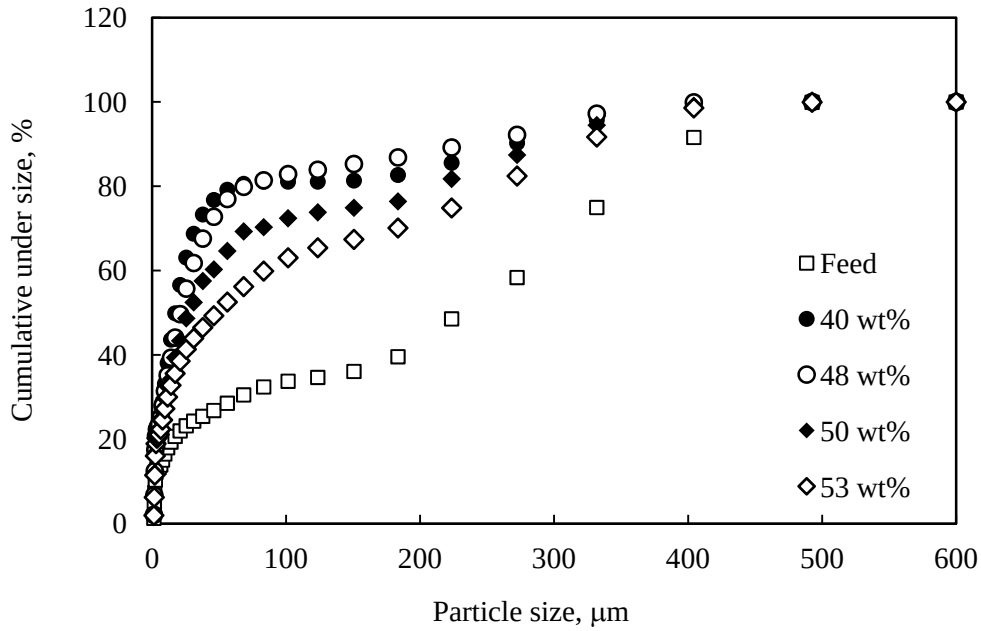

Figure 4.16 Particle size distribution of pulverized coal at various grinding ratios of coal and water.

From experimental results, it is seen that the grinding rate decrease as the solids concentration increased resulting from the increase in slurry viscosity. However, the quantity and finer size of coal particles can be significantly increased with specific conditions. Therefore, coal powder obtained from the optimized grinding conditions, which was carried out at grinding time of 24 h with 48 wt% coal loading without the addition of any dispersants, was employed for coal-water slurry preparation in the further experiment and its particle size distribution is shown in Figure 4.17.

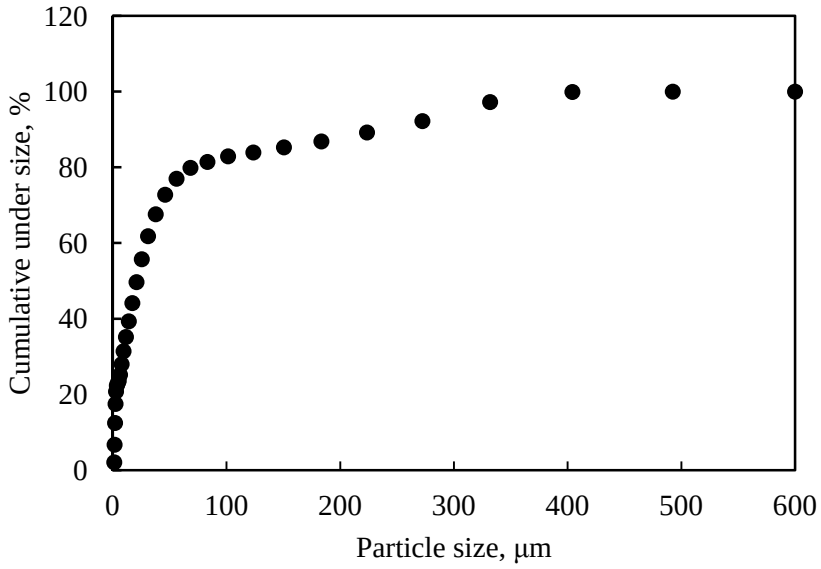

Figure 4.17 Particle size distribution of bituminous of coal sample.

4.4 Rheological property of coal-water slurry

Viscosity is an internal property of liquid which resists the motion of different layers and this opposing force arises largely due to van der Waals forces of the molecules. In order to prepare the suitable viscosity with the highly concentrated coal-water slurry for handling, transport, and atomization, the coal particles have to be in non-flocculated or non-aggregated state.

4.4.1 Effect of coal size on apparent viscosity

The effect of the particle size distribution on viscosity was investigated for various coal sizes such as -45, 45-80, 80-100, 100-125, 125-200, and +200 μm. The results of apparent viscosity measurements at 25^{o}C with shear rate of 100 s^{-1} are given in Figure 4.18. All experiments were conducted using 40, 45, 50 and 55% solid contents by weight.

As seen in Figure 4.18, it is found that the apparent viscosity of samples depends on their mean particle sizes, in which the apparent viscosity increases along the increased coal concentration and decreasing mean particle size. Even though samples have the different mean particle sizes, their viscosities differ slightly at low coal concentration whereas the difference of viscosity distinctly appears at high coal concentration. At 50% coal concentration, the coal-water slurry with fine particle size (-45 mm) shows an apparent viscosity about 1523 mPas compared to 923 mPas for the coarse ones (80-100 mm). The fineness of coal particles which increase viscosity of coal-water slurry actually causes the reduction of rheological property but improves coal-water slurry stability and may reduce stabilizing additive consumption. Generally, the viscosity of coal slurry fuel depends primarily on coal particle size distribution, viscosity of solvent, coal concentration and operating temperature. Therefore, coal slurry can be prepared by mixing different coal particle size fractions in 50% total amounts of coal concentration for which a particle size distribution with 10-80% of the particles should be in the range of 45-100 μm. Although the coal-water slurry prepared by coal particle sizes above 125 micron gave the lower viscosity, the poorer stability was obtained.

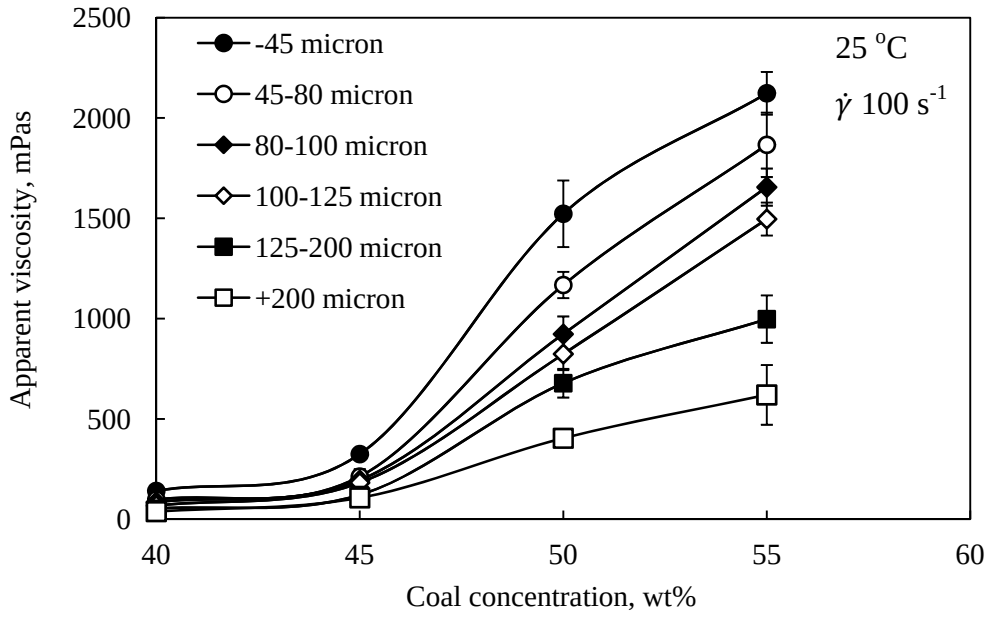

Figure 4.18 Variation of apparent viscosity of coal-water slurry without dispersant with coal concentration in slurries of different particle sizes.

4.4.2 Effect of the dispersant type on apparent viscosity

From Figure 4.19 shows the effect of coal concentration on apparent viscosity for coal-water slurry containing various dispersant types of 1.0% as diethanolamine anacardate, triethanolamine anacardate, cardanol-formaldehyde sulfonate and sodium lignosulfonate. In general, conventional coal-water slurry without additives could be piped but, due to an approximate 50% water content, exhibited high viscosity, poor long-run stability, and required dehydration before firing because of the coal nature with high degree particle-particle aggregation.

The experimental results exhibit the highest apparent viscosity of coal-water slurry without dispersant whereas coal-water slurry with each dispersant shows the lower viscosity. With a trend of apparent viscosity increasing along the increased coal concentrations, the difference of coal-water slurry with/without dispersant on apparent viscosity could be significantly observed beyond the coal concentration of 45 wt%. Sharply increasing in the apparent viscosity of coal-water slurry with the

concentration of coal is explained for the frictional forces between the particles becoming significant, and the accompanying resistance.

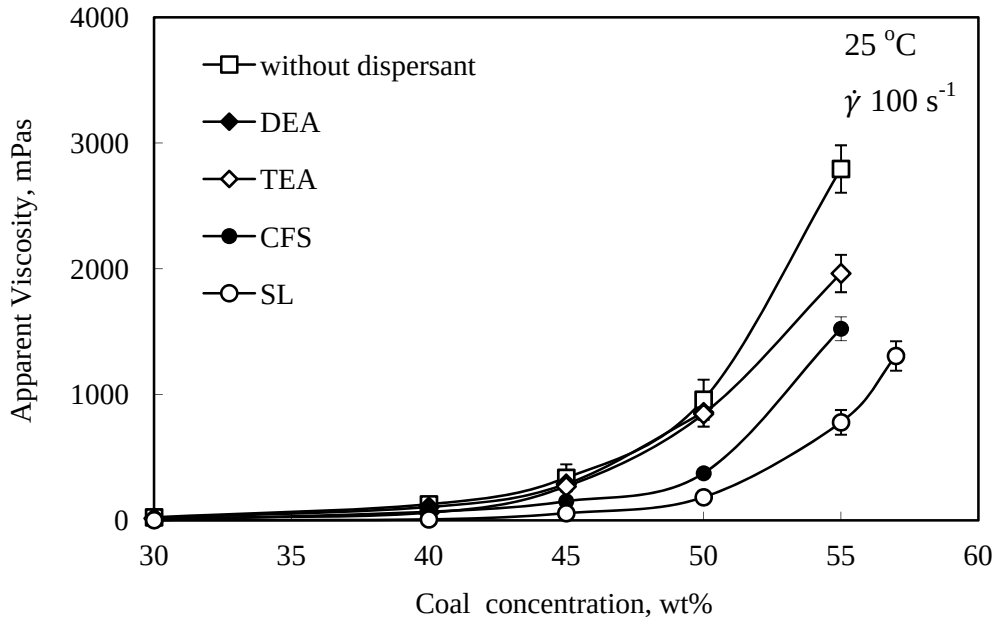

Figure 4.19 Variation of apparent viscosity with solid concentration in slurries of different dispersant at 1% concentration.

As employing diethanolamine anacardate and triethanolamine anacardate as dispersants in coal-water slurry, the apparent viscosity decreases slightly in comparison with coal-water slurry in the absence of dispersant. Although the surface activity of such kinds of carboxylic salt species derivatized from anacardic acid is better than that of cardanol-formaldehyde sulfonate due to the lower surface tension value, the viscosity of coal-water slurry containing anacardate salts was much higher than that of cardanol-formaldehyde sulfonate. This is due to the complicated structure of crosslinked cardanol-formaldehyde sulfonate acting as hydrophobic part is adsorbed on hydrophobic coal surface, and sulfonate groups acting as hydrophilic part protrude to water molecules, result in better prevention of coal particle coalescence. Furthermore, the viscosity of coal-water slurry containing cardanol-formaldehyde sulfonate also is higher than that of sodium lignosulfonate.

4.4.3 Effect of the dispersant concentration on apparent viscosity

Figure 4.20 depicts the influence of various dispersant concentrations in the range of 0.2-2.0 wt% in steps of 0.2 wt% on fixed coal concentration of 50 wt% under shear rate of 100 s^{-1}. It is revealed that the apparent viscosities of coal-water slurry containing each dispersant, decrease abruptly in proportion to the increased dispersant concentration and reach a minimum. However, coal-water slurry containing diethanolamine anacardate or triethanolamine anacardate is expected to be a good dispersant because of the strong surface activity, but the obtained viscosity is slightly different from coal-water slurry without dispersant, at a minimum viscosity of 705 mPas as detected by using diethanolamine anacardate and 715 mPas for using triethanolamine anacardate at same concentration of 1.4 wt%. There seems to be no significant difference of apparent viscosity between coal-water slurry containing diethanolamine anacardate and triethanolamine anacardate because of the similar chemical structure and surface tension to each other. This result indicates the weak influence of adding hydrophilic groups by diethanolamine and triethanomine for preparation of carboxylic salt species derivatized from anacardic acid. Moreover, it is observed clearly that the apparent viscosity of coal-water slurry containing cardanol-formaldehyde sulfonate or sodium lignosulfonate is much lower than that of coal-water slurry containing diethanolamine anacardate or triethanolamine anacardate. It’s probably because of less amount of hydrophilic group and weaker hydrophilicity of ethanolamine group. Cardanol-formaldehyde sulfonate concentration of 1.0 wt% gives almost twice higher viscosity than that of sodium lignosulfonate, the minimum viscosities of both dispersants are approximately 100 and 120 mPa s, respectively. The viscosity is likely to increase again slightly at higher dispersant concentrations because the excessive addition of dispersant concentration leads to higher flow characteristic value in consequence of the dilatant fluid behavior.

For a hydrophobic solid like coal, the most probable mechanism of adsorption of dispersant at the coal-water interface is the adsorption of dispersant with its hydrophobic group being anchored on the coal surface while the hydrophilic chains have to remain dangled in the bulk water. This orientation of di/triethanolamine

anacardate at the coal-water interface is supported by adsorbing non polar group that some di/triethanolamine anacardate molecules exist in water is expected act as micelle form, while there are still many di/triethanolamine anacardate molecules dissolve independently in water. Because of the short hydrophobic chain in di/triethanolamine anacardate, less interaction of hydrophobic force with coal surface occurs. Therefore, the apparent viscosity of coal-water slurry containing di/triethanolamine anacardate is much higher than that of coal-water slurry containing cardanol-formaldehyde sulfonate and sodium lignosulfonate indicating the poorer dispersing performance. In conclusion, both diethanolamine anacardate and triethanolamine anacardate are not the suitable dispersant used for coal-water slurry application. Therefore, cardanol-formaldehyde sulfonate was employed for coal-water slurry preparation for further study of rheological behavior, in comparison with sodium lignosulfonate.

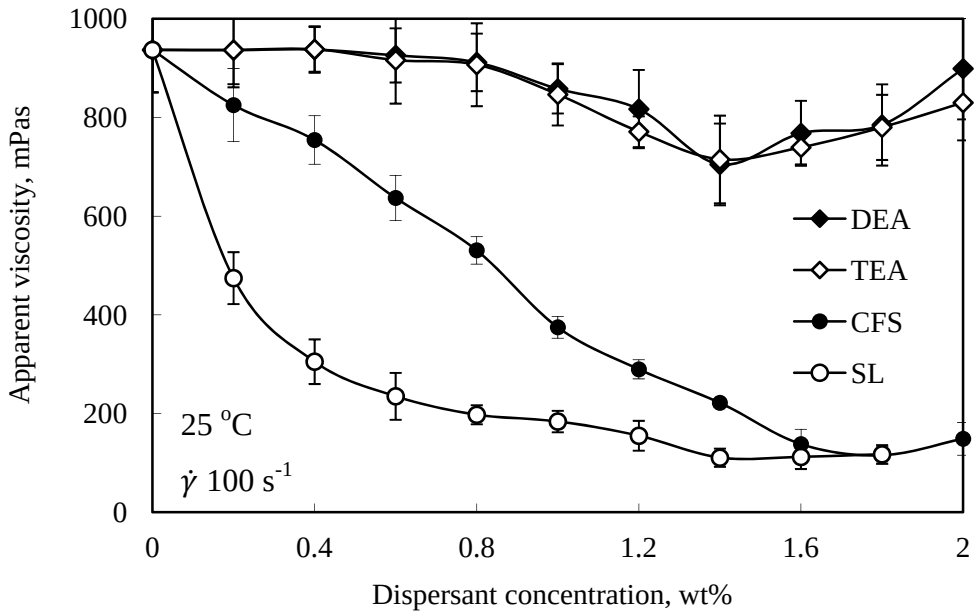

Figure 4.20 Effect of dispersant concentration on apparent viscosity of coal-water slurry.

From the above results indicate that coal concentration of 50 wt% or more with the cardanol-formaldehyde sulfonate concentration in range of 1.0-1.8 wt% is suitable for the coal-water slurry preparation in the present experiment. In order to clarify the rheological behavior, coal-water slurry in the presence of dispersant,

cardanol-formaldehyde sulfonate, was prepared in two concentrations; one is 1.0 wt% for commercial industrial possibility and the other is 1.8 wt% for the best coal-water slurry behavior expectation.

4.5 Rheological behavior studies of coal-water slurry

A theoretical understanding of the factors influencing coal slurry rheology is type of coal, coal concentration, particle size distribution, temperature, type and concentration of dispersant for the formulation of slurry. The characterization of the rheological behavior of the coal-water slurry is studied to understand the phenomenon involving in the preparation and handling of coal-water slurry to achieve the highest possible coal concentration at desired slurry viscosity level while maintaining slurry stability.

The principle of rheological examination is a basis for calculations of transports suspension with high concentration within the laminar flow. In general, pastes consisting of mineral particles and water perform rheological phenomenon as the pseudoplastic (shear thinning) fluids for which the Bingham's law is applied to define properties of the concentrated suspensions with a good approximation given by 4.5 [37];

$$\tau = \tau_0 + \eta_p \, \mathrm{dv/dr} = \tau_0 + \eta_p \dot{\gamma} \qquad 4.5$$

where τ is shear stress in N/m, τ_0 is yield limit or minimum yield stress in N/m^2, η_p is defined as plastic viscosity in Pa s, and $\dot{\gamma}$ is applied shear rate in s^{-1}.

4.5.1 Effect of coal concentration

The Bingham relation is a two parameter model used for describing viscoplastic fluids exhibiting a yield response. The ideal Bingham material is an elastic solid at low shear stress values and a Newtonian fluid above a critical value

called the Bingham yield stress, σ_B. Using the Bingham plastic model in an equation 5, the estimated values of yield stress are computed graphically from the plot of shear stress versus shear rate, are seen in Figure 4.21. The yield stress evaluated from shear stress in response to applied shear and the apparent viscosity measured at shear rate of 100 s^{-1} by using cardanol-formaldehyde sulfonate as dispersant at the concentration of 1 wt% with variation of coal concentrations, are listed in Appendix B-17.

The flow is governed by the usual conservation equations of mass, momentum and energy for incompressible fluids and laminar flow. To model the stress-deformation behavior of viscoplastic materials, different constitutive equations have been proposed. In simple shear flow takes the form as seen in Figure 4.21 [40].

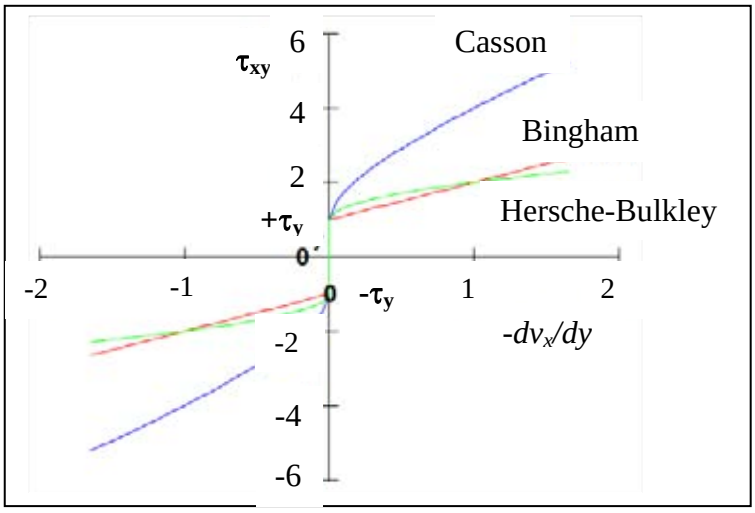

Figure 4.21 Shear stress (τ_{xy}) vs. shear rate ($\dot{\gamma}_{xy}= dv_x/dy$) for different types of viscoplastic models [40].

This model was selected and applied throughout this work to estimate the flow models such as Bingham plastic and Herschel-Bulkley. The Newtonian fluid is representing a straight line, the Bingham fluid appears to be linear but do not extrapolate through the origin, whereas Herschel-Bulkley fluid in which the strain experienced by the fluid is related to the stress in a complicated, non-linear way. In the fluid diagram with arithmetic plot all curves (Figure 4.22), the characterization of

the rheological behavior in coal-water slurry containing cardanol-formaldehyde sulfonate at 1% concentration were studied with the variation of coal loadings. It is revealed that the shear stress increases from a minimum with shear rate, indicating the Bingham behavior at coal concentration 40-53 wt%. While fluids at coal concentration between 53-57 wt% are classified as the Herschel-Bulkley fluid model, in which a certain minimum stress is required to initiate flow, but less stress with increasing shear.

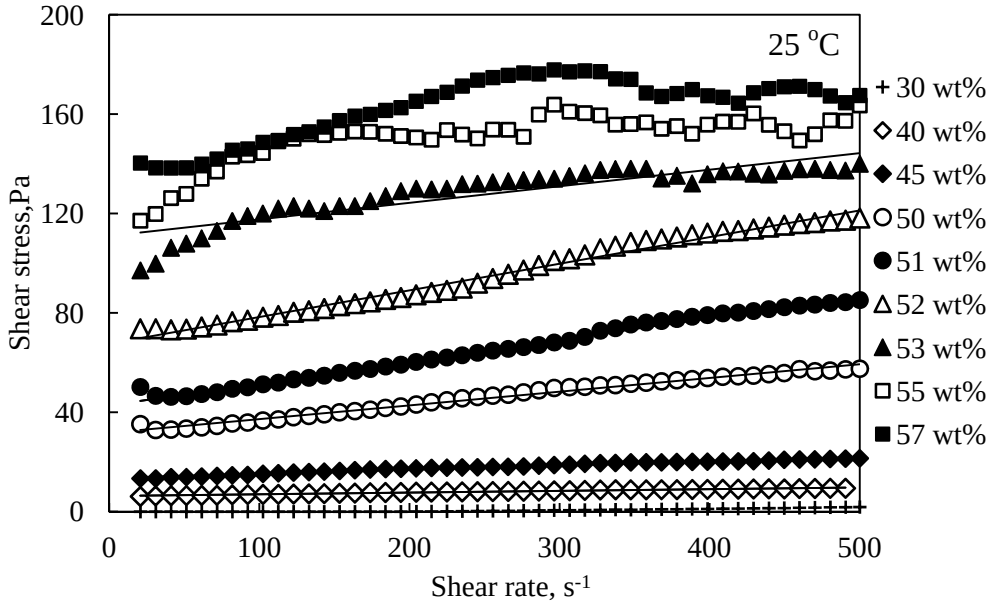

Figure 4.22 Rheogram of coal-water slurry containing cardanol-formaldehyde sulfonate of 1.0 wt% at different coal concentrations.

Using the Bingham plastic model, the experimental results from Figure 4.22 were correlated and the estimated values of yield stress were listed in Table 4.2 and the curve fitting of each coal concentration were shown in Appendix B-2, B-3, and B-4, respectively.

Table 4.2 Rheological parameters derived from Bingham Plastic model fit to the data of Figure 4.22

Coal concentration (wt%)	R^2	Yield stress
30	0.99	-1.25
40	0.98	6.28
45	0.98	13.59
50	0.99	31.71
51	0.99	42.73
52	0.98	67.60
53	0.79	110.94
55	0.53	136.79
57	0.59	145.69

In concentrated suspensions, when attractive forces prevail, solid particles aggregate to form extended structures within the suspension and the strength of such network manifests by the presence of a yield stress which exhibit the higher value with higher coal concentration. The highly concentrated suspensions did not behave exactly according to the Bingham's law because of the exceeded aggregation, the viscosity of these fluids was defined as an apparent one. On the contrary, repulsive particles became dispersed suspension that result in the yield stress decrease. At low coal concentration up to 45 wt%, the coal-water slurry exhibits a linearly Newtonian fluid. As the coal concentration is increased, it is seen that beyond 50 wt% the onset of a yield stress is apparent due to the higher degree of aggregation between coal particles. These results correspond with the apparent viscosity which moderately increases with the increase of coal concentrations as shown in Figure 4.23. It is observed that the coal-water slurry viscosity rises as an exponential curve at high concentrations that increase sharply in the region of 50-57%.

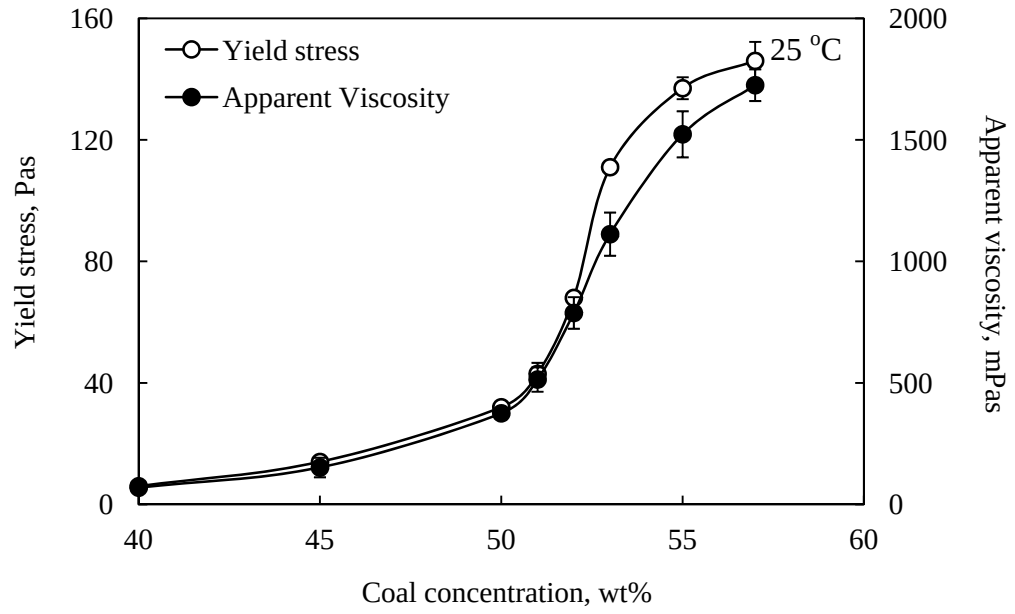

Figure 4.23 Changing in yield stress and apparent viscosity of coal-water slurry containing cardanol-formaldehyde sulfonate of 1.0 wt% as function of coal concentrations.

4.5.2 Effect of dispersant concentration

Figure 4.24 summarizes the effect of dispersant concentration on apparent viscosity with coal concentration of 50 wt%. The optimum concentration of synthesized dispersant, cardanol-formaldehyde sulfonate is in range of 1.0-1.8 wt%, at which low apparent viscosities are obtained. For a good-quality of highly concentrated coal-water slurry, the requirement is not only the low viscosity, but also good stability and low concentration of dispersants. Therefore, the dispersant concentration of 1.0 and 1.8 % were studied to explain the rheological behavior of coal-water slurry containing cardanol-formaldehyde sulfonate compared with that containing sodium lignosulfonate.

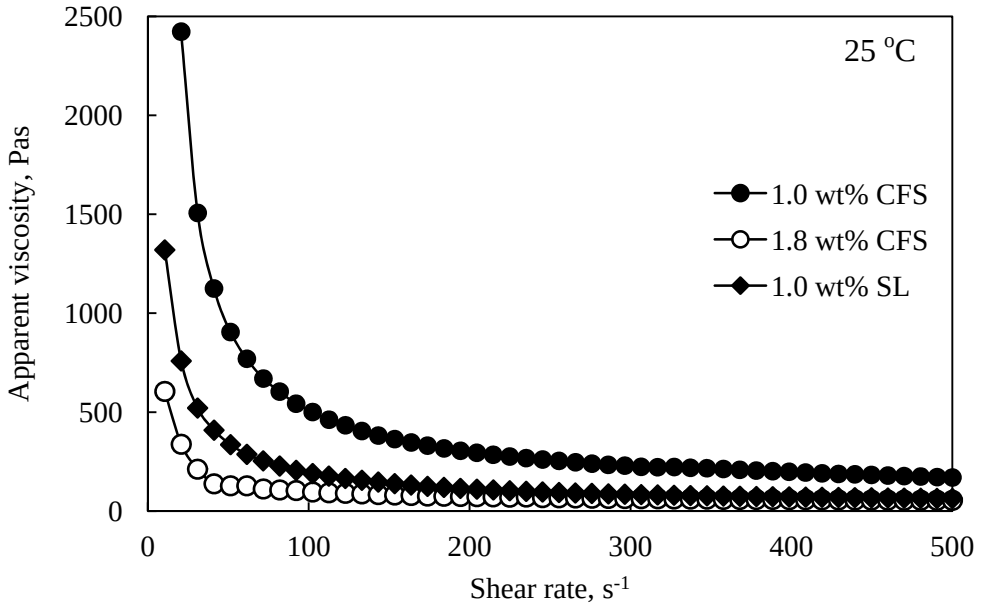

Figure 4.24 Plot of the apparent viscosity for coal-water slurry with the variation of the shear rates (50 wt% of coal in coal-water slurry).

From the above discussion, it is well known that the rheological behavior of coal-water slurry is a non-Newtonian fluid characteristic because the viscosity is influenced from the variation of shear rates. The variation in the rheological behavior due to the changes in colloid interactions among the coal particles is clearly seen in the plots of apparent viscosity against shear rate in Figure 4.24. It is evident from the results that all the suspensions show shear-thinning behavior, i.e., the apparent viscosity rapidly decreases with increasing shear rate up to 100 s^{-1}, above which it becomes constant. At a higher shear rate, the breaking of coal agglomerates occurs. This is the case for all the three types of coal-water slurry. Noticeably, the viscosity of coal-water slurry containing cardanol-formaldehyde sulfonate of 1.8 wt% shows little change to no effect at the various applied shear rates.

In the Bingham model, the apparent viscosity is represented by the ratio between the shear stress above minimum yield stress and shear rate. The plots of shear stress with variation of shear rates of coal-water slurry in the presence of 1.0 and 1.8 wt% of cardanol-formaldehyde sulfonate and 1.0 wt% of sodium lignosulfonate were shown in Figure 4.25. A linear shear stress-shear rate relationship

with an initial shear stress threshold is found. The variation of shear stress with shear rate indicated Bingham behavior.

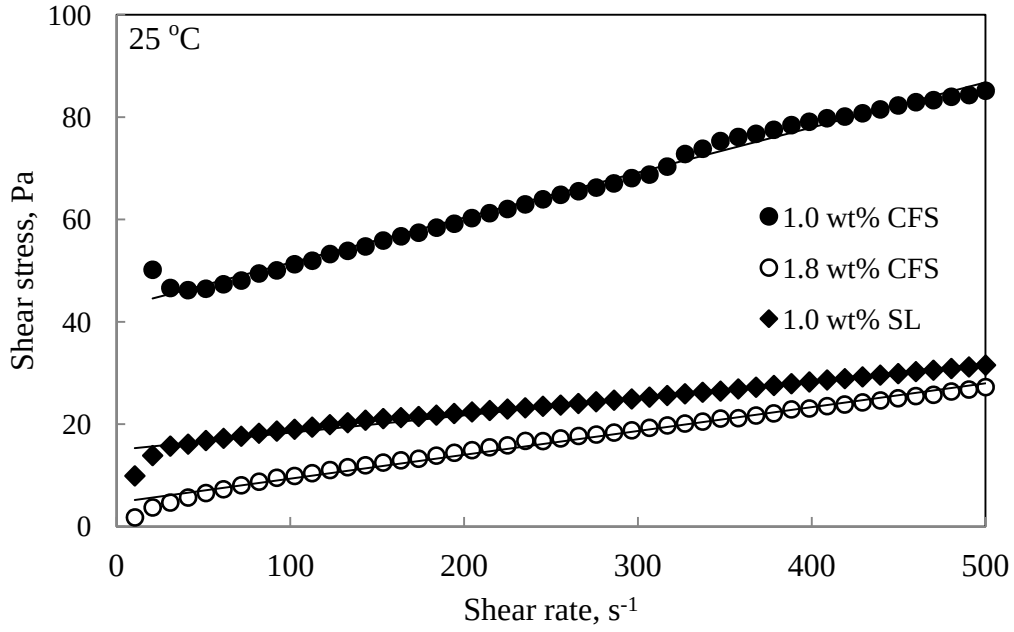

Figure 4.25 Effect of the cardanol-formaldehyde sulfonate concentration comparable to sodium lignosulfonate on rheological behavior of coal-water slurry.

Since the yield stress is governed by the resistance of the particle aggregation against shear deformation, it is desired to enhance the interacting force among the particles. From Figure 4.25, it is found that by increasing cardanol-formaldehyde sulfonate concentration from 1.0 to 1.8 wt% at a shear rate of 100 s^{-1}, the rheological behavior of coal-water suspension changes from Bingham-plastic through Newtonian with simultaneous decrease of yield point from 40.29 to 3.92, respectively. In addition, at sodium lignosulfonate concentration of 1.0 wt%, the yield stress was 15.14. It indicates that the flocculation (i.e., aggregation of particles) of coal-water slurry is substantially reduced with the increase of cardanol-formaldehyde sulfonate concentration, which thereby causes reduction in yield stress and apparent viscosity.

4.6 Temperature dependence on apparent viscosity of coal-water slurry

Temperature is related to the average kinetic energy of the molecules of a substance which correspond with mobility rate of the molecules. If temperature is measured in Kelvin degrees, then this number is directly proportional to the average kinetic energy of the molecules.

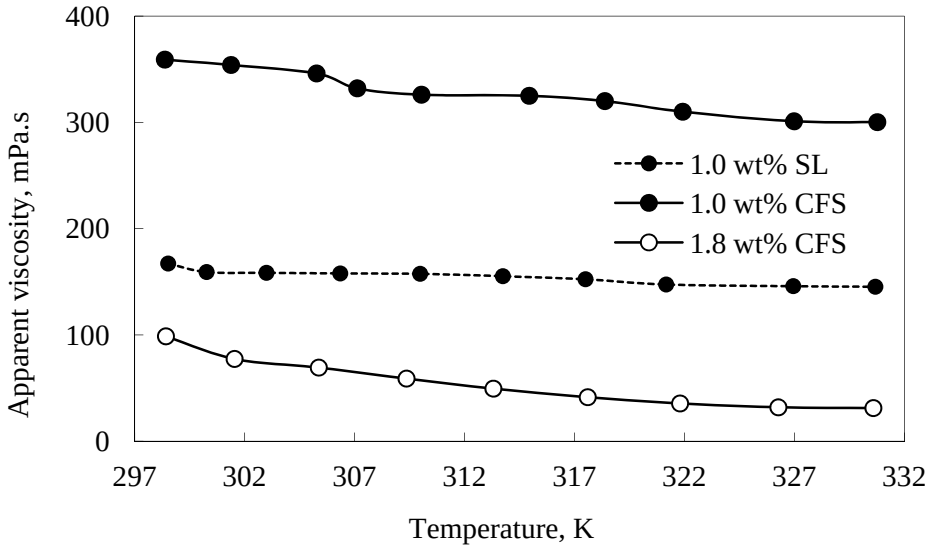

Figure 4.26 Effect of temperature on apparent of coal-water slurry (50 wt%coal loading) containing each dispersant as cardanol-formaldehyde sulfonate (CFS) and sodium lignosulfonate (SL) at a shear rate of 100 s^{-1}.

Figure 4.26 shows the temperature dependence of the apparent viscosity of coal-water slurry at shear rate of 100 s^{-1}. It is found that at the concentration of dispersant as 1.0 and 1.8 wt%, the apparent viscosity of coal-water slurry tends to decrease significantly as its temperature increases even the different viscosity levels. The slight increase in temperature promoted the possibility of collision between the carbonaceous particles and resulted in an increase in the coagulation tendency of the particles. While at higher temperature, the increased kinetic energy in the faster molecules did not promote the aggregation between coal particles demonstrating the dispersibility [54].

The temperature dependence of liquid viscosity is the phenomenon by which liquid viscosity tends to decrease as its temperature increases. The rheological properties of a Newtonian fluid or polymer liquid obey consistently with the Arrhenius equation for molecular kinetics as shown below in equation 4.6 [6,54**]**.

$$\eta = A\, exp(Ea/RT) \qquad 4.6$$

where η is the apparent viscosity at a particular shear rate, A is the characteristic constant for polymers of a specific shear rate and molecular weight, Ea is the fluid flow activation energy, R is the universal gas constant, and T is temperature in Kelvin.

Another common modification is the stretched exponential form in equation 4.7.

$$ln\,(\eta) = E/RT + ln\,(A) \qquad 4.7$$

According to equation 4.7, a plot of $ln\,(\eta)$ versus $1/T$ (Kelvin) gives a straight line, in which shows a slope of E/R and intercept of $ln\,A$, as seen in Figure 4.27.

Figure 4.27 shows the variation of natural logarithmic of apparent viscosity as a function of the reciprocal temperature for cardanol-formaldehyde sulfonate at 1.0 and 1.8 wt% concentrations. As is well known, at higher temperatures, the probability that two molecules will collide is higher. This higher collision rate results in a higher kinetic energy, which has an effect on the activation energy of the reaction. The activation energy is the amount of energy required to ensure that a reaction happens. This results in a decrease in the viscosity of the coal-water slurry.

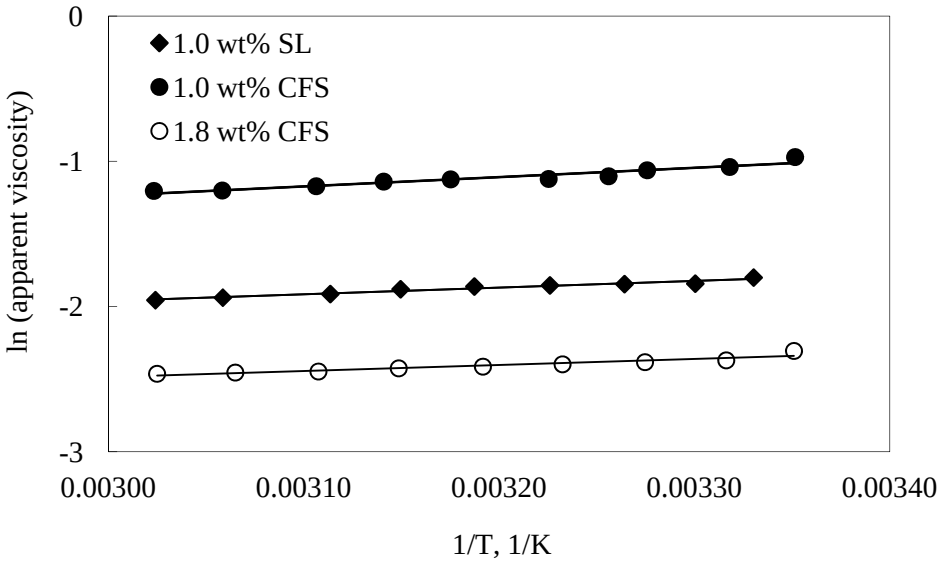

Figure 4.27 Arrhenius plot of viscosity versus temperature for coal-water slurry containing cardanol-formaldehyde sulfonate of 1.0 and 1.8 wt%.

In the experimental result, the values of linear lines with correlation coefficient and the fluid flow activation energy for the coal-water slurry of 50 wt% coal concentration at the shear rate of 100 s^{-1}, is reported in Table 4.3. It may be noted that there is little change in the apparent activation energy with concentration of dispersant. The fluid flow activation energy due to viscous flow is found to depend on the type of coal used being highest for low ash coal and lowest for high ash coal, whereas is essentially independent of the rate of shear and coal concentration [5,37].

Table 4.3 Fluid-flow activation energy as a function of the solid concentration for coal-water slurry of different coal samples

Sample	Activation Energy [kJ/mol]	R^2
1.0 wt% SL	55.60	0.96
1.0 wt% CFS	76.87	0.92
1.8 wt% CFS	50.18	0.93

4.7 Zeta potential investigation

A simple micro electrophoresis apparatus was used to determine the zeta potential of the coal particles at various pH levels and under conditions of dilute concentration. The measurements were made using an electrophoresis cell, a regulated voltage supply and a microscope. An electrical potential is applied across the two electrodes which are spaced at a specified distance from each other. According to the extended Derjaguin–Landau–Verwey–Overbeek (DLVO) theory of colloid stability describes the force between charged surfaces interacting through a liquid medium. It combines the degree of particle dispersion/aggregation is governed by a balance between repulsive (electrostatic, hydration, steric) and attractive (van der Waals, hydrophobic) interparticle forces [43]. In coal-water suspension, the ionic dispersant adsorbed on coal surface improves the hydrophilic property and increasing the electrical properties of the coal surface. The coal surface is charged with negative electrons in coal-water suspension, and the adsorbed anionic dispersant can modify the electrical properties of the coal water interface.

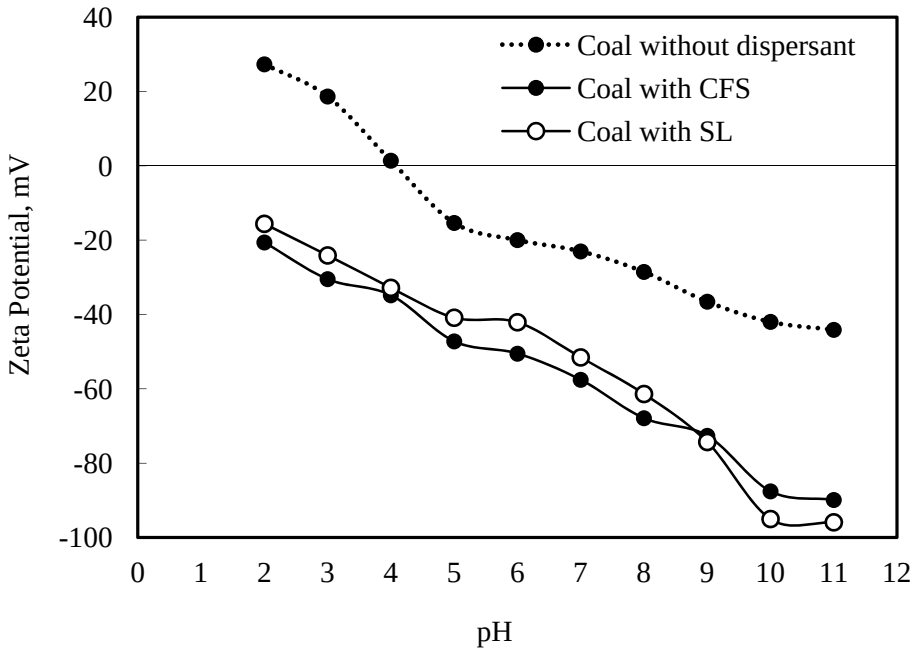

Figure 4.28 Variation of the zeta potentials for Indonesian bituminous coal with changing in pH using deionized water.

In the experiment, the electrophoretic mobility (zeta potential) of the coal particles was determined with the variation of pHs and various concentrations of the anionic dispersants; cardanol-formaldehyde sulfonate and sodium lignosulfonate. Coal surface contains polar groups such as -COOH and-OH attached to the hydrocarbon skeleton connected by cross-links. Depending on the pH of the solution, the polar groups get protonated or ionized when suspended in water. At acidic pH, protonated hydroxyl and carboxyl group will render positive charge and at alkaline pH dissociated hydroxyl and carboxyl group would render negative charge to the coal surface. These charges account for its zeta potential when electric field is applied.

As shown in Figure 4.28, the effect of pH on the zeta potential of coal particles was conducted using samples in the absence and presence of dispersants for each test. The initial dispersant concentrations used were 200 mgL^{-1} and coal of 10 wt% for all measurements. For Indonesian bituminous coal, the natural pH of a prepared coal-water suspension used in this experimental trial is slightly acidic at pH levels of approximately 6.7. The zeta potential of the coal particles in this case is approximately -23 mV. Over the pH range of 2.0-6.0 the zeta potential lies in the range of +27 mV to -20 mV. This particle surface characteristic is referred to the isoelectric point at pH of approximately 4.0. Since at the isoelectric point the residual charge on coal particle becomes zero, greater cooperative interaction of the cardanol-formaldehyde sulfonate adsorbed on coal particles takes place. Therefore, coal particles settle down easily because of highest yield stress. Consequently, at this pH, more energy for pumping is required for the slurry flow than for any other pHs. In Figure 4.27, it is important to note that the addition of dispersant affects dramatic low-zeta potential of coal samples. The zeta potentials are negative over the whole pH range for coal in the presence of the dispersant. However, cardanol-formaldehyde sulfonate and sodium lignosulfonate is used at same initial loadings, no signicant differences were observed at the zeta potential values. The marked decrease of zeta potential point is due to the large number of hydroxyl and sulfonate groups demonstrating adsorbed cardanol-formaldehyde sulfonate which may also be dissociated and protonated depending on the pH of the solution. The electrostatic repulsion between intense negative charges developed on coal surface due to the

ionization of the polar groups preventing particle-particle association as the pH of slurry increases.

This results in reduction of apparent viscosity. The coal sample acquires -88 and -95 mV zeta potential values around pH 10 in the presence of dispersant as cardanol-formaldehyde sulfonate and sodium lignosulfonate, respectively. This finding is important since above these absolute zeta potential values adequate dispersion can be sustained. As a result, highly negative charges on coal surface from the interaction of dispersant would prevent particle-particle association and affect the dispersing achievement.

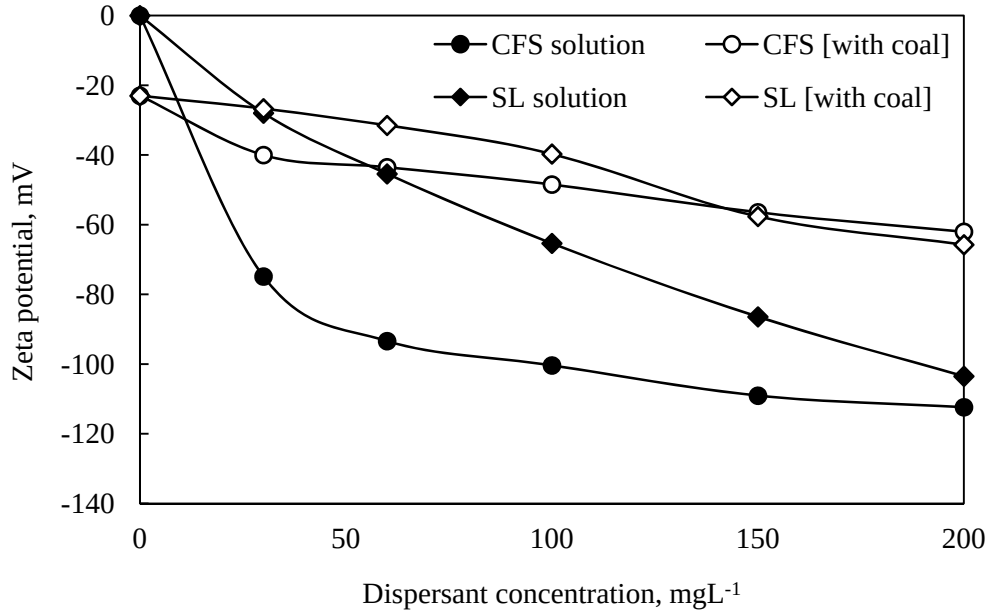

Figure 4.29 Effect of dispersant concentrations on zeta potentials of coal surface.

The important to the disclosure of the mechanism between the dispersant and the coal particles is explained by the zeta potential of the coal particles performed at various concentrations of the anionic dispersants. In Figure 4.29, it is clearly seen that the zeta potential of cardanol-formaldehyde sulfonate and sodium lignosulfonate solutions with coals are negative and more negative in the case of without coal. With increasing cardanol-formaldehyde sulfonate concentration in solution without coal particles, the negative values of zeta potential increase sharply when the cardanol-formaldehyde sulfonate concentration is less than 50 mgL^{-1}. This phenomenon also

appears in sodium lignosulfonate solution but shows the much steeper incline. While the zeta potential of bare coal in distilled water used in the experiments was -23 mV and it shifted towards more negative values as the dispersant concentration increased. This result indicates that the adsorption of the dispersant influences the zeta potential value, causes the repulsion of coal particles. Although, coal-water slurry containing sodium lignosulfonate demonstrates the same behavior of the zeta potential as that containing cardanol-formaldehyde sulfonate but the lower zeta potential of sodium lignosulfonate is obtained in range of 150-200 mgL^{-1}. The main adsorption form of cardanol-formaldehyde sulfonate on coal surface is the adsorption between hydrophobic groups of coal and hydrophobic chains (aromatic rings and methylene groups) of the polymer unit. Moreover, the electrostatic bonding take place between the positives sites of coal and anionic of head groups (sulfonic groups). Furthermore, this result provides strong evidence that the magnitude of the zeta potential of the coal particles in suspension is an important driving force in electrokinetically enhanced pipe flow techniques.

4.8 Stability

Because coal-water slurry contains solid coal particles suspended in water, unsuitably prepared coal-water slurry, shows sedimentation of coal particles during storage in a tank or the difficulty to flow during transportation of the coal-water slurry. These facts would cause many problems such as pumping and spraying for coal utilization processes. The additives are used to prevent the sedimentation of coal particles. Therefore, research and evaluation of the stability of coal-water slurry are important for the applications of coal-water slurry.

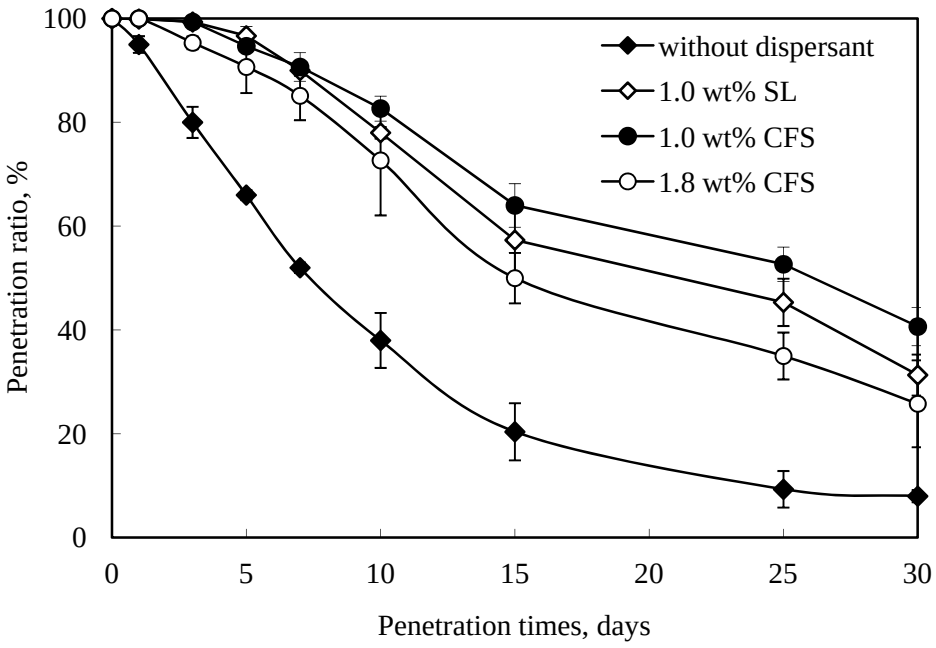

Figure 4.30 Stability of coal-water slurry containing cardanol-formaldehyde sulfonate and sodium lignosulfonate of 1.0 and 1.8 wt% concentration within 30 days.

In this study, the relation between the stability of coal-water slurry and variation of dispersant types at concentrations of 1.0 and 1.8 wt% is described by a plot of penetration ratio against penetration times, which is illustrated in Figure 4.30. In this study, the apparent viscosity of coal-water slurry formulated with 50 wt% coal concentration is less than 1000 mPa s, in which the coal-water slurry without dispersant gives poor stability among all samples.

The coal-water slurry prepared by using cardanol-formaldehyde sulfonate concentration of 1.0 wt% shows larger content of coal particles dispersed in solution among all slurries within 30 days. Although, the coal-water slurry prepared using sodium lignosulfonate concentration of 1.0 wt% shows lower viscosity than that using cardanol-formaldehyde sulfonate concentration of 1.0 wt% in Figure 4.20, but inferior stability. The apparent viscosity of coal-water slurry containing cardanol-formaldehyde sulfonate concentration of 1.8 wt% is also less than that of 1.0 wt% but poorer stability. In general, the coal-water slurry has low viscosity, affects the low stability when storing for a long time. For practical application, coal-water slurry should have low viscosity and gives good stability, depends on the dispersant concentration, coal type, particle size distribution of coal, and coal concentration, etc., corresponding with the above-mentioned explanation.

(a) (b) (c) (d) (e) (f)

Figure 4.31 Schematic of the stability evaluation of coal-water slurry containing dispersant with coal loading of 50 wt%, settled for 15 days: (a) coal with H_2O, (b) coal with diethanolamine anacadate solution of 1.0 wt%, (c) coal with triethanolamine anacadate solution of 1.0 wt%, (d) coal with sodium lignosulfonate solution of 1.0 wt%, (e) coal with cardanol-formaldehyde sulfonate solution of 1.0 wt%, (f) coal with cardanol-formaldehyde sulfonate solution of 1.8 wt%.

Figure 4.31 shows the stability of coal-water slurry, each containing dispersant in range of 1-1.8 wt%, for which was kept for 15 days. From the experimental result, it seems that the soft sediments were seen in coal-water slurry containing dispersant whereas the sedimentary coal becomes compacted into hard layer obtained for bare coal mixed with deionized water. This phenomenon is explained for the different

density between coal particles and water, that the coal particles may be subjected to a centrifugal force, which may cause the outward compaction of solid particles. Besides, the effect of the swelling action of dispersant on coal particles leads to an enhancement on slurry stability. On the contrary, the strong swell behavior of coal particles may give higher viscosities occuring in coal-water slurry containing diethanolamine anacadate or triethanolamine anacadate. Clearly, the poor stability is observed in coal-water slurry, each containing diethanolamine anancardate and triethanolamine anancardate. In case of coal-water slurry containing cardanol-formaldehyde sulfonate, it is noted that there are still a lot of dispersed coal particles in an upper portion of a dispersant solution demonstrating a good static stability, as shown in Figure 4.31 (e). However, smaller amount of fine coal particles is observed for coal-water slurry containing cardanol-formaldehyde sulfonate of 1.8 wt% as compared to that containing cardanol-formaldehyde sulfonate of 1.0 wt%. Moreover, the results that indicate the stability of coal-water slurry containing cardanol-formaldehyde sulfonate is better than that containing sodium lignosulfonate, may be related to the molecular configuration in aqueous solution of the dispersant. The chemical structure shows that cardanol-formaldehyde sulfonate is a macromolecular compound with network structure and its molecular weight is higher than that of sodium lignosulfonate. Because of the characteristics of long chain macromolecule, flexibility and several polar groups of cardanol-formaldehyde sulfonate, a network structure can be formed by cross-linking in solution medium. Thus, coal-water slurry with cardanol-formaldehyde sulfonate does not bleed water easily. Furthermore, the network structure can also be formed by the molecular attraction and partial hydrogen bond, which has the feature of thixotropy. Therefore, the network structure can be destroyed under the external force and reformed after storing to enhance the whole stability of coal-water slurry. While diethanolamine anacadate or triethanolamine anacadate is a linear polymer, therefore, it is hard to form a network structure in aqueous solution, therefore weakly affects the stability of coal-water slurry. Actually, the stability of coal-water slurry results from not only the rheological behavior of slurry but also the impurities that have generally a larger size than that of top size of coal particles. Indeed, the tendency to settle of the pure coal particles prevented by the action of the chemical additives and the inner structure of the coal-water slurry

provided by the residual adhesion forces among the coal particles, are sufficient to avoid settling at rest. On the other hand, impurities in coal powder having a different chemical structure, do not react with the additives, so the settling of these particles can not be controlled, leading to a sediment build-up at the bottom of the slurry when the coal-water slurry is in pipeline at long distances. In such a case, the solid concentrations of coal-water slurry may vary along the radial distance from the inner cylinder. When the shear rate is zero, the coal-water slurry shows a large amount of hard pack layer deposit.

From the stability result, the stability can be ascribed to the action of the chemical agent, especially the highly polar dispersant molecules that coat the coal particles with anionic charges so that mutual repulsive forces prevent natural sedimentation. Finally, we can thus conclude that the coal-water slurry containing cardanol-formaldehyde sulfonate of 1.0 wt% concentration performing above 80% of the penetration ratio within 10 days and below 50% penetration ratio within 30 days, is effective in preventing the sedimentation of coal particles and expected to be the clean coal fuel having good stability and low viscosity.

4.9 Suspension observation using SEM analysis

The molecular configuration of cardanol-formaldehyde sulfonate in solution is also an important factor affecting its adsorption on coal surface. Therefore, cardanol-formaldehyde sulfonate aqueous solution (pH 9) is observed by means of SEM to investigate the microscopic molecular shape and the existence status in aqueous solution. In addition, the suspension behavior of coal particle prepared in aqueous solution of cardanol-formaldehyde sulfonate, was also studied with minimum diameters of 1 μm. With this experiment, the shape and the diameter of the dispersant molecules can be estimated roughly in Figure 4.32 and 4.33.

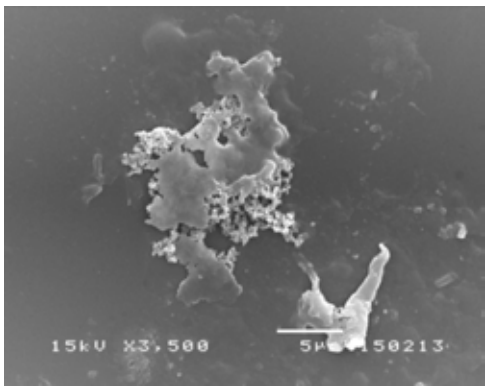

Figure 4.32 SEM micrography of cardanol-formaldehyde sulfonate performed as flocculent structure at low concentration of 1 g L^{-1}.

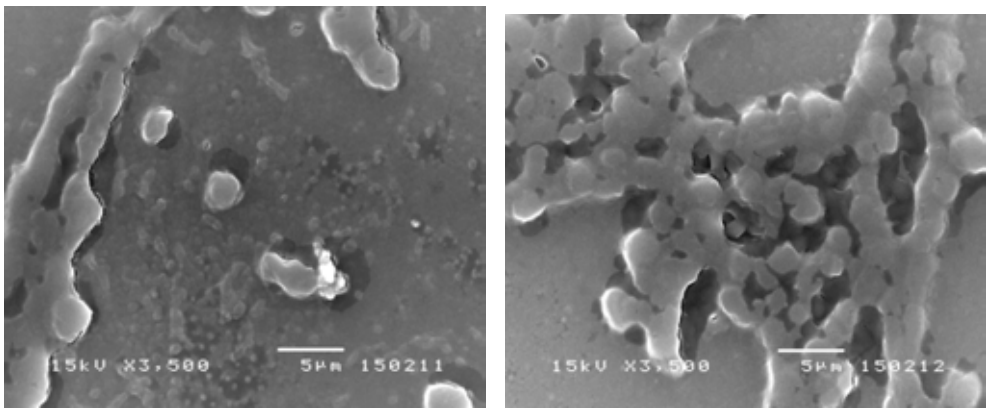

Figure 4.33 SEM micrography of cardanol-formaldehyde sulfonate performed as globular micelle at high concentration of 20 g L^{-1}.

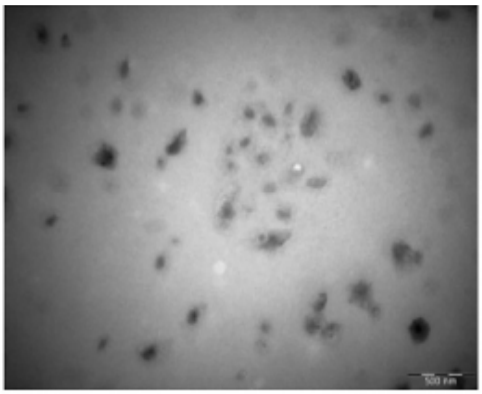

Figure 4.34 SEM micrography of sodium lignosulfonate performed as semi-colloidal structure at concentration of 10 g L^{-1} [48].

In SEM images, Figure 4.32 shows the globular micelle and the flocculent structure of cardanol-formaldehyde sulfonate molecules. It is possible that, at lower concentration of 1 gL^{-1}, most of molecules may be induced the irregular flocculent branches and packaged in the micelles. Within the experimental concentration of 10 gL^{-1}, small molecules can combine with each other and form bigger ones in solution in Figure 4.33. These molecules exist as micelle form and disperse uniformly in water. Generally, aggregation of dispersant usually occurs in order to minimize the free energy of the solution. Moreover, the average molecular length of cardanol-formaldehyde sulfonate is less than 30 nm and about 600-2000 nm at low and high concentration, respectively. Zhou et al [48] reported that sodium lignosulfonate molecules existed in water as semi-colloidal form, as seen in Figure 4.34. Most of the sodium lignosulfonate molecules formed the globular micelles in water, together with many sodium lignosulfonate molecules dissolving independently in water.

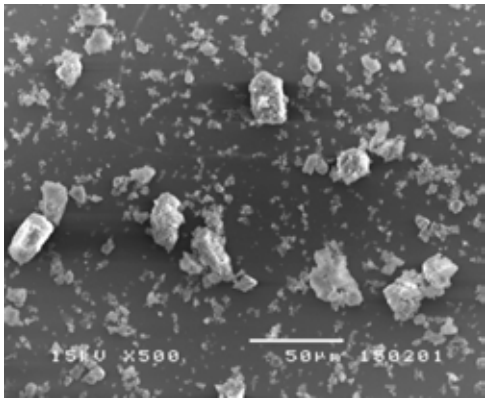

Figure 4.35 SEM micrography of coal particles with irregular shape.

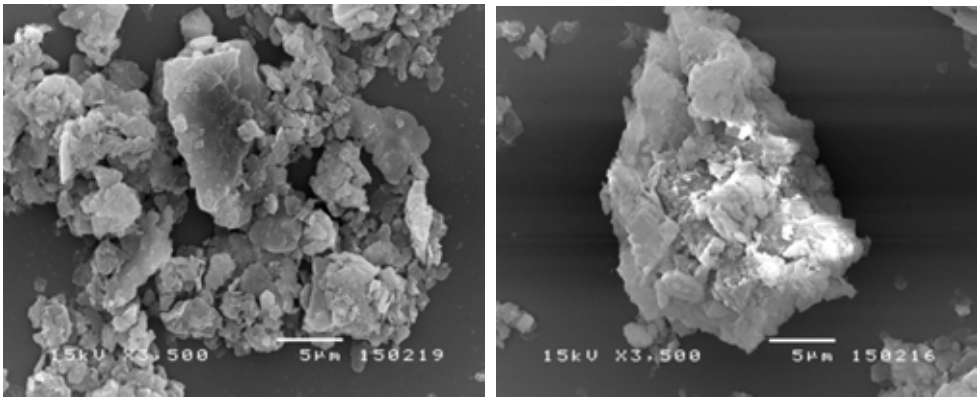

Figure 4.36 SEM micrography of aggregation of coal particles with sharp edges.

Figure 4.35 and 4.36 show that the coal particles are irregular in shape with various sized fractions and exhibit sharp edges. However, a phenomenon of particle-to-particle adhesion, leading to formation of strong aggregates cannot be avoided even at very low coal concentration, aggregation between the fine and coarse coal particles is also found sporadically in this study. The micrography images of coal particles immersed in cardanol–formaldehyde sulfonate solution are clearly shown in Figure 4.37. It is revealed that there is adsorption affinity between the cardanol–formaldehyde sulfonate molecules and coal surface because of the presence of many flocculent branches and a lot of anchoring sites of cardanol–formaldehyde sulfonate on coal surface. This is proved by FTIR spectrum of the cardanol–formaldehyde sulfonate that the appearance of weak absorbance in the bands at 1620 and 1556 cm^{-1} (aromatic skeletal vibrations), and sharp absorbance in the bands at 1188 cm^{-1} and 1051 cm^{-1} (sulfonic group), which indicates that much of the aromatic ring in lignin molecules is broken, and many irregular flocculent branches are engrafted. Thus, the cardanol–formaldehyde sulfonate molecules can easily adsorb on coal surface tightly, and exhibit excellent dispersing effect for coal-water slurry.

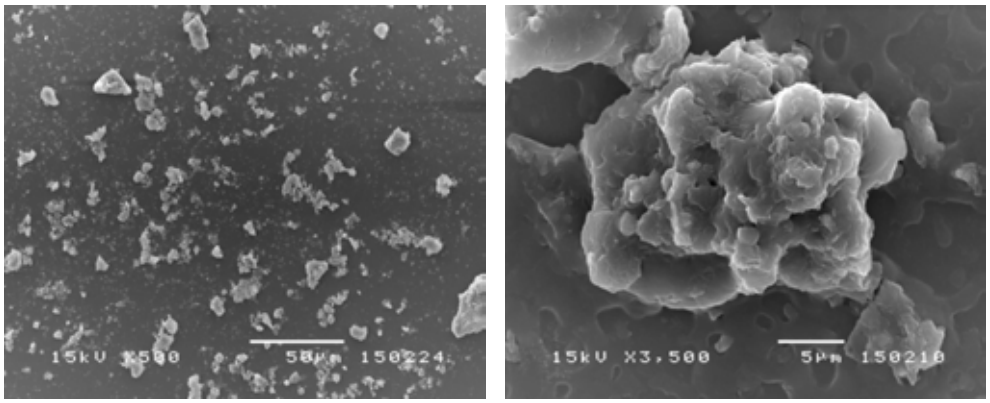

Figure 4.37 SEM micrography of cardanol-formaldehyde sulfonate absorbed on coal surface.

4.10 Thermal Behavior

Coal is a fuel with a high percentage of fixed carbon but low volatile matter content. The combustion of volatile matter occurs in a molecular dispersion state and is complete in a very short time. However, combustion of fixed carbon occurs on the surface of the solids and the combustion rate is controlled by the surface area of the fuel. In coal–fired power plants, the coal is usually crushed to very fine particles and blown into the furnace to increase combustion rate.

Thermal analysis: TG (weight loss in relation to the temperature of thermal degradation) and DTG (weight loss rate) curves of the coal-water slurry was performed to examine the combustion phenomena and its decomposition characteristics. Determination of weight loss was operated as the sample burns in air against crucible temperature while the furnace was heated at 15 ^{o}C min^{-1} starting from room temperature and an air flow rate of 90 ml.min^{-1}.

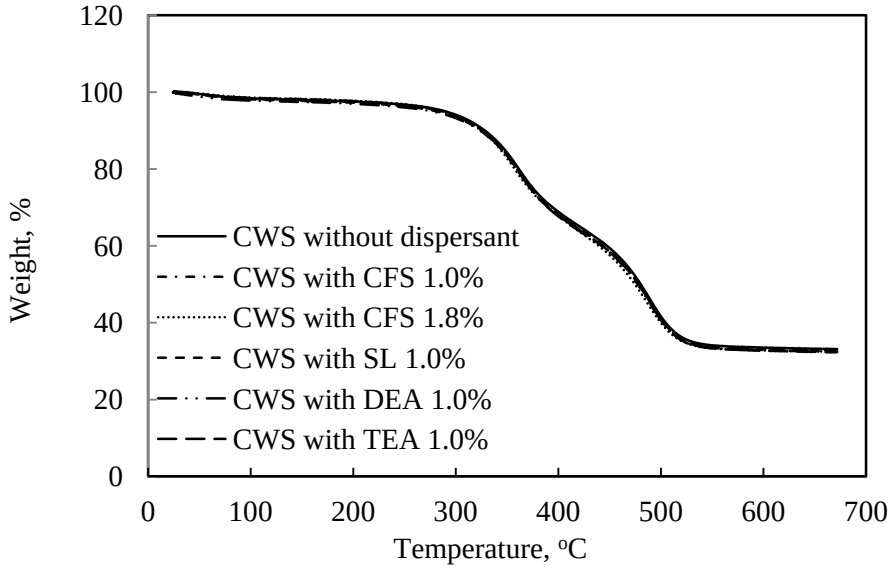

Figure 4.38 TG thermograms for coal-water slurry without and with dispersant composed of 50 wt% bituminous coal in water.

Figure 4.38 and 4.39 illustrate the TG and DTG curves of coal-water slurry, fired in air in the temperature range of 25–700 ^{o}C. The weight losses of all samples in

inert atmosphere occur into three stages in TG curve. In general, coal particles have continuous weight loss between 200 and 900 ^{o}C. When coal sample is first heated in nitrogen gas in order to dry it and to expel any volatiles, atmosphere is switched to oxygen and the carbon content is burnt to CO_2. Weight loss in the last step can be used to calculate the carbon content [4,34,41,51,55]. While coal-water slurry shows an exothermic peak with slow burning nature of coal.

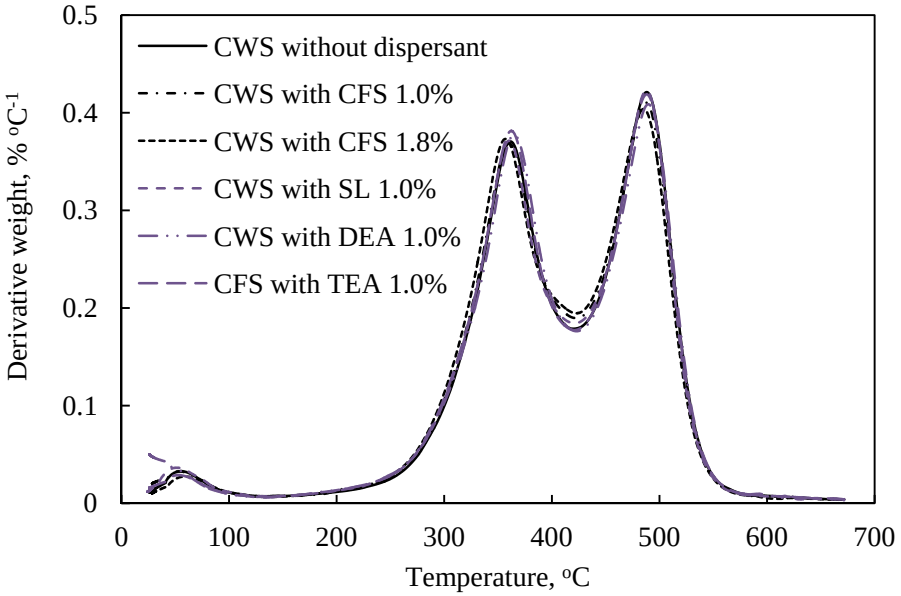

Figure 4.39 DTG thermograms for coal-water slurry without and with dispersant composed of 50 wt% bituminous coal in water.

From Figure 4.39, DTG results display an exothermic event starting at 45 ^{o}C for the initial weight loss. The strong exothermic peak appears in DTG curves between 200 ^{o}C and 700 ^{o}C corresponding to the combustion of coal particles and dispersant compounds. This was confirmed by the continuous weight loss between 200 ^{o}C and 700 ^{o}C in TG curves (Figure 4.38). For coal-water slurry without dispersant, the first stage range between 25 and 125 ◦C shows about 5% loss in weight. This is thought to be due to inherent moisture vaporization which does not normally include in the burning profile characterization. While the second stage appears at about 360 ^{o}C corresponding weight loss of about 33% attributed to the decomposition of volatiles matter. At the last stage, the main characteristic point was

around 490 ^{o}C which indicates that the rate of weight loss was at maximum, also called the peak temperature, and was the parameter used chiefly in the assessment of coal combustibility. The total weight loss of the sample at about 600 ^{o}C is 65%.

Table 4.4 Thermogravimetric analysis of the coal-water slurry

Sample	Weight loss (%)	
	2nd Stage	3rd Stage
CWS without dispersant	32.9	63.8
CWS with CFS 1.0%	34.2	65.4
CWS with CFS 1.8%	34.7	65.9
CWS with SL 1.0%	33.4	64.8
CWS with DEA 1.0%	33.9	65.9
CWS with TEA 1.0%	34.0	64.0

The TG and DTG thermograms displaying the similar behavior of combustion is also observed in coal-water slurry with each dispersant. This indicates no dramatic changes in the carbon structure after adsorption of dispersant. The desorption phenomena occur at low temperature probably during drying/water vaporization period. Adsorption of dispersant on coal surface may influence to the reduction of surface area available for combustion leading to low combustion rate with incomplete combustion. From the experimental result, there seem to be no significant shift in the peak temperature between coal-water slurry with and without dispersant. This behaves in the same way with the result reported by Ramachandran et al [56]. According to them, the coal in the slurry had 30 percent lower BET surface area, probably due to blinding of some pores by additives, the two chars had nearly identical BET areas. It appeared that there were no basic differences in carbon burnout potential between the two fuels when compared on an equal particle size basis. In case of coal-water slurry containing cardanol-formaldehyde sulfonate, the

first stage obtained at 30-125 °C indicates the loss of adsorbed water that was about 4.0%. Volatile components and light gases such as CO and CO_2 might also be released at the second stage because the weight loss of the sample is much higher than the moisture content with 34%, as shown in Table 4.3. The decomposition of the cardanol-formaldehyde sulfonate structure is expected to begin above 200 °C. A sharp weight loss observed over 315 °C may be simultaneous combustion of cardanol-formaldehyde sulfonate molecule and volatile matters. With the predominant weight loss between 425 and 600 °C, the high weight loss rate DTG peaks correspond to the decomposition of the major components of carbon. Finally, it is important to note that the addition of cardanol-formaldehyde sulfonate between 1.0-1.8 wt% in coal-water slurry does not affect the deterioration in combustion behavior, although there is no significant improvement on fast combustion rate corresponding to the complete combustion during the short residence time, typical of boilers designed originally for burning oil.

4.11 Fundamental discussion of cardanol-formaldehyde sulfonate acting as high-performance dispersant of coal-water slurry

The cardanol cannot be used to prepare highly concentrated coal-water slurry, while the modified cardanol as cardanol-formaldehyde sulfonate can be used as high-performance dispersant to prepare highly concentrated coal-water slurry made up from bituminous coals. Because of the nature of coal, the coal-water slurry suspension tends to weakly acidic system, so cardanol without modification have no dispersing ability in coal-water slurry. Consequently, the grafting of sulfonic groups in cardanol molecules plays an important role with strong increasing the water-soluble property of cardanol. As shown in Appendix A.15, the spectrum of the cardanol-formaldehyde sulfonate shows sharp absorbance in the bands at 1188 and 1051 cm^{-1}, denoting sulfonic groups, while the spectrum of the cardanol has no absorbance in the above bands. It indicates that the chemical treatment reaction increases the contents of sulfonic groups. Therefore, the water-soluble cardanol-formaldehyde sulfonate can be adsorbed on coal surface and the hydrophilic groups provide hydrophilicity and electronegativity for coal particles. The hydrophilic hydration layer on coal surface and the electrostatic repelling force between coal particles make the coal particles disperse in water. Moreover, the increased molecular weight of cardanol-based dispersant is another important factor influencing its dispersing ability. As shown in Figure 4.8 and 4.9, the chemical treatment reaction makes the molecular weight of cardanol-formaldehyde sulfonate from cardanol increases remarkably, the average molecular weight (Mw) is about 14,631 Dalton, the number average molecular weight (Mn) is 9667 Dalton and the polydispersity (Mw/Mn) is 1.51. It has been reported that a high molecular weight dispersant has more adsorption potential on coal surface and has better dispersing effect for coal-water slurry [5,6,41,52,57]. So the increase of the molecular weight and sulfonate group improves the dispersing ability of cardanol-formaldehyde sulfonate for coal-water slurry.

CHAPTER 5

CONCLUSION

In utilization of coal–water slurry in industrial plants, highly concentrated coal–water slurry is desired and it is necessary for coal–water slurry to perform excellent properties such as good fluidity and stability suitable for its handling in preparation, storage, transport and combustion processes. To obtain suitable coal–water slurry, usage of the appropriate type and amount of chemical dispersant is necessary. Because the slurry particles cannot avoid the agglomeration entirely, it is still necessary to prevent high concentrations of the coal-water slurry in the water based fluid. Such dispersants are essential for dispersion of the coal particles by breaking the aggregates and agglomerates, for stability against settling of the particles. Dispersing agents adsorb on the particle surface, thus modifying their surface properties.

In this study, three anionic dispersants are modified from cashew nut shell liquid obtained from processing cashew nut, to give diethanolamine anacardate, triethanolamine anacardate and cardanol-formaldehyde sulfonate, respectively. Then these dispersants were evaluated for their properties in which focus on the suitable dispersing performance for coal–water slurry preparation. Therefore, this research was classified and concluded into two parts as shown below:

Part 1: Synthesis and selection of a suitable dispersant for coal–water slurry preparation

The isolation of cashew nut shell liquid was neutralized by diethanolamine and triethanolamine till pH of 8.0 that gives diethanolamine anacardate and triethanolamine anacardate product with approximately 98 %yield, respectively. Their structures were proved by IR and NMR spectroscopy. Although, both diethanolamine anacardate and triethanolamine anacardate exhibit high surface activity with the reduction of the surface tension, the apparent viscosity of coal-water slurry decreases slightly compared with that of coal-water slurry without dispersant. Therefore, it is

revealed that diethanolamine anacardate and triethanolamine anacardate are the inappropriate dispersant for coal-water slurry application.

The cardanol was used to prepare the cardanol-formaldehyde sulfonate obtained by sulfomethylation reaction with sulfomethylating agent, for which gives 35% yield product with aromatic ring and aliphatic high polymer containing hydroxyl and sulfonic groups. Its structure was confirmed by IR and NMR techniques. In the result of varying conditions, it is found that the dispersing effect of cardanol-formaldehyde sulfonate is influenced greatly by the molecular weight and sulfonic group content which is affected by the amount of sodium sulfite and formaldehyde, reaction time and temperature. The optimum condition was carried out at 80 ^{o}C for 8 hours with the sodium sulfite and formaldehyde dosages as 15.25 and 24.21 %, respectively, which gives cardanol-formaldehyde sulfonate having the molecular weight of 14,631 daltons and the average quantity of sulfur as 17%. With this condition, obtained cardanol-formaldehyde sulfonate shows the better dispersing effect of coal-water slurry with the average viscosity of 380 mPas. The physicochemical properties investigation shows that cardanol-formaldehyde sulfonate has certain surface activity and can reduce the surface tension of distilled water from 71 to 52 mN·m^{-1} beyond the concentration of 0.2 wt%.

From the preliminary result, cardanol-formaldehyde sulfonate is expected to act as a good dispersant for coal-water slurry, so the rheological behavior of coal-water slurry containing cardanol-formaldehyde sulfonate is further studied in the second part.

Part 2: Clarification of various factors on the rheological behavior of coal-water slurry containing synthesized dispersant

This study emphasizes the following fundamental properties of coal-water slurry: viscosity, rheology, stability and combustion behavior by using the mixture of coal and water in the presence of cardanol-formaldehyde sulfonate as a dispersant.

- The rheological investigation showed that the coal-water slurry containing cardanol-formaldehyde sulfonate is classified as a Newtonian fluid at low coal concentrations up to 45 wt% and as a Bingham plastic at higher coal concentration values in range of 50-53 wt%. The yield stress of coal-water slurry increases with increasing coal concentrations.

- The viscosity of coal-water slurry increases rapidly with coal concentration especially at high coal concentration above 50 wt% because the saturation percentage of coal in water is approached. Further, the apparent viscosity of coal-water slurry containing cardanol-formaldehyde sulfonate tends to decrease exponentially with the increased coal size and temperature.

- As employing cardanol-formaldehyde sulfonate of 1.8 wt% exhibits the best effect on reducing the viscosity of the coal-water slurry which the similar behavior is also observed with coal-water slurry containing commercial sodium lignosulfonate at 1.4 wt% with the minimum viscosity. Although, the coal-water slurry containing cardanol-formaldehyde sulfonate at 1.0 wt% gave the higher viscosity but it still hold in the applicable viscosity ranges of 1000 mPas. Additionally, the addition of dispersant was necessary to increase the absolute value of zeta potentials of experimental coal sample to sustain stability. The adsorption of dispersant is also shown in SEM observation.

- In the stability study, the slurry with cardanol-formaldehyde sulfonate at 1.0 wt% concentration exhibited the penetration approximately 80% within 10 days and goes down significantly below 50% within a maximum of 30 days. Commercially, the cardanol-formaldehyde sulfonate amount at 1.0 wt% was suitable for the coal-water slurry preparation of 50% coal concentration due to required small amount of dispersant, the low viscosity and better stability, results in storage and transport through the pipe line without precipitation of coal particles in few days.

-Thermal analysis by DTG/TG of coal-water slurry without and with dispersant presents three stages for combustion phenomena; moisture evaporation (around 25-125 ^{o}C), volatile matters (around 357-366 ^{o}C), and solid phases

combustion (around 485-490 ^{o}C). In each sample, there is no significant difference of temperature range between coal-water slurry with dispersant when compared to that without dispersant. This demonstrates no effect of using dispersant in coal-water slurry on the combustion behavior.

As above mentioned results, it revealed that cardanol-formaldehyde sulfonate synthesized from sulfomethylation of cardanol exhibited the similar properties to commercial dispersant, sodium lignosulfonate, and gave the value of each property defined in the specification. Therefore, such kind of natural dispersant, cardanol-formaldehyde sulfonate, would be another choice for dispersant employed in coal-water slurry application.

REFERENCES

[1] Thielemann, T., Schmidt, S., and Gerling, J.P. Lignite and hard coal: Energy suppliers for world needs until the year 2100-An outlook. International Journal of Coal Geology 72 (September 2007): 1-14.

[2] Wolde-Rufael, Y. Coal consumption and economic growth revisited. Applied Energy 87 (January 2010): 160–167.

[3] Miller, B.G. Clean coal technologies for advanced power generation. Clean Coal Engineering Technology 12 (January 2011): 251-300.

[4] Shalaurov, V.A., Anushenkov, A.N., and Freidin, A.M. Preparation and transportation of coal slurry. Journal of Mining Science 33 (September 1997): 481-486.

[5] Kaymakci, E., and Didari, V. Relations between coal properties and spontaneous combustion parameters. Turkish Journal of Engineering & Environmental Sciences 26 (October 2002): 59-64.

[6] Das, D., Panigrahi, S., Misra, P.K., and Nayak, A. Effect of organized assemblies. part 4. formulation of highly concentrated coal-water slurry using a natural surfactant. Energy & Fuels 22 (January 2008): 1865–1872.

[7] Yang, D., Qiu, X., Zhou, M., Lou, H. Properties of sodium lignosulfonate as dispersant of coal water slurry. Energy Conversion and Management 48 (June 2007): 2433–2438.

[8] Pawlik, M. Polymeric dispersants for coal-water slurries, Colloids and Surfaces A: Physicochem. Colloids and Surfaces A: Physicochemical and Engineering Aspects 266 (April 2005): 82–90.

[9] Patel, R.N., Bandyopadhyay, S., Ganesh, A. Extraction of cashew (*Anacardium occidentale*) nut shell liquid using supercritical carbon dioxide. Bioresource Technology 97 (April 2006): 847–853.

[10] Rajapakse, R.A., Gunatillake, P.A., Wijekoon, K.B. A preliminary study on processing of cashew-nuts and production of cashew-nut shell liquid (CNSL) on a commercial scale in Sri Lanka. Journal of the National Science Council of Sri Lanka 5 (July 1977): 117-124.

[11] Jekayinfaa, S.O., Bamgboyeb, A.I. Estimating energy requirement in cashew (*Anacardium occidentale L.*) nut processing operations. Energy 31 (April 2006): 1305–1320.

[12] Gedam, P.H., and Sampathkumaran, P.S. Cashew nut shell liquid: extraction, chemistry and applications. Progress in Organic Coatings. 14 (March 1986): 115– 157.

[13] Tyman, J.H.P., Johnson, R.A., Muir, M., and Rokhgar, R. The extraction of natural cashew nut-shell liquid from the cashew nut *(Anacardium occidentale).* Journal of the American Oil Chemists' Society 6 (April 1989): 553-557.

[14] Setiantoa, W.B., Yoshikawab, S., Smith Jr,R.L., Inomatab, H., Florussed, L.J., and Peters, C.J. Pressure profile separation of phenolic liquid compounds from cashew (*Anacardiumoccidentale*) shell with supercritical carbon dioxideand aspects of its phase equilibria. The Journal of Supercritical Fluids 48 (2009): 203–210.

[15] Kasemsiria, P., Hiziroglub, S., and Rimdusit, S. Effect of cashew nut shell liquid on gelation, cure kinetics, and thermomechanical properties of benzoxazine resin. Thermochimica Acta 520 (April 2011): 84-92.

[16] Andrade, T., et al. A. Antioxidant properties and chemical composition of technical cashew nut shell liquid (CNSL). Food Chemistry 126 (November 2011): 1044–1048.

[17] Dantasa, T.N.C., Dantasa, M.S.G., Dantas-Netoa, A.A., D'Ornellasb, C.V., and Queiroza, L.R. Novel antioxidants from cashew nut shell liquid applied to gasoline stabilization. Fuel 82 (April 2003): 1465–1469.

[18] Kumar, P.P., Paramashivappa, P.J., Vithayathil, P.J., SubraRao, P.V., and Srinivasa Rao A. Process for isolation of cardanol from technical cashew (Anacardiumoccidentale.) nut shell liquid. Journal of Agricultural and Food Chemistry 50 (September 2002): 4705-4708.

[19] Mythili, C.V., Retina, A.M., and Gopalakrishnan, S. Synthesis, mechanical, thermal and chemical properties of polyurethanes based on cardanol. Bulletin of Materials Science 27 (June 2004): 235-241.

[20] Paramshivappa, R., Phani Kumar, P., Vithayathil, P. J., and Rao, A.S. Novel method for isolationof major phenolic components from cashew (*Anacardiumoccidentale L.)* nut shell liquid. Journal of Agricultural and Food Chemistry 49 (May 2001): 2548-2551.

[21] Devi, A., and Srivastava, D. Studies on the blends of cardanol-based epoxidized novolac type phenolic resin and carboxyl-terminated polybutadiene (CTPB) I. Materials Science and Engineering A 458 (June 2007): 336–347.

[22] Prabhakaran, K., Narayanan, A., and Pavithran, C. Cardanol as a dispersant plasticizer for an alumina/toluene tape casting slip. Journal of the European Ceramic Society 21 (December 2001): 2873–2878.

[23] Yu, J., Yang, J., and Huang, Y. The transformation mechanism from suspension to green body and thedevelopment of colloidal forming. Ceramics International 37 (July 2011): 1435–1451.

[24] Javadian, S., Gharibi, H., Sohrabi, B., Bijanzadeh, H., Safarpour, M.A., and Behjatmanesh-Ardakani, R. Determination of the physico-chemical parameters and aggregation number of surfactant in micelles in binary alcohol–water mixtures. Journal of Molecular Liquids 137 (January 2008): 74–79.

[25] Kiinig, S., Quitzsch, K., Knig, B., Hornmel, R., Haferburg, D., and Kleber, H.P. Physicochemical investigations in systems of composition biosurfactant/sodium dodecylsulfate/water around the critical micelle concentration. Colloids and Surfaces Biointerfaces 23 (1993): 33-41.

[26] Malik, M.A., Hashim, M.A., Nabi, F., AL-Thabaiti, S.A., and Khan, Z. Anti-corrosion ability of surfactants: A review. International Journal of Electrochemical Science 6 (June 2011): 1927-1948.

[27] Rosety, M., Ordóñez, F.J., Rosety-Rodríguez, M., Rosety, J.M., Carrasco, C., and Ribelles, A. Acute toxicity of anionic surfactants sodium dodecyl sulphate (SDS) and linear alkylbenzene sulphonate (LAS) on the fertilizing capability of gilthead *(Sparus aurata* L.) sperm. Histol Histopathol 16 (May 2001): 839-843.

[28] Rosen, M.J. Adsorption of surface-active agents at interfaces: The electrical double layer, Surfactants and interfacial phenomena, pp.34-55. New Jersey : John Wiley & Sons, 2004.

[29] Laughlin, R.G. Fundamentals of the zwitterionic hydrophilic group. Langmuir 7 (June 1991): 842-847.

[30] Bloch, H., Rafiq, S., and Salim, R. Coal consumption, CO_2 emission and economic growth in China: Empirical evidence and policy responses. Energy Economics 34 (August 2012): 518–528.

[31] Peng-wei, L., Dong-jie, Y., Hong-ming, L., and Xue-qing, Q. Study on the stability of coal water slurry using dispersion-stability analyzer. Journal of Fuel Chemistry and Technology 36 (October 2008): 524−529.

[32] Kesavan, S., and Schruben, D. L. Stabilization of coal particle suspensions using coal liquids. Fuel Science and Technology International 4 (February 1986): 87-101.

[33] Brownlie, D. Carbonization of coal-oil mixtures: A review of recent developments. Industrial And Engineering Chemistry 28 (1936): 629-633.

[34] Bird, S.O. Coal-in-water: Fuel of the future. Virginia Division of Energy 32 (August 1986): 21-30.

[35] Ekmann**,** A.C. Viscosities of coal-water-methanol mixtures. Fuel 63 (August 1984): 1182-1184.

[36] Lee, S. Coal slurry fuel. In S. Lee, J.G. Speight, and S.K. Loyalka (ed.), Handbook of alternative fuel technologies, pp.125-148. New York : Taylor & Francis, 2007.

[37] Becerra Signe. Straw and coal ash rheology. Ph.D. Thesis, Department of Chemical and Biochemical Engineering Technical University of Denmark, 2001.

[38] Peker, S.M., and Helvacı, S.S. Non-newtonian behavior of solid-liquid suspensions, Solid-liquid two phase flow, pp.71–166. Netherland : Elsevier, 2008.

[39] Partal, P., and Franco, J.M. Non-newtonian fluids. Rheology 1 (2008): 1-10.

[40] Eberl, E., and Eberl, U., Parameters of transport of non-newtonian fluids through the pipes. The Mining-Geological-Petroleum Engineering Bulletin 7 (1995): 65-69.

[41] Zhua, H., Kimb, Y.D., and De Kee, D. Non-newtonian fluids with a yield stress. Journal of Non-Newtonian Fluid Mechanics 129 (June 2005): 177–181.

[42] Papachristodoulou, G., and Trass, O. Coal-slurry fuel technology. Journal of Chemical & Engineering Data 65 (March 1987): 177-201.

[43] Rowell, R.L. The cinderella synfuel. Chemtech (April 1989): 244-248.

[44] Kawatra, S.K. Coal-water slurries. In S. Lee (ed.), Encyclopedia of Chemical Processing, pp.495–503. New York : Taylor & Francis, 2005.

[45] Kawatra, S.K., and Bakshi, A.K. The on-line pressure vessel rheometer for concentrated coal slurries. Journal of Coal Preparationand Utilization 22 (July 2002): 41-56.

[46] Xu, R., Zhuang, W., He, q., Cai, J., Hu, B., and Shen, J. Effects of chemical structure on the propertiesof carboxylate-type copolymer dispersant for coal-water slurry. Environmental and Energy Engineering Journal 55 (September 2009): 2461-2467.

[47] Horsfall, D.W. The properties and uses of mixtures of coal, and water or oil. Journal of the South African Institute of Mining and Metallurgy 90 (August 1990): 199-204.

[48] Zhou, M., Qiu, X., Yang, D., Lou, H., and Ouyang, X. High-performance dispersant of coal–water slurry synthesized from wheat straw alkali lignin. Fuel Processing Technology 88 (November 2007): 375–382.

[49] Mishra, S.K., Kanungo, S.B., Rajeev. Adsorption of sodium dodecyl benzenesulfonate onto coal. Journal of Colloid and Interface Science 267 (May 2003): 42–48.

[50] Boylu, F., Ates¸ok, G., and Dincer, H. The effect of carboxymethyl cellulose (CMC) on the stability of coal-water slurries. Fuel 84 (October 2005): 315–319.

[51] Shin, Y., and Shen, Y.H. Preparation of coal slurry with organic solvents. Chemosphere 68 (February 2007): 389–393.

[52] Scorzza, C., Nieves, J., Vejar, F., and Bullon, J. Synthesis and physicochemical characterization of anionic surfactants derived from cashew nut shell oil. Journal of Surfactants and Detergents 13 (June 2010): 27–31.

[53] Chen, R.H., Tsaih, M.L. Effect of temperature on the intrinsic viscosity and conformation of chitosans in dilute HCl solution. International Journal of Biological Macromolecules 23 (October 1998): 135–141.

[54] Mishra, S.K., Senapati, P.K., and Panda, D. Rheological behavior of coal-water slurry energy sources. Energy Source 24 (2002): 159-167.

[55] Whitehouse, A.E., and Mulyana, A.A.S. Coal fires in Indonesia. International Journal of Coal Geology 59 (July 2004): 91– 97.

[56] Ramachandran, P., Tsai, C-Y., and Schanche, G.W. An evaluation of coal water slurry fuel burners and technology. Usacerl Technical Report (November 1992): 1-112.

[57] Qiu**,** X**.,** Zhou**,** M., Yang**,** D., Lou**,** H., Ouyang, X.**,** and Pang, Y. Evaluation of sulphonated acetone-formaldehyde (SAF) used in coal water slurries prepared from different coals. Fuel 86 (2007): 1439–1445.

APPENDICES

APPENDIX A

^{1}H-NMR, ^{13}C-NMR and IR SPECTRA OF SYNTHESIZED DISPERSANT

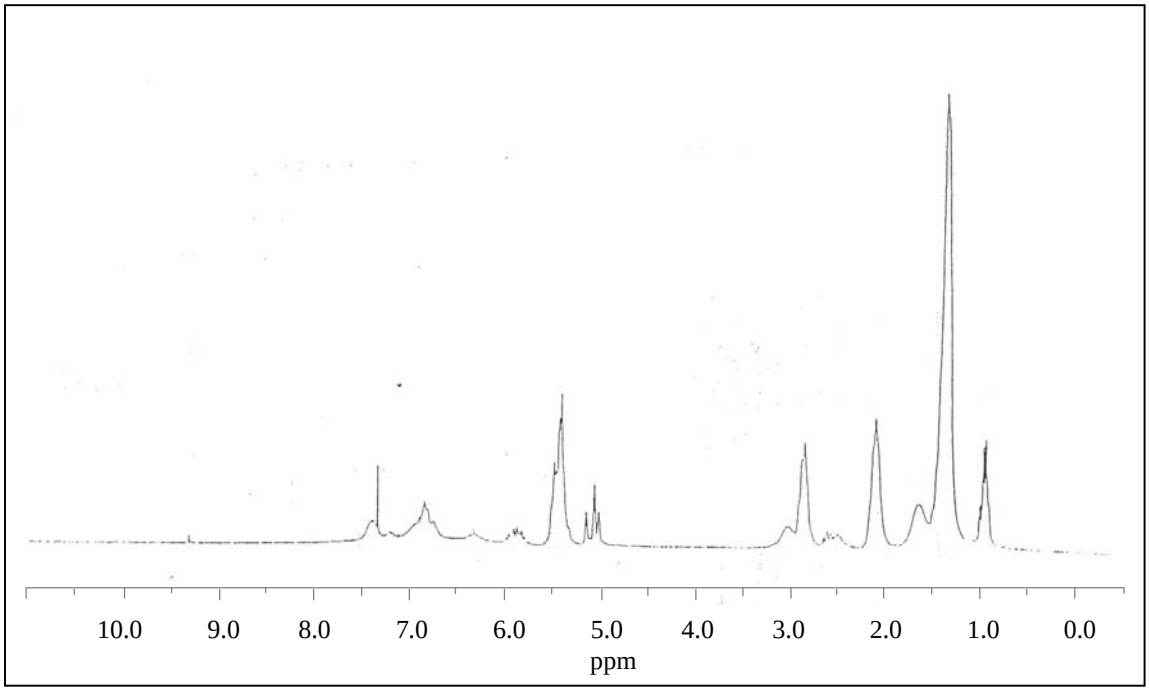

Figure A-1 ^{1}H-NMR spectrum of cashew nut shell liquid.

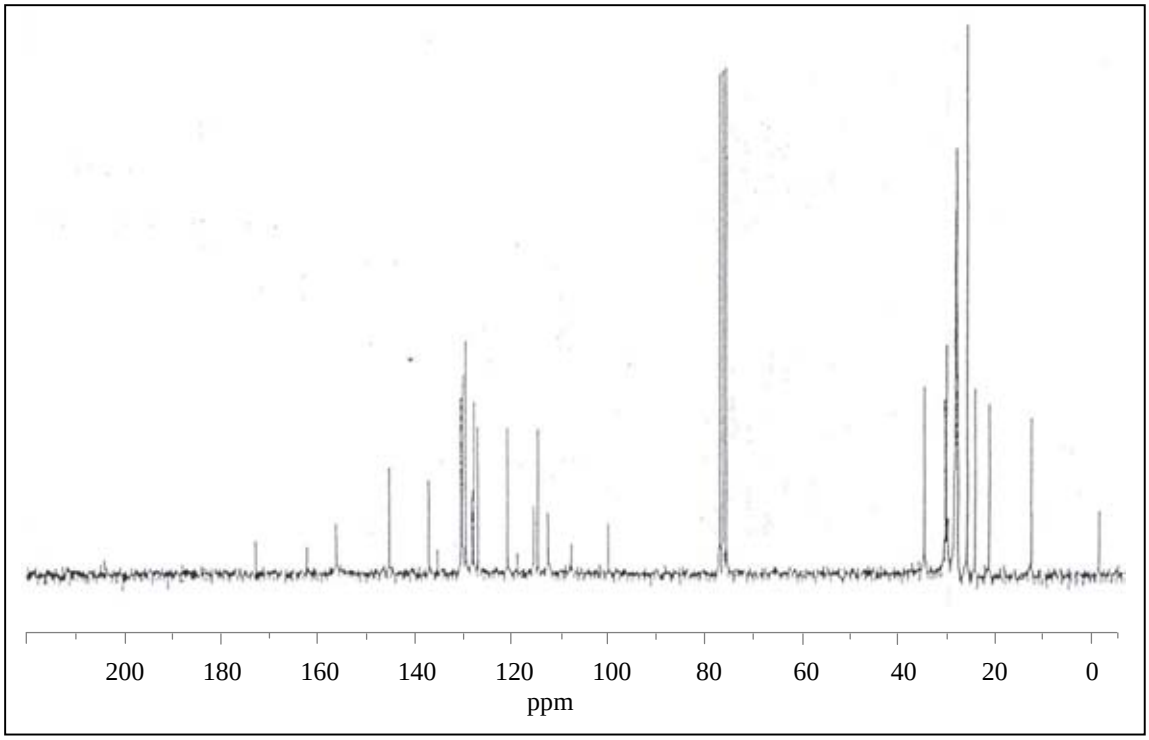

Figure A-2 ^{13}C-NMR spectrum of cashew nut shell liquid.

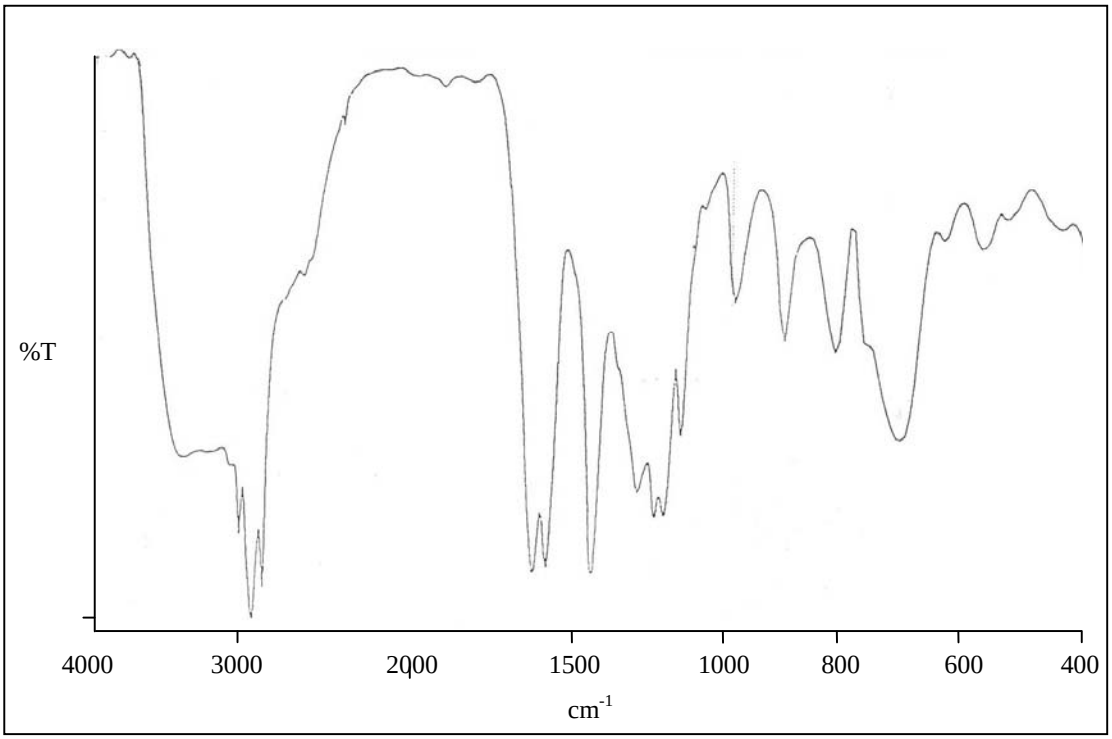

Figure A-3 Infrared spectrum of cashew nut shell liquid.

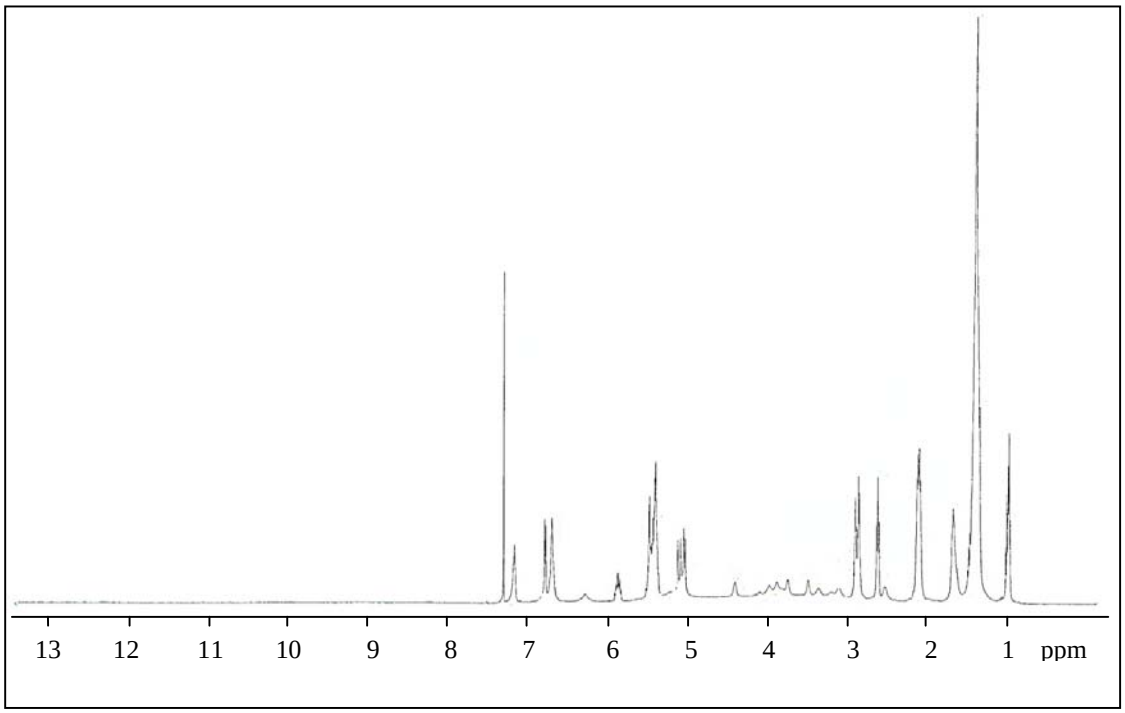

Figure A-4 ^{1}H-NMR spectrum of diethanolamine anacardate.

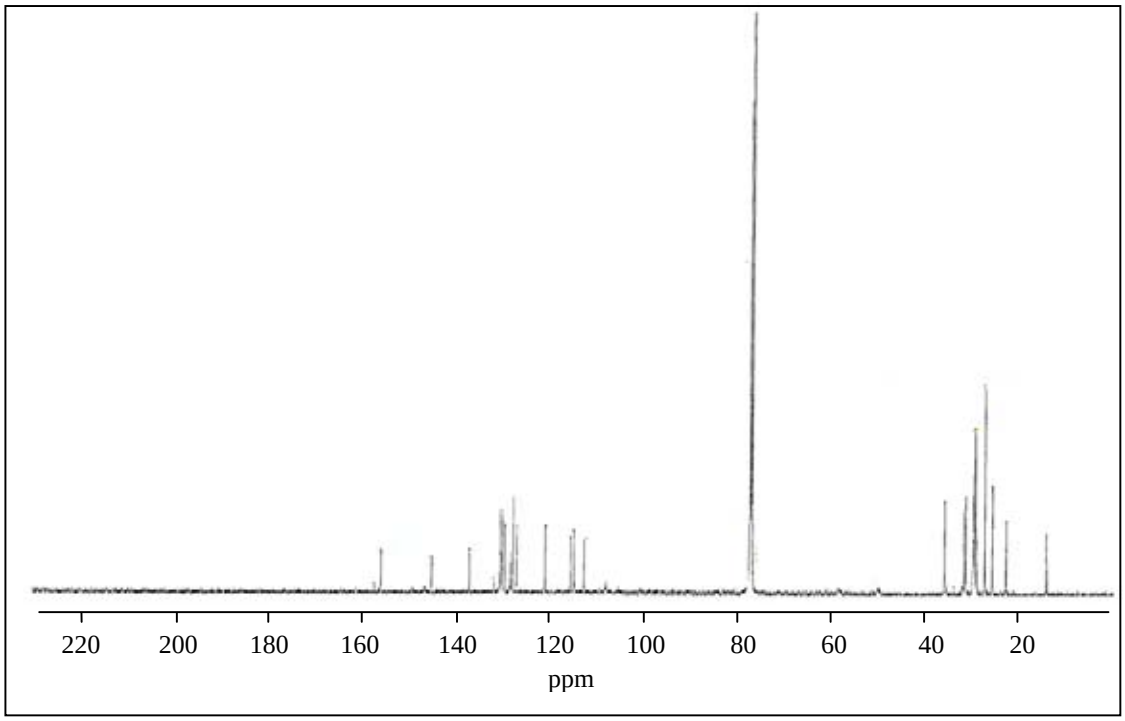

Figure A-5 ^{13}C-NMR spectrum of diethanolamine anacardate.

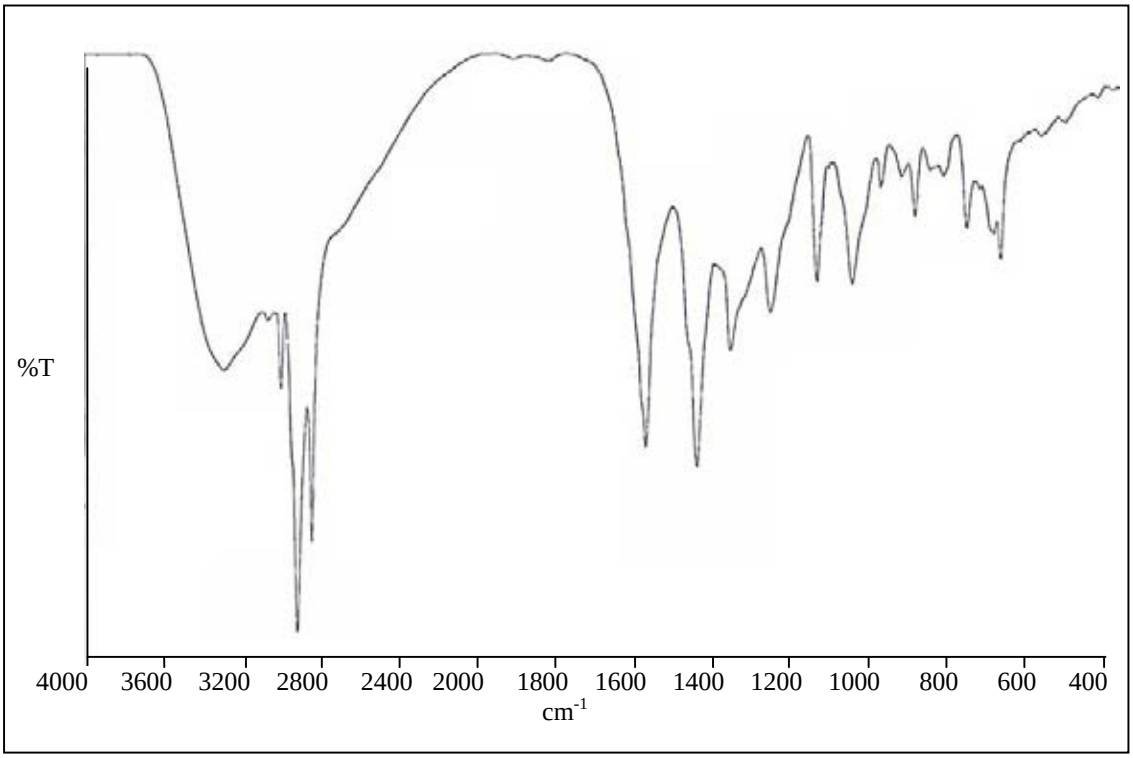

Figure A-6 Infrared spectrum of diethanolamine anacardate.

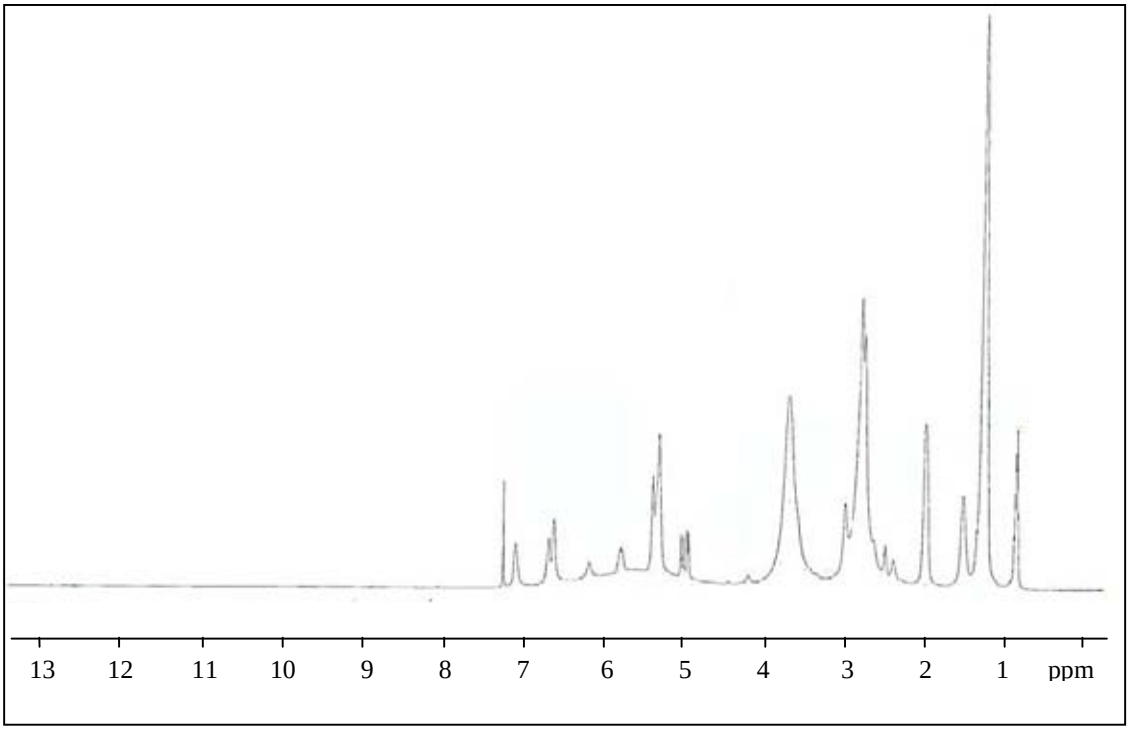

Figure A-7 ^{1}H-NMR spectrum of triethanolamine anacardate.

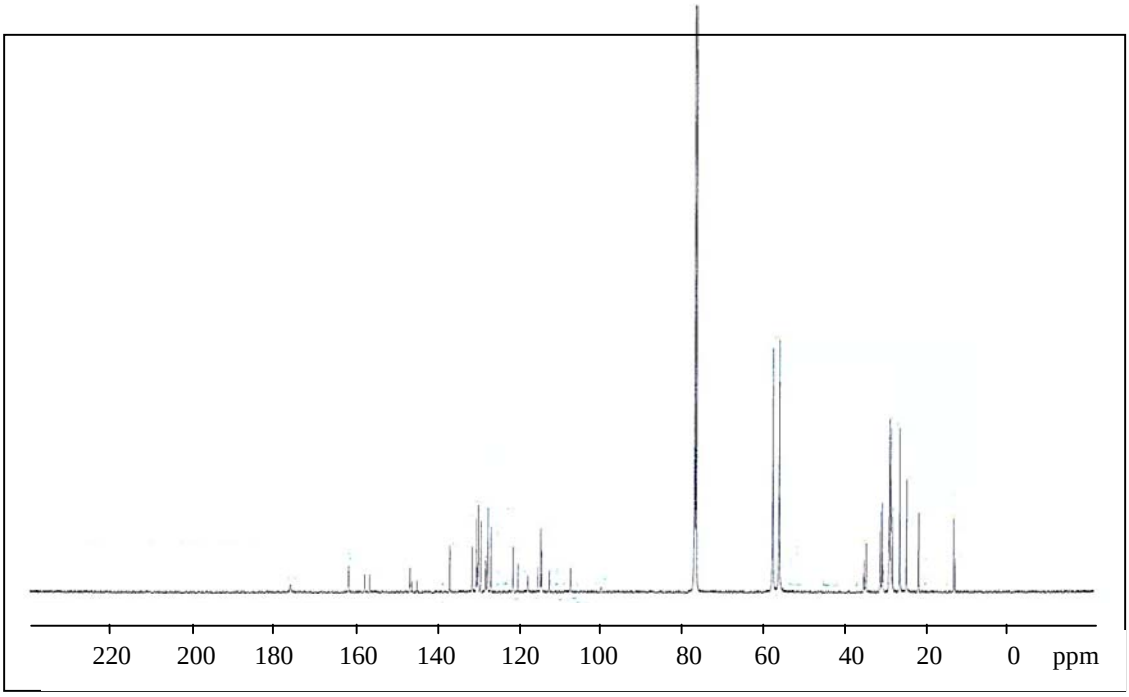

Figure A-8. ^{1}C-NMR spectrum of triethanolamine anacardate.

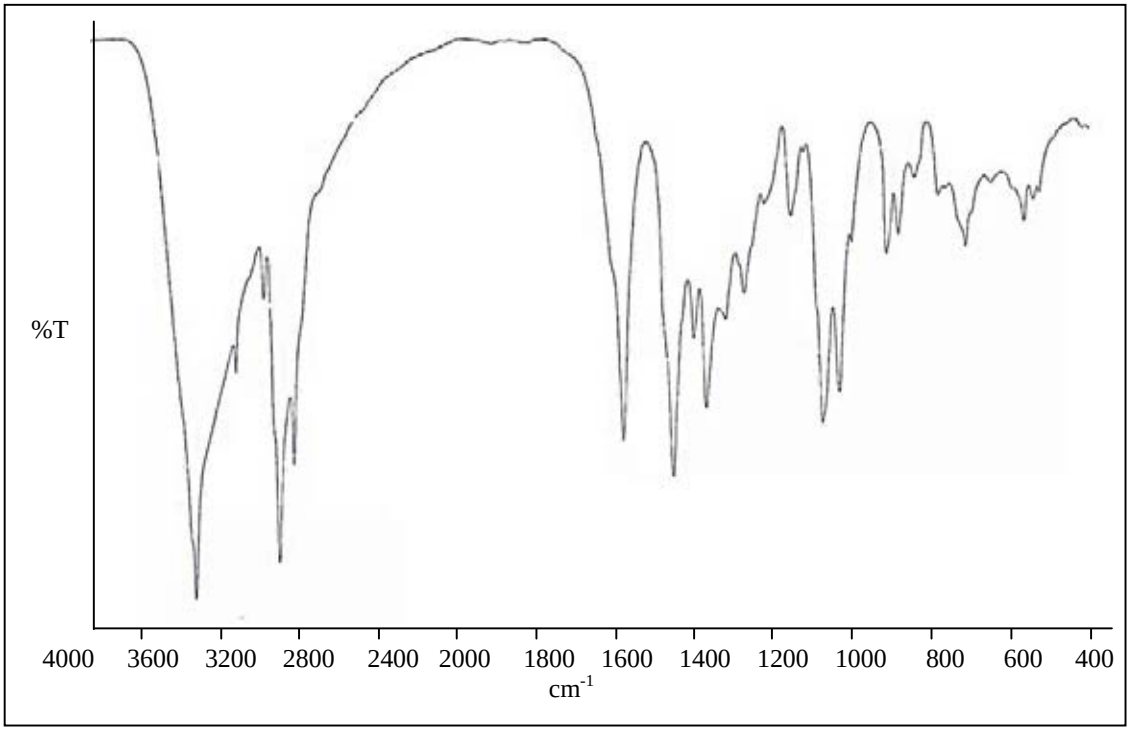
%T
4000
3600
3200
2800
2400
2000
1800
1600
1400
1200
1000
800
600
400
cm-1

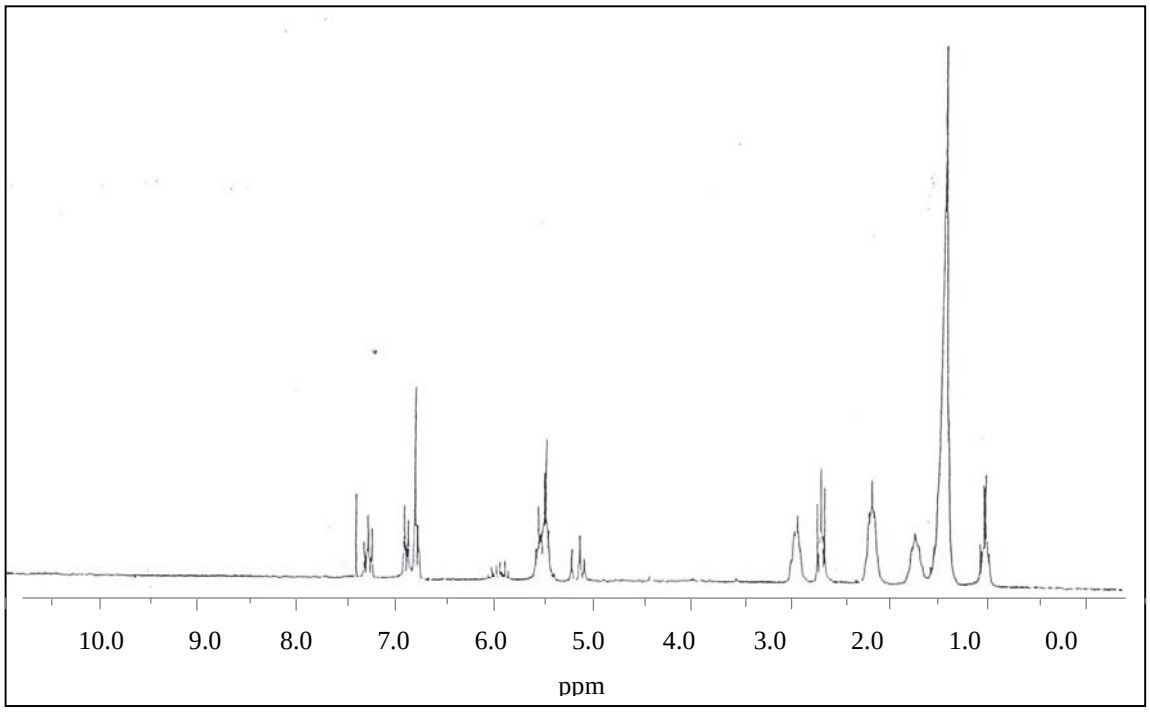

Figure A-10 ^{1}H-NMR spectrum of cardanol.

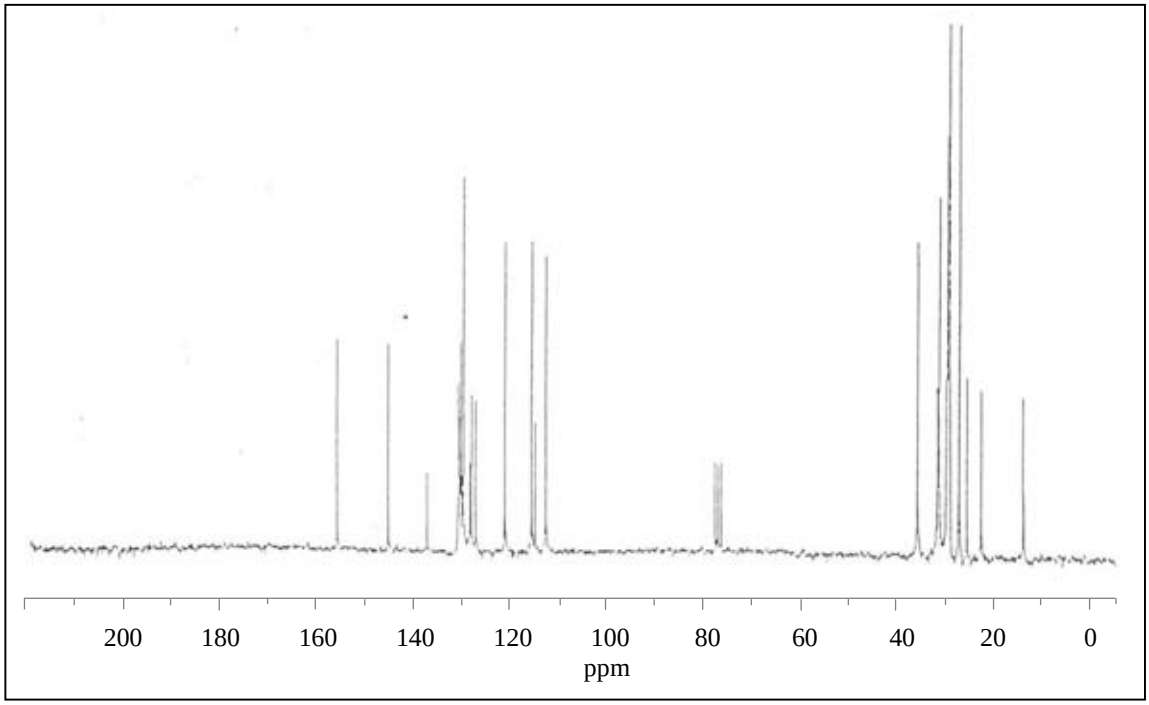

Figure A-11 ^{13}C-NMR spectrum of cardanol.

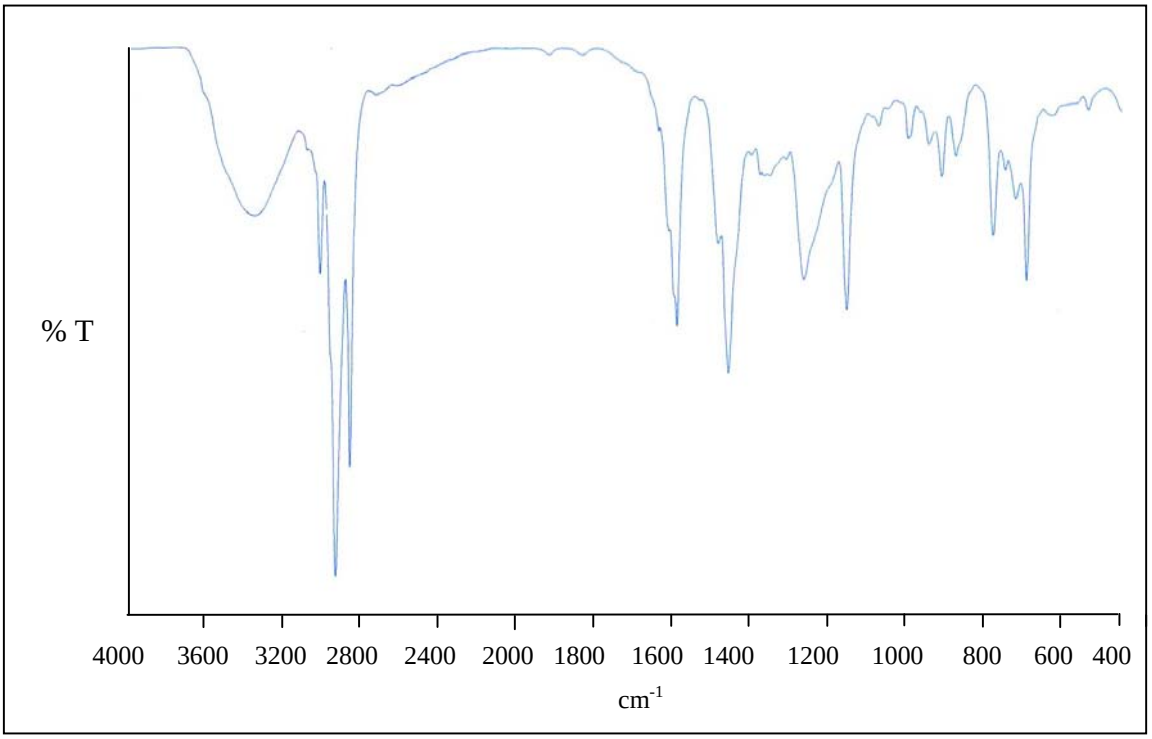

Figure A-12 Infrared spectrum of cardanol.

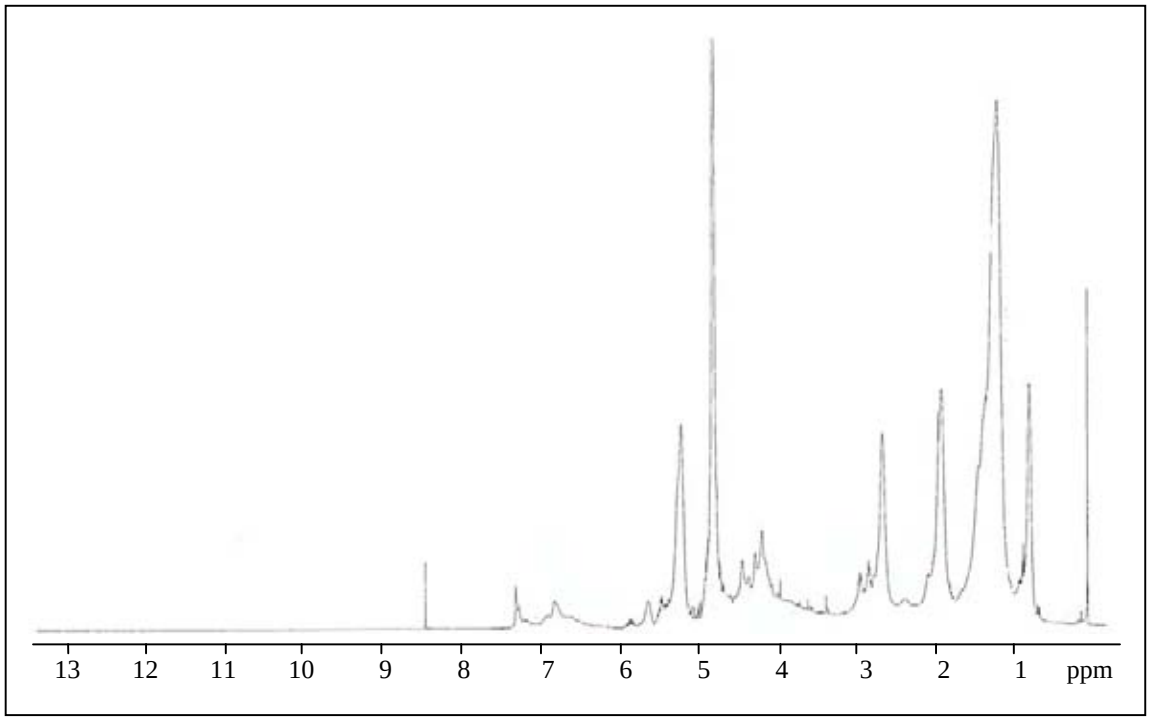

Figure A-13 ^{1}H-NMR spectrum of cardanol-formaldehyde sulfonate.

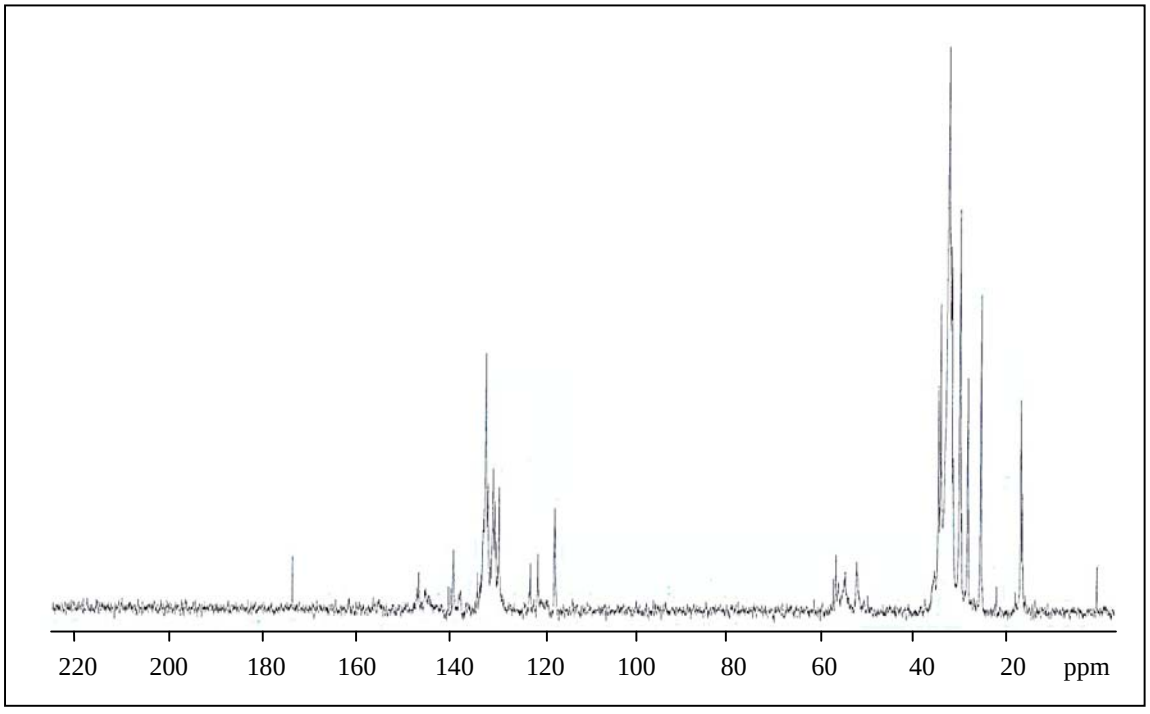

Figure A-14 ^{13}C-NMR spectrum of cardanol-formaldehyde sulfonate.

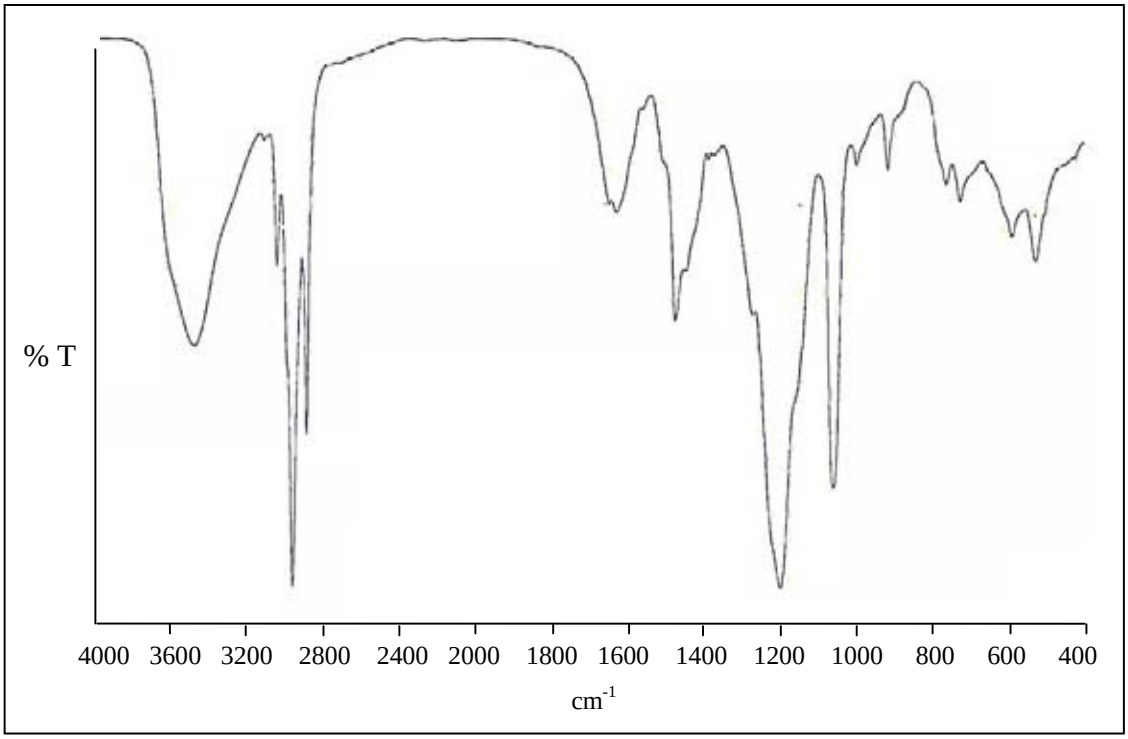

Figure A-15 Infrared spectrum of cardanol-formaldehyde sulfonate.

APPENDIX B

PROPERTIES OF BITUMINEOUS COAL AND COAL-WATER SLURRY CONTAINING SYNTHESIZED DISPERSANT

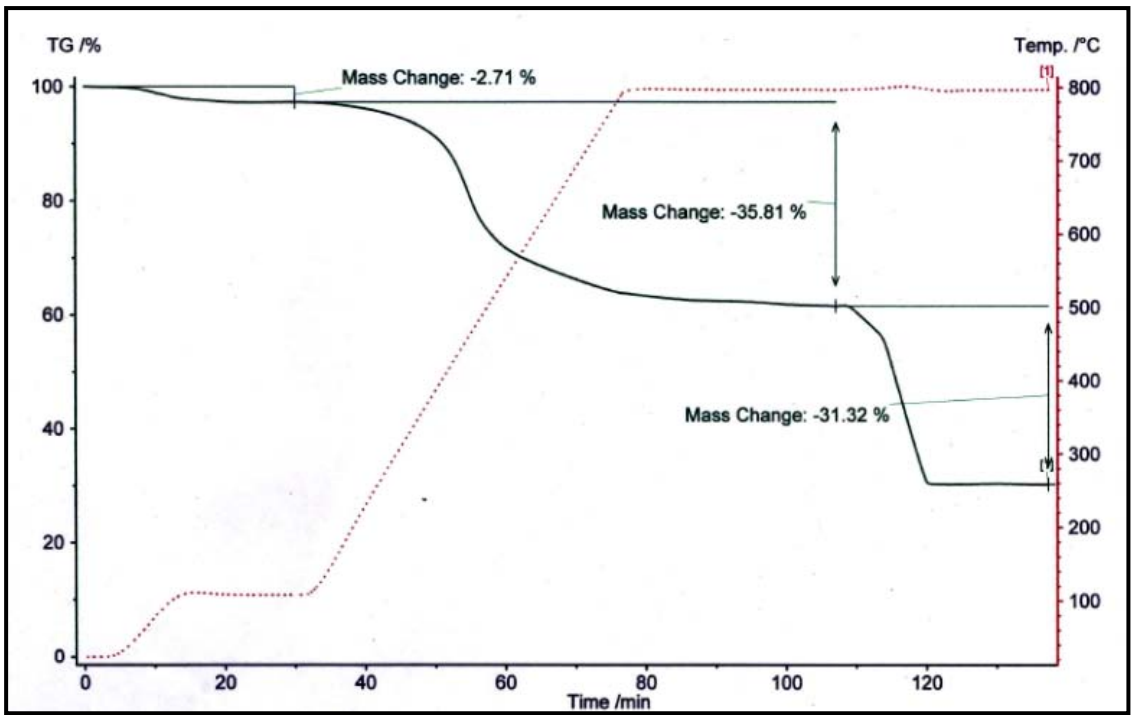

Figure B-1 Proximate analysis of bituminous coal

Instrument: NETZSCH STA 409 C/CD		
Project: Proximate	Material: coal	Segments: 1-55
Identity: 1704	Temp. Cal/Sens. Files: Tcalzero.tcx	Cruclible: DTA/TG crucible Al_2O_3
Laboratory: STREC	Range: 18….810/0.0…15.0K/min	Atmosphere: N_2-02/50 / N_2/ - / N_2
Operator: SOPA	Sample Car./TC: TG HIGH RG 2/ S	30ml/min/-
Sample: Coal, 29.910 mg	Mode/Type of Meas.: TG/Sample + Correction	TG Corr./M.Range: 020/50 mg

Table B-2 GPC data of cardanol-formaldehyde sulfonate

Peak Name	Retention Time (min)	% Area	Mn	Mw	MP	Poly dispersity	Area (μV*sec)	Height (mV)
1	20.698	97.56	9667	14631	13141	1.513495	338916627	2276924
2	26.242	1.75	835	868	970	1.039282	60948224	109936
3	29.223	0.68	256	258	256	1.005998	2369891	94875

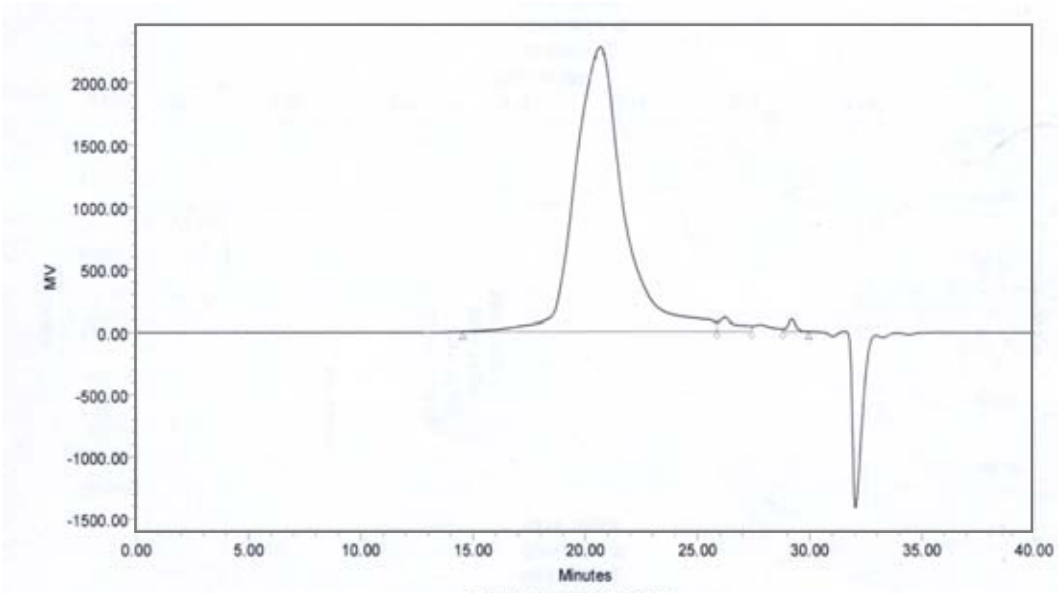

Figure B-2 GPC chromatogram of cardanol-formaldehyde sulfonate.

Table B-3 The effect of the variation of the sodium sulfite mass in sulfomethylation reaction on sulfur contents of cardanol-formaldehyde sulfonate

Cardanol:Na_2SO_3:CH_2O	Na_2SO_3 (%)	Sulfur Content (%)	Apparent Viscosity mPas
1:01:20	5.66	4.5	891
1:02:20	10.72	12.1	785
1:03:20	15.25	16.9	394
1:04:20	19.35	15.5	456

Table B-4 The effect of the variation of formaldehyde mass in sulfomethylation reaction on sulfur content and molecular weight of cardanol-formaldehyde sulfonate

Cardanol:Na_2SO_3:CH_2O	CH_2O (%)	Sulfur Content (%)	Mw	Apparent Viscosity (mPas)
1:03:10	13.77	10.9	11,090	667
1:03:20	24.21	16.2	14,333	399
1:03:30	32.40	16.1	12,789	565
1:03:40	38.99	16.4	9,556	599

Table B-5 Surface tension of diethanolamine anacardate at various concentrations

Dispersant concentration (% by weight)	Surface tension (mN/m)			Average
	1	2	3	
0	71.2	71.2	71.2	71.2
0.001	36.4	36.2	36.4	36.3
0.005	34.8	35.3	34.0	35.1
0.01	35.0	34.5	34.8	34.8
0.05	31.8	32.0	32.0	31.9
0.1	32.0	32.5	32.3	32.3
0.2	31.9	31.9	31.9	31.9
0.6	31.4	31.0	32.2	31.5
1	31.1	31.4	32.1	31.5
1.4	32.4	32.1	31.0	31.8
1.8	32.0	30.8	32.0	31.6
2	32.3	32.0	31.8	32.0

Table B-6 Surface tension of triethanolamine anacardate at various concentrations

Dispersant concentration (% by weight)	Surface tension (mN/m)			Average
	1	2	3	
0	71.2	71.2	71.2	71.2
0.001	39.1	39.2	39.2	39.2
0.005	35.9	36.0	35.8	35.9
0.01	34.9	35.0	35.0	35.0
0.05	31.5	31.9	31.7	31.7
0.1	32.6	32.1	32.0	32.2
0.2	33.0	33.0	32.0	32.7
0.6	32.5	31.8	32.2	32.2
1	32.6	31.8	31.8	32.1
1.4	32.1	32.1	32.1	32.1
1.8	32.5	32.4	32.4	32.4
2	32.4	32.2	32.2	32.3

Table B-7 Surface tension of cardanol-formaldehyde sulfonate at various concentrations

Dispersant concentration (% by weight)	Surface tension (mN/m)			Average
	1	2	3	
0	71.2	71.2	71.2	71.2
0.001	68.0	68.1	68.1	68.1
0.005	67.1	67.0	67.1	67.1
0.01	65.3	65.3	65.3	65.3
0.05	59.1	59.4	59.4	59.3
0.1	58.9	57.9	58.5	58.4
0.2	52.0	52.3	52.8	52.4
0.6	51.7	51.8	52.1	51.9
1	50.0	50.1	50.0	50.0
1.4	50.0	50.9	51.4	50.8
1.8	50.8	50.7	50.5	50.7
2	51.0	50.0	50.5	50.5

\

Table B-8 Surface tension of sodium lignosulfonate at various concentrations

Dispersant concentration (% by weight)	Surface tension (mN/m)			Average
	1	2	3	
0	71.2	71.2	71.2	71.2
0.001	70.1	70.0	70.0	70.0
0.005	69.0	69.5	69.0	69.2
0.01	68.9	68.4	68.8	68.7
0.05	68.6	68.7	68.8	68.7
0.1	68.0	68.4	68.3	68.2
0.2	62.0	62.8	62.1	62.3
0.6	59.5	59.0	59.0	59.2
1	59.0	59.0	58.8	58.9
1.4	59.0	59.0	59.8	59.3
1.8	58.8	58.5	57.0	58.1
2	53.7	53.1	52.8	53.2

Table B-9 Sulfur content of cardanol-formaldehyde sulfonate obtained at specific condition

Summary of results

Sample:	Cardanol-formaldehyde sulfonate
Condition	
Mass ratio: (cardanol: Na_2SO_3:CH2O)	1:3:20
Reaction temperature:	80^{o}C
Reaction time:	8 h
Measured:	530705-F
Sum:	18.9%
RMS:	0.000
Used lines:	4
Traces:	Si
Qual. Program:	SemIQ2004

Analyte	Type	Calibration status	Compound	Concentration (%)	Calculation method
Na	Sample	Calibrated	Na	1.696	Calculate
Si	Sample	Calibrated	Si	17.154	Calculate
S	Sample	Calibrated	S	0.0023	Calculate
Zn	Sample	Calibrated	Zn	0.014	Calculate

Sample Preparation

Sample type:	solid
Area ratio:	5.29
Additives sample:	0.
normalise:	no
X-ray path:	Helium

Quantify parameters

Recipe:	C:\superq\data\new.rcp
Spectrometer resp. file:	C:\superq\data\semiq.sti
Use compound list:	No
Apply drift corr.:	No
Apply medium corr.:	No
Apply film corr:	Yes
Disall. elem. set:	None
Disall. lines set:	None
Error weighting:	Root
Max. Flow detector intensity:	2000 kcps
Max. Sealed detector intensity	1000 kcps
Max. Scint detector intensity:	1000 kcps
Max. Duplex detector intensity:	3000 kcps

Table B-10 Sulfur content of commercial sodium lignosulfonate

Summary of results

Sample:	SL
Measured:	530705-A
Sum:	13.2%
RMS:	0.001
Used lines:	7
Traces:	Mg Si Fe
Qual. Program:	SemIQ2004

Analyte	Type	Calibration status	Compound	Concentration (%)	Calculation method
Na	Sample	Calibrated	Na	1.389	Calculate
P	Sample	Calibrated	P	0.006	Calculate
S	Sample	Calibrated	S	10.621	Calculate
Cl	Sample	Calibrated	Cl	0.192	Calculate
K	Sample	Calibrated	K	0.612	Calculate
Ca	Sample	Calibrated	Ca	0.39	Calculate
Mn	Sample	Calibrated	Mn	0.039	Calculate

Sample Preparation

Sample type:	solid
Area ratio:	7.55
Additives sample:	0.
normalise:	no
X-ray path:	Helium

Quantify parameters

Recipe:	C:\superq\data\new.rcp
Spectrometer resp. file:	C:\superq\data\semiq.sti
Use compound list:	No
Apply drift corr.:	No
Apply medium corr.:	No
Apply film corr:	Yes
Disall. elem. set:	None
Disall. lines set:	None
Error weighting:	Root
Max. Flow detector intensity:	2000 kcps
Max. Sealed detector intensity	1000 kcps
Max. Scint detector intensity:	1000 kcps
Max. Duplex detector intensity:	3000 kcps

Table B-11 Apparent viscosity of coal-water slurry without dispersant

t [s]	t_seg [s]	$\dot{\gamma}$ [1/s]	T [°C]	f [Pas]	σ [Pa]	f [mPas]
14.18	12.28	100	25.45	0.826	82.56	826
20.32	18.42	100	25.44	0.823	82.34	823
26.4	24.5	100	25.44	0.829	82.95	829
32.52	30.62	100	25.46	0.839	83.91	839
38.65	36.75	100	25.47	0.841	84.11	841
44.76	42.86	100	25.48	0.849	84.85	849
50.91	49.01	100	25.48	0.854	85.44	854
57.07	55.17	100	25.48	0.855	85.53	855
63.14	61.24	100	25.48	0.861	86.11	861
69.29	67.39	100	25.48	0.866	86.58	866
75.38	73.48	100	25.48	0.865	86.55	865
81.51	79.61	100	25.5	0.87	86.99	870
87.62	85.72	100	25.51	0.875	87.47	875
93.79	91.89	100	25.52	0.873	87.27	873
99.91	98.01	100	25.51	0.878	87.76	878
106	104.1	100	25.52	0.882	88.2	882
112.1	110.2	100	25.51	0.879	87.9	879
118.3	116.4	100	25.51	0.884	88.36	884
124.4	122.5	100	25.51	0.885	88.52	885
130.5	128.6	100	25.5	0.881	88.11	881
136.6	134.7	100	25.49	0.883	88.34	883
142.7	140.8	100	25.48	0.887	88.71	887
148.9	147	100	25.47	0.881	88.08	881
155	153.1	100	25.46	0.878	87.79	878
161.1	159.2	100	25.47	0.881	88.09	881
167.2	165.3	100	25.47	0.875	87.47	875
173.3	171.5	100	25.47	0.877	87.74	877
179.5	177.6	100	25.47	0.882	88.21	882
185.6	183.7	100	25.48	0.878	87.79	878
191.7	189.9	100	25.5	0.879	87.89	879
197.8	196	100	25.51	0.874	87.43	874
203.9	202	100	25.51	0.873	87.29	873
210.1	208.2	100	25.51	0.879	87.93	879
216.2	214.4	100	25.52	0.876	87.57	876
222.3	220.5	100	25.53	0.872	87.24	872
228.5	226.6	100	25.52	0.881	88.07	881
234.6	232.7	100	25.52	0.878	87.81	878
240.7	238.8	100	25.52	0.876	87.55	876
246.8	244.9	100	25.51	0.88	88.04	880
252.9	251	100	25.51	0.877	87.72	877
259.1	257.2	100	25.51	0.875	87.53	875
265.2	263.3	100	25.51	0.877	87.73	877
271.3	269.4	100	25.51	0.878	87.81	878
277.4	275.5	100	25.52	0.874	87.39	874
283.5	281.6	100	25.51	0.876	87.59	876
289.7	287.8	100	25.51	0.878	87.83	878
295.8	293.9	100	25.5	0.875	87.53	875

Table B-12 Apparent viscosity of coal-water slurry containing triethanolamine anacardate of 1.0 wt%

t [s]	t_seg [s]	$\dot{\gamma}$ [1/s]	T [°C]	f [Pas]	σ [Pa]	f [mPas]
20.22	18.38	100	25.67	0.78	78.01	780
26.37	24.53	100	25.66	0.79	78.98	790
32.48	30.64	100	25.65	0.798	79.81	798
38.58	36.74	100	25.65	0.799	79.91	799
44.74	42.9	100	25.64	0.806	80.61	806
50.86	49.02	100	25.62	0.81	80.98	810
57	55.16	100	25.62	0.811	81.09	811
63.09	61.25	100	25.62	0.818	81.81	818
69.24	67.4	100	25.62	0.819	81.94	819
75.31	73.47	100	25.62	0.82	81.98	820
81.47	79.63	100	25.62	0.826	82.57	826
87.61	85.77	100	25.62	0.826	82.63	826
93.7	91.86	100	25.63	0.827	82.73	827
99.85	98.01	100	25.64	0.833	83.3	833
105.9	104.1	100	25.62	0.834	83.37	834
112.1	110.2	100	25.61	0.834	83.38	834
118.2	116.4	100	25.61	0.84	83.95	840
124.3	122.5	100	25.61	0.839	83.88	839
130.4	128.6	100	25.6	0.84	83.97	840
136.5	134.7	100	25.6	0.844	84.42	844
142.7	140.9	100	25.59	0.845	84.46	845
148.8	147	100	25.59	0.845	84.48	845
154.9	153.1	100	25.57	0.849	84.89	849
161	159.2	100	25.56	0.851	85.09	851
167.2	165.3	100	25.56	0.85	85.01	850
173.3	171.5	100	25.56	0.856	85.64	856
179.4	177.6	100	25.56	0.856	85.61	856
185.6	183.7	100	25.57	0.856	85.55	856
191.7	189.9	100	25.59	0.863	86.28	863
197.8	195.9	100	25.59	0.863	86.27	863
203.9	202.1	100	25.6	0.863	86.31	863
210	208.2	100	25.6	0.869	86.86	869
216.1	214.3	100	25.6	0.87	86.96	870
222.3	220.5	100	25.6	0.868	86.81	868
228.4	226.6	100	25.6	0.875	87.48	875
234.5	232.7	100	25.59	0.874	87.43	874
240.6	238.8	100	25.59	0.874	87.37	874
246.8	244.9	100	25.57	0.88	88.02	880
252.9	251.1	100	25.58	0.881	88.12	881
259	257.2	100	25.57	0.88	88.01	880
265.1	263.3	100	25.57	0.885	88.54	885
271.3	269.4	100	25.56	0.887	88.68	887
277.4	275.5	100	25.56	0.887	88.67	887
283.5	281.7	100	25.57	0.89	89.02	890
289.6	287.8	100	25.59	0.89	89.01	890
295.7	293.9	100	25.6	0.888	88.8	888

Table B-13 Apparent viscosity of coal-water slurry containing cardanol-formaldehyde sulfonate of 1.0 wt% at specific condition

t [s]	t_seg [s]	$\dot{\gamma}$ [1/s]	T [°C]	f [Pas]	σ [Pa]	f [mPas]
20.29	18.41	100	25.96	0.384	38.42	384
26.42	24.54	100	25.94	0.377	37.69	377
32.54	30.66	100	25.93	0.375	37.47	375
38.66	36.78	100	25.91	0.377	37.68	377
44.75	42.87	100	25.88	0.377	37.72	377
50.91	49.03	100	25.88	0.375	37.47	375
57.02	55.14	100	25.85	0.376	37.6	376
63.13	61.25	100	25.83	0.376	37.6	376
69.26	67.38	100	25.82	0.374	37.42	374
75.4	73.52	100	25.8	0.376	37.64	376
81.48	79.6	100	25.78	0.376	37.57	376
87.62	85.74	100	25.77	0.377	37.66	377
93.76	91.88	100	25.76	0.376	37.64	376
99.86	97.98	100	25.75	0.38	38.02	380
106	104.1	100	25.73	0.374	37.37	374
112.1	110.3	100	25.71	0.376	37.63	376
118.2	116.3	100	25.71	0.375	37.49	375
124.4	122.5	100	25.7	0.377	37.75	377
130.5	128.6	100	25.7	0.376	37.55	376
136.6	134.8	100	25.69	0.375	37.54	375
142.7	140.9	100	25.68	0.373	37.28	373
148.8	146.9	100	25.68	0.375	37.51	375
155	153.1	100	25.69	0.375	37.48	375
161.1	159.2	100	25.7	0.373	37.32	373
167.2	165.4	100	25.7	0.375	37.48	375
173.3	171.4	100	25.7	0.374	37.44	374
179.5	177.6	100	25.7	0.373	37.26	373
185.6	183.7	100	25.68	0.374	37.4	374
191.7	189.8	100	25.68	0.374	37.4	374
197.8	196	100	25.66	0.374	37.43	374
204	202.1	100	25.66	0.374	37.4	374
210	208.2	100	25.65	0.374	37.44	374
216.2	214.3	100	25.64	0.372	37.19	372
222.3	220.4	100	25.64	0.374	37.36	374
228.4	226.6	100	25.62	0.374	37.44	374
234.6	232.7	100	25.61	0.372	37.2	372
240.7	238.8	100	25.61	0.374	37.4	374
246.8	245	100	25.61	0.373	37.34	373
252.9	251.1	100	25.6	0.371	37.13	371
259	257.1	100	25.6	0.373	37.31	373
265.2	263.3	100	25.59	0.373	37.34	373
271.3	269.4	100	25.59	0.372	37.16	372
277.4	275.6	100	25.57	0.373	37.34	373
283.5	281.6	100	25.58	0.374	37.43	374
289.7	287.8	100	25.58	0.372	37.23	372
295.8	293.9	100	25.57	0.374	37.39	374
301.9	300	100	25.57	0.374	37.42	374

Table B-14 Apparent viscosity of coal-water slurry containing sodium lignosulfonate of 1.0 wt%

t [s]	t_seg [s]	$\dot{\gamma}$ [1/s]	T [°C]	f [Pas]	σ [Pa]	f [mPas]
20.26	18.42	100	25.45	0.172	17.21	172
26.38	24.54	100	25.44	0.174	17.37	174
32.48	30.64	100	25.44	0.175	17.48	175
38.63	36.79	100	25.44	0.175	17.5	175
44.71	42.87	100	25.44	0.176	17.62	176
50.85	49.01	100	25.46	0.177	17.72	177
57.01	55.17	100	25.46	0.177	17.73	177
63.08	61.24	100	25.47	0.178	17.83	178
69.21	67.37	100	25.46	0.179	17.91	179
75.36	73.52	100	25.46	0.179	17.93	179
81.44	79.6	100	25.46	0.18	18.01	180
87.56	85.72	100	25.47	0.181	18.09	181
93.68	91.84	100	25.47	0.181	18.06	181
99.82	97.98	100	25.47	0.182	18.19	182
105.9	104.1	100	25.47	0.183	18.25	183
112	110.2	100	25.47	0.182	18.23	182
118.2	116.4	100	25.47	0.183	18.31	183
124.3	122.5	100	25.46	0.184	18.36	184
130.4	128.6	100	25.46	0.183	18.33	183
136.5	134.7	100	25.47	0.184	18.41	184
142.7	140.9	100	25.46	0.185	18.47	185
148.8	147	100	25.46	0.184	18.44	184
154.9	153.1	100	25.47	0.185	18.53	185
161	159.2	100	25.47	0.186	18.59	186
167.2	165.3	100	25.46	0.185	18.52	185
173.3	171.5	100	25.46	0.186	18.64	186
179.4	177.6	100	25.44	0.187	18.69	187
185.6	183.7	100	25.44	0.186	18.63	186
191.7	189.9	100	25.44	0.187	18.74	187
197.8	196	100	25.44	0.188	18.79	188
203.9	202.1	100	25.44	0.187	18.72	187
210	208.2	100	25.44	0.188	18.79	188
216.1	214.3	100	25.44	0.188	18.84	188
222.3	220.4	100	25.44	0.188	18.77	188
228.4	226.6	100	25.43	0.189	18.86	189
234.5	232.7	100	25.42	0.189	18.89	189
240.7	238.8	100	25.43	0.188	18.83	188
246.8	244.9	100	25.44	0.189	18.93	189
252.9	251.1	100	25.44	0.189	18.93	189
259	257.2	100	25.44	0.189	18.89	189
265.1	263.3	100	25.45	0.19	18.96	190
271.3	269.4	100	25.46	0.19	18.98	190
277.4	275.5	100	25.44	0.189	18.94	189
283.5	281.7	100	25.44	0.19	18.99	190
289.6	287.8	100	25.46	0.19	19.04	190
295.7	293.9	100	25.46	0.19	18.98	190

Table B-15 Apparent viscosity of coal-water slurry containing cardanol-formaldehyde sulfonate of 1.8 wt%

t [s]	t_seg [s]	$\dot{\gamma}$ [1/s]	T [°C]	f [Pas]	σ [Pa]	f [mPas]
53.2	36.74	100	26.23	0.01796	1.796	17.96
59.35	42.89	100	26.2	0.01714	1.714	17.14
65.46	49	100	26.18	0.01724	1.724	17.24
71.58	55.12	100	26.16	0.01722	1.722	17.22
77.75	61.29	100	26.14	0.01643	1.643	16.43
83.82	67.36	100	26.11	0.0166	1.66	16.6
89.95	73.49	100	26.09	0.01692	1.692	16.92
96.06	79.6	100	26.06	0.01605	1.605	16.05
102.2	85.75	100	26.05	0.01624	1.624	16.24
108.4	91.89	100	26.03	0.01647	1.647	16.47
114.5	98.01	100	26.02	0.01561	1.561	15.61
120.6	104.1	100	26.01	0.01582	1.582	15.82
126.7	110.3	100	26	0.01614	1.614	16.14
132.8	116.4	100	25.98	0.01581	1.581	15.81
138.9	122.5	100	25.98	0.01572	1.572	15.72
145.1	128.6	100	25.98	0.01613	1.613	16.13
151.2	134.7	100	25.97	0.01515	1.515	15.15
157.3	140.8	100	25.97	0.01513	1.513	15.13
163.4	147	100	25.98	0.01546	1.546	15.46
169.6	153.1	100	25.97	0.01483	1.483	14.83
175.7	159.2	100	25.97	0.01482	1.482	14.82
181.8	165.4	100	25.96	0.01507	1.507	15.07
187.9	171.5	100	25.94	0.01431	1.431	14.31
194	177.6	100	25.94	0.01443	1.443	14.43
200.2	183.7	100	25.94	0.01493	1.493	14.93
206.3	189.8	100	25.93	0.01413	1.413	14.13
212.4	196	100	25.92	0.01406	1.406	14.06
218.5	202	100	25.91	0.01438	1.438	14.38
224.7	208.2	100	25.9	0.01396	1.396	13.96
230.8	214.3	100	25.89	0.01388	1.388	13.88
236.9	220.4	100	25.88	0.01433	1.433	14.33
243	226.5	100	25.87	0.01377	1.377	13.77
249.1	232.7	100	25.87	0.01353	1.353	13.53
255.3	238.8	100	25.87	0.01434	1.434	14.34
261.4	244.9	100	25.87	0.01384	1.384	13.84
267.5	251.1	100	25.87	0.01423	1.423	14.23
273.6	257.2	100	25.87	0.01435	1.435	14.35
279.7	263.3	100	25.87	0.01391	1.391	13.91
285.9	269.5	100	25.86	0.01413	1.413	14.13
292	275.6	100	25.85	0.01429	1.429	14.29
298.1	281.6	100	25.84	0.01388	1.388	13.88
304.2	287.8	100	25.84	0.0138	1.38	13.8

Table B-16 Apparent viscosity of coal-water slurry containing sodium lignosulfonate 0f 1.4 wt%

t [s]	t_seg [s]	$\dot{\gamma}$ [1/s]	T [°C]	f [Pas]	σ [Pa]	f [mPas]
26.43	24.54	100	25.49	0.107	10.7	107
32.56	30.67	100	25.47	0.109	10.93	109
38.64	36.75	100	25.45	0.108	10.76	108
44.78	42.89	100	25.44	0.125	12.47	125
50.89	49	100	25.42	0.109	10.87	109
57.04	55.15	100	25.41	0.108	10.81	108
63.12	61.23	100	25.42	0.114	11.38	114
69.28	67.38	100	25.43	0.115	11.45	115
75.42	73.52	100	25.45	0.104	10.36	104
81.56	79.66	100	25.45	0.112	11.18	112
87.65	85.75	100	25.46	0.117	11.73	117
93.75	91.85	100	25.46	0.113	11.34	113
99.86	97.96	100	25.46	0.105	10.48	105
106	104.1	100	25.47	0.109	10.91	109
112.1	110.2	100	25.47	0.107	10.67	107
118.2	116.3	100	25.47	0.107	10.73	107
124.4	122.5	100	25.47	0.108	10.8	108
130.5	128.6	100	25.47	0.106	10.61	106
136.6	134.7	100	25.46	0.114	11.38	114
142.7	140.8	100	25.45	0.109	10.89	109
148.9	147	100	25.44	0.113	11.32	113
155	153.1	100	25.42	0.107	10.65	107
161.1	159.2	100	25.41	0.114	11.37	114
167.2	165.3	100	25.4	0.105	10.55	105
173.4	171.5	100	25.38	0.111	11.12	111
179.4	177.6	100	25.37	0.11	10.97	110
185.6	183.7	100	25.37	0.11	10.96	110
191.7	189.8	100	25.37	0.111	11.14	111
197.8	196	100	25.37	0.109	10.91	109
204	202.1	100	25.38	0.11	11.02	110
210.1	208.2	100	25.38	0.114	11.37	114
216.2	214.3	100	25.38	0.111	11.07	111
222.4	220.5	100	25.38	0.11	10.97	110
228.4	226.6	100	25.39	0.11	11.02	110
234.6	232.7	100	25.38	0.108	10.75	108
240.7	238.8	100	25.4	0.109	10.95	109
246.8	244.9	100	25.41	0.111	11.08	111
253	251.1	100	25.41	0.109	10.94	109
259.1	257.2	100	25.42	0.111	11.05	111
265.2	263.3	100	25.43	0.112	11.21	112
271.3	269.4	100	25.44	0.109	10.89	109
277.4	275.5	100	25.45	0.107	10.73	107

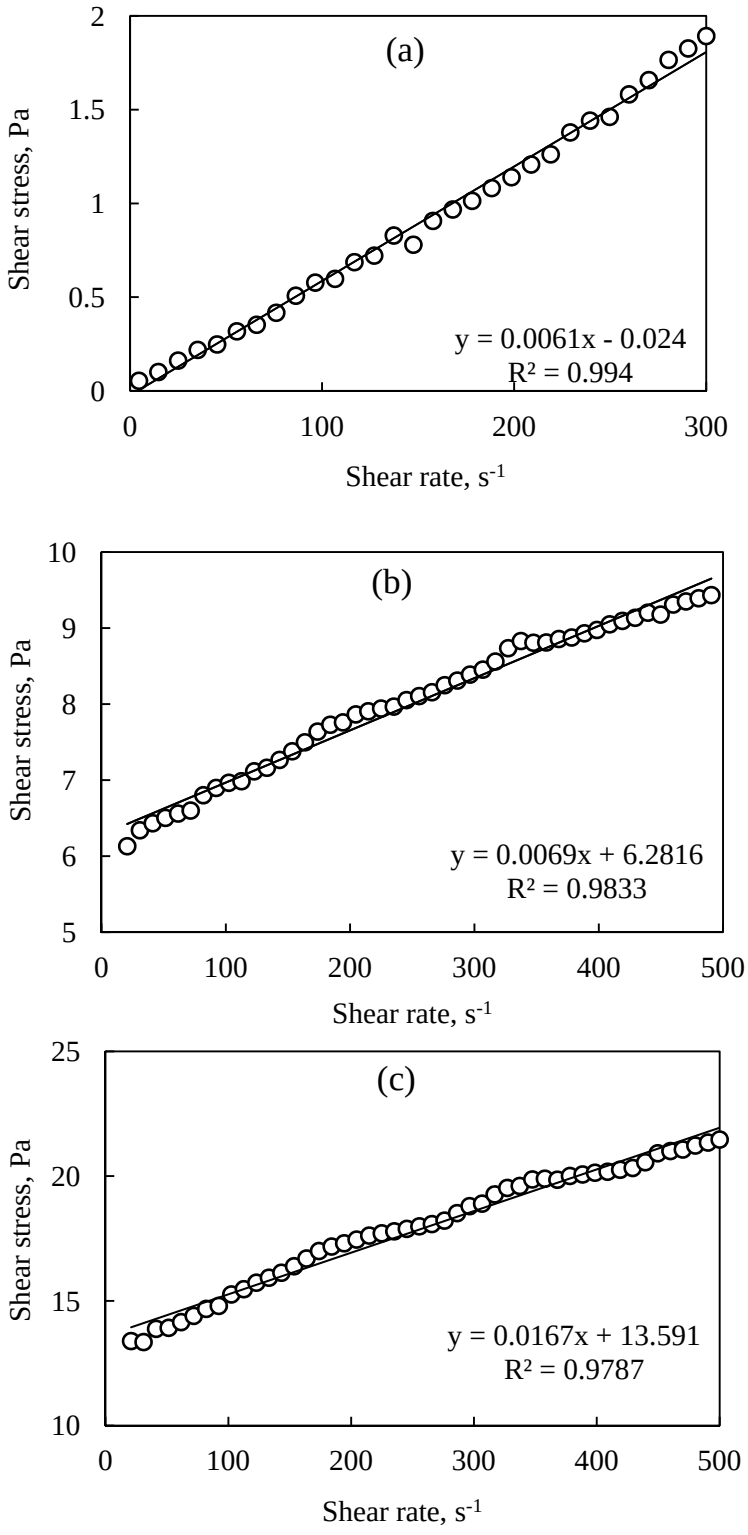

Figure B-2 The shear stress–shear rate curves fitted to the Bingham plastic model of coal-water slurry containing cardanol-formaldehyde sulfonate of 1.0 wt% at different coal concentrations; (a) 30% coal, (b) 40% coal, and (c) 50% coal.

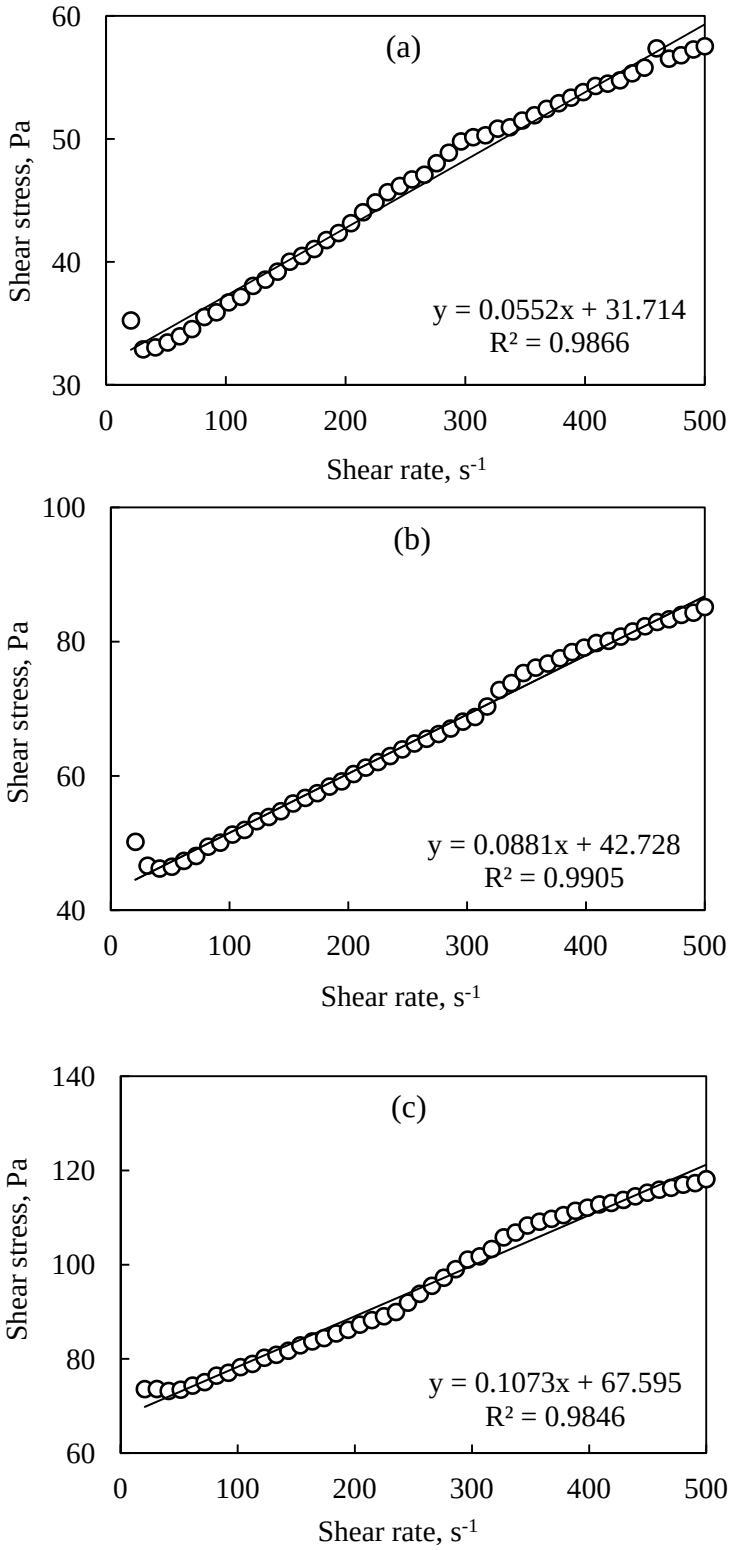

Figure B-3 The shear stress–shear rate curves fitted to the Bingham plastic model of coal-water slurry containing cardanol-formaldehyde sulfonate of 1.0 wt% at different coal concentrations; (a) 50% coal, (b) 51% coal, and (c) 52% coal.

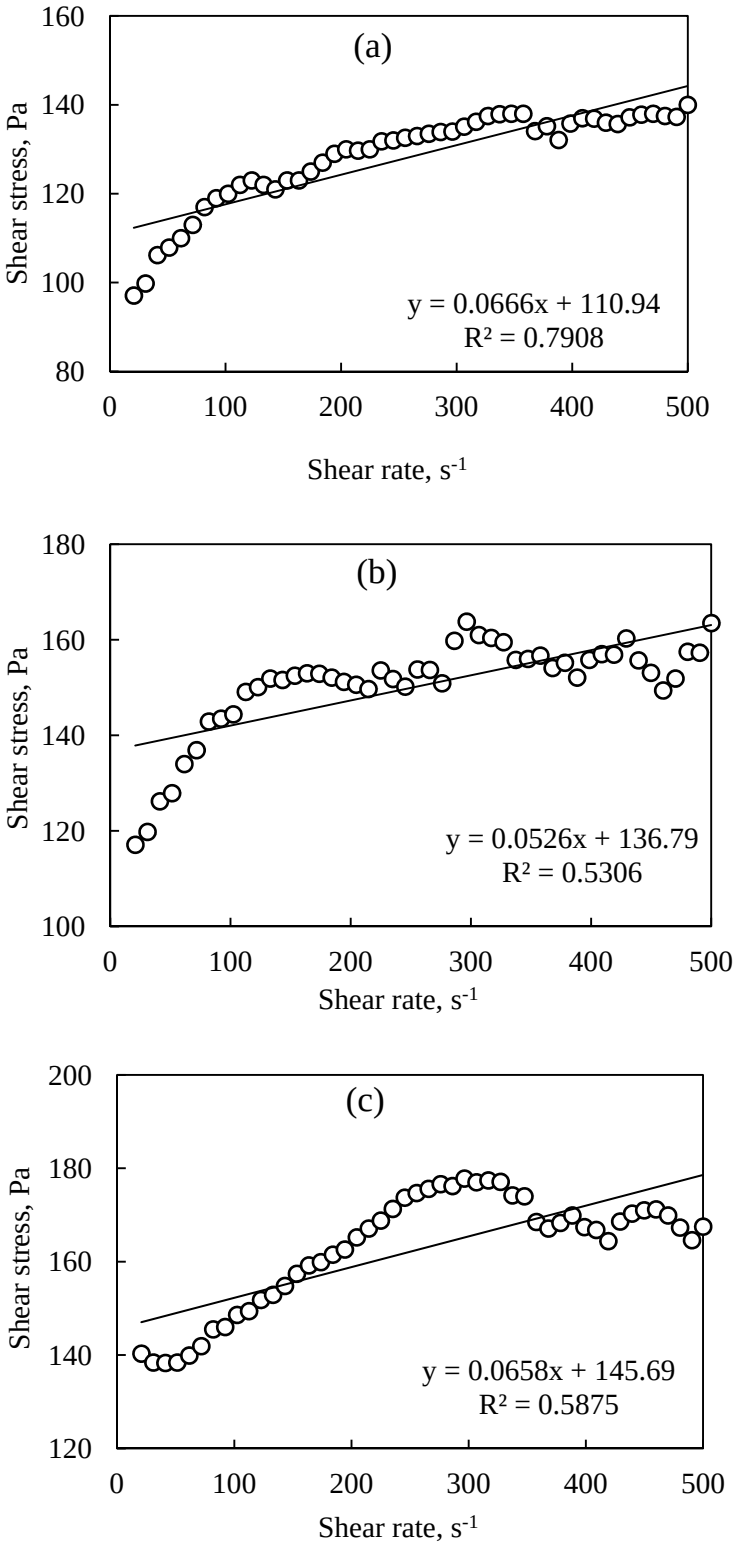

Figure B-4 The shear stress–shear rate curves fitted to the Bingham plastic model of coal-water slurry containing cardanol-formaldehyde sulfonate of 1.0 wt% at different coal concentrations; (a) 53% coal, (b) 55% coal, and (c) 57% coal.

Table B-17 Apparent viscosity and yield stress of coal-water slurry at the shear rate of 100 s^{-1} with the variation of coal concentrations

Coal concentration [wt%]	Apparent viscosity [mPa.s]	Yield stress [Pa]
40	69	6
45	152	14
50	375	32
51	514	43
52	788	68
53	1112	111
55	1523	137
57	1725	146

VITAE

Miss Panitha Phulkerd was born on April 7, 1983, in Petchaburi, Thailand. She received the Bachelor Degree of Science, majoring in Chemistry in 2005 and graduated with Master's Degree of Science majoring in Petrochemistry and Polymer Science from Faculty of Science, Chulalongkorn University in 2007. She began her PhD study in Program of Petrochemistry, Faculty of Science, Chulalongkorn University in the academic year of 2008. Further, she has entered the joint-dual education program between Faculty of Science, Chulalongkorn University and School of Materials Science, Japan Advanced Instituted of Science and Technology, Japan in 2010. Following the joint-dual degree agreement, she will be completed both programs in 2012.

Awards:

December 2010	Best Poster Presentation, the 9th Asian Workshop on Polymer Processing (AWPP2010), Hanoi, Vietnam
April 2012	Best Poster Award (ANTEC 2012 Graduate Student Poster Competition, Ken J. Braney International Award), Annual Technical Conference 2012, organized by the Society of Plastic Engineering, Orlando, USA.

Publications:

1. M. Yamaguchi, Y. Irie, **P. Phulkerd**, H. Hagihara, S. Hirayama, S. Sasaki, Plywood-like structure of injection-moulded polypropylene polymer, *Polymer*, 51, 5983-89 (2010).
2. **P. Phulkerd**, S. Nobukawa, Y. Uchiyama, M. Yamaguchi, Anomalous mechanical anisotropy of β form polypropylene sheet with *N*,*N*′-dicyclohexyl-2,6-naphthalenedicarboxamide, *Polymer*, 52, 4867-72 (2011).